Peptide-Polymer-Hybrid Materials for Advanced Retroviral Gene Transfer Agents

Diploma Thesis by

Oliver Ceyhun

Born on the 06.08.1987

in Flörsheim (am Main)

Matriculation number: 2658612

Max Planck Institute for Polymer Research (MPI-P)

Fachbereich 09 Johannes Gutenberg Universität Mainz (JGU)

Supervisor: Prof. Dr. Tanja Weil

Referee: Prof. Dr. Pol Besenius

March 2018 – Septemper 2018

Acknowledgements

I would like to thank my supervisor Prof. Dr. Tanja Weil for the opportunity to work in her group.

Further I would like to thank Dr. Christopher Synatschke for his support and guidance during my diploma thesis. I am thankful for the interesting research project I was able to work on.

Die Arbeit wurde vom 07.03.2018 bis zum 30.09.2018 am Max-Planck-Institut für Polymerforschung in Mainz unter der Leitung von Prof. Dr. Tanja Weil durchgeführt.

The work was carried out from 07.03.2018 to 30.09.2018at the Max Planck Institute for Polymer Research under the supervision of Prof. Dr. Tanja Weil.

Abstract

The supramolecular structures formed by self-assembling peptides are in the focus of many scientific projects for their huge potential in biomedical applications. As a result, the interest in understanding the parameters which influence the self-assembly is growing with every year. The group of T. Weil investigates the self-assembly behavior of short peptide sequences into nanofibers and, in cooperation with other groups, their potential in enhancing retroviral gene transfer.

The aim of this thesis was to further the understanding of different parameters to enhance the controllability of peptide self-assembly. To investigate the morphology of assembled supramolecular architectures, transmission electron microscopy was used. It was possible to demonstrate the influence on supramolecular assembly behavior by selected parameters. The pH value was identified as one of the most significant parameters that influences self-assembly. Changes in the range of two orders of magnitude in pH resulted in either well-defined fibers or ill-defined aggregates. This could completely change the morphology of the structures assembled. A similar effect had the oxidation of a terminal methionine group in one of the peptide sequences. Both parameters could be used to transform the morphology from fibrillar structures to wider ribbon like structures. The salt concentration of the solution the self-assembly took place in, showed the capability to enhance the effect the other parameters had. The synthesis of a polymer-peptide hybrid was successful, but unfortunately it was not possible to produce usable information about the influence of the polymer corona on the self-assembly behavior.

Consequently, this thesis is a small contribution to the understanding of self-assembly processes and the parameters to influence them.

Zusammenfassung

Supramolekulare Strukturen aus selbstassimilierten Peptiden sind im Focus vieler wissenschaftlicher Projekte aufgrund des großen Potenzials, das sie für biomedizinische Anwendungen bieten. Daher wächst das Interesse daran mit jedem Jahr die Parameter besser zu verstehen, die ihre Selbsassimilierung beeinflussen. Der Arbeitskreis von T. Weil untersucht die Selbsassimilierung kurzer Peptide in Nanofasern und, in Kooperation mit anderen Arbeitskreisen, die Möglichkeit retroviralen Gentransfer zu verstärken.

Das Ziel dieser Abschlussarbeit war es das Verständnis der Parameter, die die Selbstassimilierung beeinflussen zu vertiefen. Um die Morphologien der enstandenen supramolekularen Strukturen zu untersuchen wurde die Transmissionselektronenmikroskopie eingesetzt. Es war möglich zu zeigen, wie ausgewählte Parameter das Selbstassimilierungsverhalten beeinflussen. Der pH-Wert zeigte sich als einer der Parameter mit dem größten Einfluss auf die Selbstassimilierung. Veränderungen des pH-Wertes von zwei Größenordnungen machten den Unterschied zwischen gut definierten Fasern oder schlecht definierten Aggregaten aus. Die Oxidation der endständigen Methioningruppe der Peptidsequenz übte einen ähnlichen Einfluss aus. Beide Parameter konnten genutzt werden um die Morphologie der Strukturen von einer fibrillären zu einer bänderhaften Struktur zu verändern. Die Salzkonzentration des Mediums, in dem die Selbstassimilierung stattfand, zeigte die Fähigkeit die Wirkung, welche die anderen Parameter ausübten, zu verstärken. Die Synthese des Polymer-Peptid-Hybrides war erfolgreich, leider war es nicht möglich verwendbare Erkenntnisse über den Einfluss der Polymerkorona auf das Selbstassimilierungsverhalten zu gewinnen.

Somit liefert diese Abschlussarbeit einen kleinen Beitrag zum Verständnis der Selbstassimilierungsprozesse und der Parameter, die diese beeinflussen.

Content

List of abbreviations

ACN	Acetonitrile
AIBN	Azobisisobutyronitrile
ALP	Anionic living polymerization
ATRP	Atom-transfer radical polymerization
Bib-	α-Bromoisobutyryl-
Boc	tert-Butyloxycarbonyl
CSIRO	Commonwealth Scientific and Industrial Research Organisation
CTA	Chain transfer agent
D	Dispersity
DIEA	N, N-Diisopropylethylamine
DMAA	N, N-Dimethylacrylamide
DMF	Dimethylformamide
DMSO	Dimethyl sulfoxide (
DNA	Deoxyribonucleic acid
DPBS	Dulbecco's Phosphate-Buffered Saline
ESI-MS	Electrospray ionization mass spectrometry
Fmoc	Fluorenylmethyloxycarbonyl
FRP	Free radical polymerization
GPC	Gel permeation chromatography
HFIP	Hexafluoroisopropanol
HPLC	High-performance liquid chromatography
LCMS	Liquid chromatography–mass spectrometry
M_n	Number average molar mass
mRNA	messenger RNA
M_w	Mass average molar mass
NMP	Nitroxide-mediated radical polymerization
NMR	Nuclear magnetic resonance (spectroscopy)
OEGMA	Poly(ethylene glycol) methyl ether methacrylate
RAFT	Reversible addition-fragmentation chain transfer

RDRP	Reversible-deactivation radical polymerization
RPM	Rounds per minute
RNA	Ribonucleic acid
PA	Peptide amphiphile
PBS	Phosphate-buffered saline
PEG	Polyethylene glycol
PES	Polysulfone
PRE	Persistent radical effect
PTFE	Polytetrafluoroethylene
PyBOP	Benzotriazol-1-yl-oxytripyrrolidinophosphonium hexafluorophosphate
RNA	Ribonucleic acid
SEM	Scanning electron microscope
SPPS	Solid-phase peptide synthesis
TEM	Transmission Electron Microscopy
TFA	Trifluoroacetic acid
TIPS	Triisopropylsilane
TMS	Tetramethylsilane

1. Motivation

The goal of the underlying project of this diploma thesis was the synthesis of peptide-polymer hybrid materials which are capable of facilitating a more efficient viral gene transduction. Gene transduction plays an important role in medical applications, as in the transduction of T cells.[1] It has potential uses in gene therapy of cancer or in the combat against inherent genetic disorders.[2-3] The gene transduction *via* viral vectors has the huge upside of its high biosafety.[4] Especially lentiviral vectors showed an improvement of the gene transfer compared to other methods.[5]

In their cooperative work the groups of C. Meier, T. Weil, F. Kirchhoff and J. Münch could show that nanofibrils, which self-assembled from peptides, enhance the viral gene transfer more strongly than other established systems.[6-8] These promising results are the motivation for this project. The aim is to better understand the self-assembly behavior of these peptide sequences and show how further improvement of the transduction efficiency could be achieved.

To achieve the optimal transduction performance it is necessary to have good control over the self-assembly behavior of the peptide. Ideally, it should be possible to design peptides and direct their self-assembly so that they fit perfectly to the given task and environment. There are many mechanisms to control the self-assembly behavior of peptides and this quest for better control is a growing field in biochemical and material science. To investigate the controllability of the process, various parameters such as peptide sequence, polymer corona and pH value, among others, were studied.

Obviously, the first parameter which can be varied is the design of the peptide sequence. S. Sieste, in the group of T. Weil at the University of Ulm, showed in her work that by changing even a single amino acid in a peptide sequence can have dramatic effects on their self-assembly behavior and consequently its biological performance. Other projects also highlight the influence of sequence variation on the establishing supramolecular architecture.[9-11] Due to the cost-efficient method of automated solid phase peptide synthesis, these sequence-specific-modifications are easily accessible.[12]

A more drastic change is the coating of peptide assemblies with a synthetic polymer corona. This technique offers a wide array of engineering tools in control of the self-assembly and later behavior of the supramolecular structure.[13-15] The group of T. Weil was able to demonstrate the improvement of fibril building peptides in applications for regenerative medicine, by coating them with polydopamine.[16] To achieve the goal of synthesizing a peptide-polymer hybrid material, which can enhance the gene transduction, a three step approach was taken in this thesis (**Figure 1**). In the first step the peptide should be synthesized and coupled to a radical polymerization initiator. In the second step the macroinitiator will be used to synthesize the polymer-peptide hybrid. Which will then be sent to the group of Prof. J. Münch in the University of Ulm. The reversible-deactivation radical polymerization (RDRP) was considered as an appropriate polymerization method. This method combines the positive features of both free radical polymerization and anionic living polymerization.[17] Therefore, the ATRP and RAFT polymerization were chosen for the synthesis of the peptide-polymer conjugates. ATRP offers a high control over the functionality, mass average molar mass (Mw) and dispersity (D).[18] It has proven to be an excellent tool of designing and producing bioconjugates.[19] RAFT polymerization is known as the most versatile method of the RDRPs. It offers a high tolerance against a variety of functional groups, mild reaction conditions and the added benefit of a metal free reaction.[20-21] Therefore, it is no surprise that RAFT polymerization is a fast growing method in the development of polymer-bioconjugates.[20, 22-24]

The work in this thesis is supposed to enhance the understanding of the mechanisms which influence the self-assembly of peptides into supramolecular structures. This improved understanding will make it possible to plan preparation and synthesis pathways to design the outcome of the self-assembling process of the peptides.

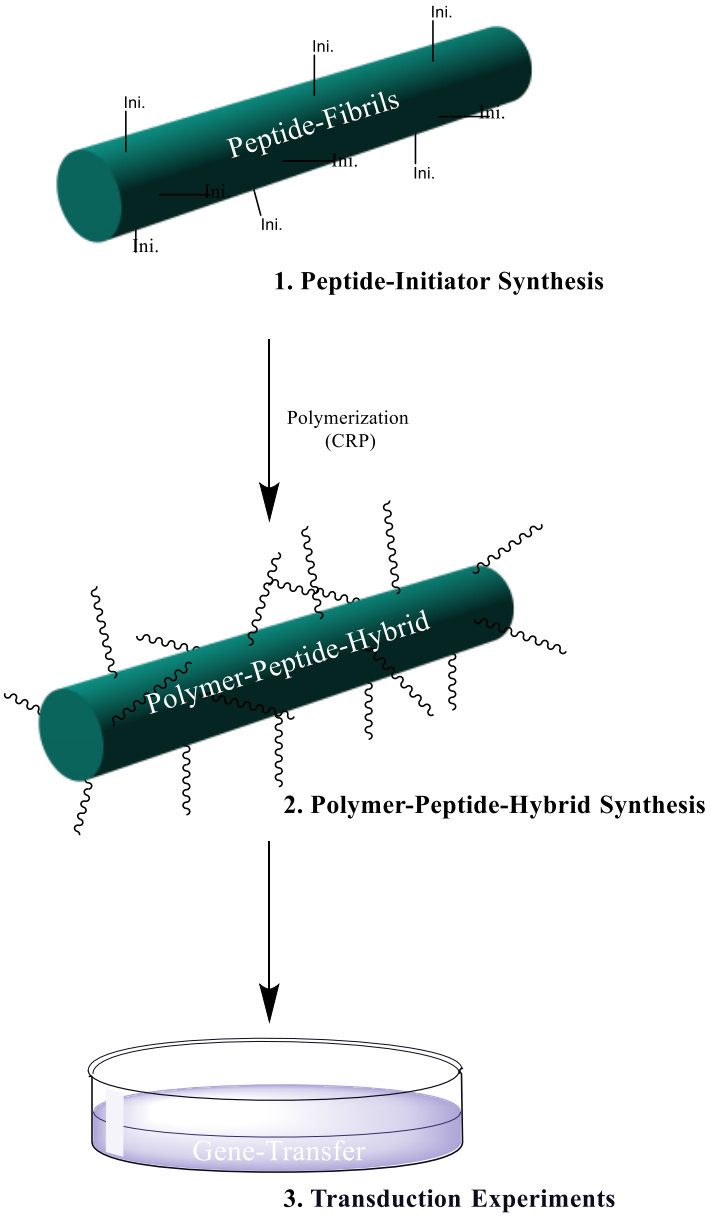

Figure 1: Three step approach to synthesize and test polymer-peptide hybrid materials for their capability of enhancing the gene transfer of viruses.

2. Theory

2.1. Molecular Self-Assembly

The mechanism of molecular self-assembly makes supramolecular architectures attainable which would not exist without this process. There are two distinct types of molecular self-assembly, the intermolecular one and the intramolecular one. The second describes for example the folding process in which proteins achieve their three-dimensional structure. For this project the intermolecular self-assembly is important and will be presented in more detail. The process of intermolecular self-assembly is part of the concept of supramolecular chemistry. It first appeared in the mid-1930s under the name of "Übermoleküle" as a model to illustrate the molecular architecture of combined covalent saturated molecules.[25] This concept is essential for the understanding of biological and medical phenomena. The supramolecular structure is formed with intermolecular forces like hydrogen bonding, van der Waals forces, π-π interactions, and others.[26] In nature, this intermolecular self-assembly is a cornerstone of the "bottom-up" process which forms multitude of natural occurring supramolecular architectures.[27] Over billions of years, nature created many different self-assembling systems, for example, lipids, nucleic acids, and amino acids.[28] Lipids are small amphiphilic molecules which can self-assemble into many different biological components, such as the cell membrane consisting of phospholipids.[29] The nucleic acids comprise the ribonucleic acid (RNA) and the deoxyribonucleic acid (DNA) and can be described as the most important biomolecules for life. In **Figure 2** various examples for self-assembled structures out of these building stones are shown. Peptides and their building blocks, the amino acids are the subject of this thesis and will therefore be discussed more thoroughly in the next chapters.

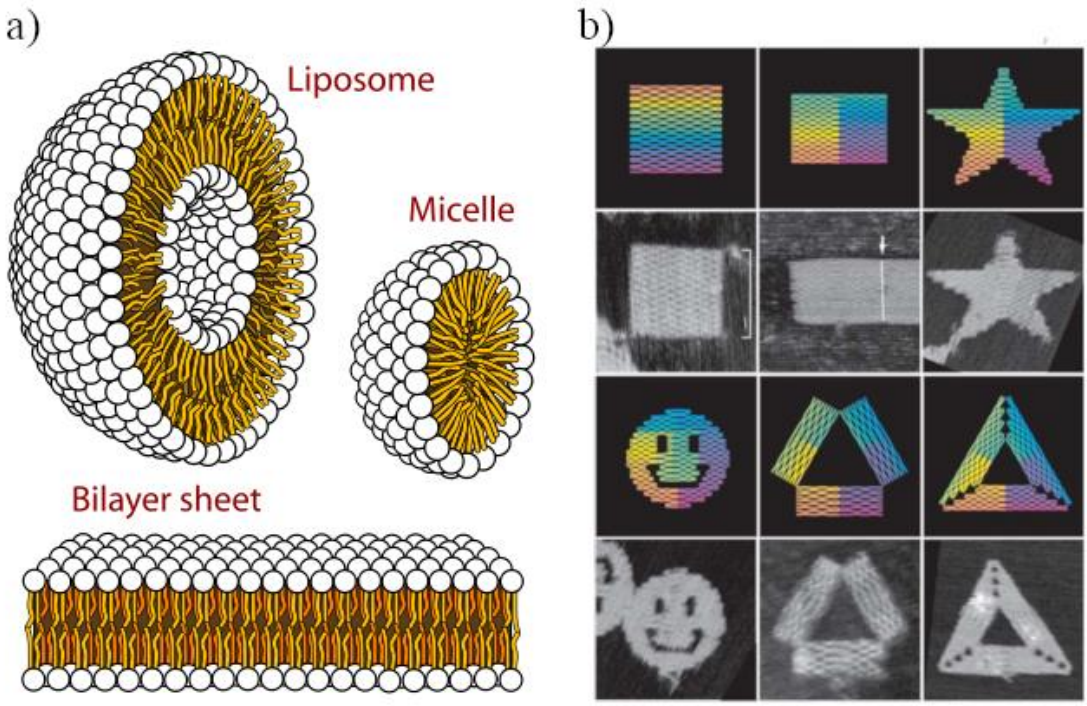

Figure 2: Example of a) a natural self-assembly process: supramolecular lipid architectures and b) a synthetic self-assembly process: supramolecular DNA architectures.[30]

2.1.1. Peptides

2.1.1.1. Proteins

As mentioned before amino acids are the building blocks of peptides and proteins. Proteins have a 3D structure which dictates their function, and which is predetermined by their 1D polypeptide chain. It is this highly evolved natural system of folding a sequence of amino acids into a protein that captures the interest of scientists for decades. The mimicking of this natural process with a synthetic one is the goal of many chemists today.

The protein biosynthesis starts with the transcription of the genome. In this process the information is read out from the DNA by the RNA polymerase which writes the information into a so-called messenger RNA (mRNA) single strand. The mRNA is then translated by the ribosome into a polypeptide chain. The finished chain is afterwards released from the

ribosome; the folding begins during the translation at the ribosome when the coupled amino acids start to interact.

The polypeptide chain structure is the random coil, the amino acids are covalently linked to their neighbors. During the folding process, the random coil self-assembles into the fully functional 3D protein structure.[31] The amino acid sequence is called the primary structure. Its intermolecular interaction defines the 3D protein structure.[32] The forces controlling this folding process are hydrogen bonds, van der Waals interactions, Backbone angle preferences, electrostatic interactions, and hydrophobic interactions.[33]

The first step is the formation of the secondary structure. This process is governed by the formation of intramolecular hydrogen bonds to from structures like the α-helices and the β-sheets.[33-34] The formation of this structures determines the next step in the folding process, the tertiary structure. The α-helices and β-sheets can have parts which are hydrophobic or hydrophilic and the orientation of these parts in relation to the surrounding *aqueous* environment controls the formation of the 3D structure of the protein.[35] Some tertiary structures interact with others to form the quaternary structure, in contrast to proteins with tertiary structure, proteins with quaternary structure consist of multiple polypeptide chains.

In contrast to proteins which consist in some cases of tens of thousands amino acids most peptides have less than a hundred. The synthesis of peptides longer than 70 amino acids pushes limits of the current possibilities.[36] The peptides in this thesis are not longer than seven amino acids and can therefore be defined as oligopeptides, which consist of an amino acid chain between 2 and 20 amino acids.

The use of peptides has advantages over the use of proteins. They have a much narrower sequence space, they also have a high structural programmability. Another benefit is their versatile functionality, their easy availability and a high-cost efficacy.[37-42] In contrast to synthetic polymers they are also capable of a folding response and can therefore be better controlled with external stimuli like the pH value.[42]

Peptides are a widely used component in biomedical chemistry. They are investigated for their application as therapeutics, due to their good biocompatibility, low immunogenicity, and biodegradability. Examples of peptide applications as potential therapeutics are fibrils in tissue engineering, peptides to combat cardiovascular diseases, or as drug delivery system for cancer

therapeutics.[42-44] They are even studied in terms of their use as in electronic applications for example as semiconductors or as piezoelectric elements.[45-46]

2.1.1.2. Amino Acids

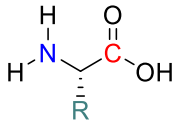

Figure 3: Amino acid with marked N-terminus (blue), C-terminus (red) and the residue (green).

Amino acids are the building blocks of peptides and proteins. The first amino acids were discovered in the time span from the early 19th century to the first half of the 20th century. [47] Amino acids have a common scaffold with a so called N-terminus (-NH_2) on one end and the C-terminus (-COOH) on the other end of the molecule. The part giving every amino acid its individual behavior is its residue. With more than 500 known natural amino acids, their variety is sheer breathtaking.[48] But only a few are part of the protein building process, the so called proteinogenic amino acids, which are shown in Error! Reference source not found..

Table 1: Table of proteinogenic amino acids.

Arginine (R)	Histidine (H)	Lysine (K)	Aspartic acid (D)	Glutamic acid (E)	Serine (S)	Threonine (T)
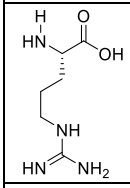	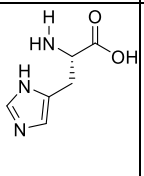	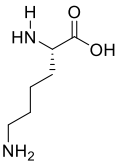	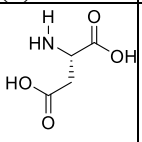	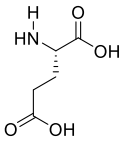	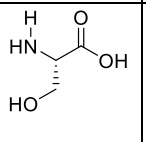	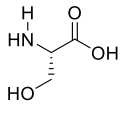
Asparagine (N)	Glutamine (Q)	Cysteine (C)	Selenocysteine (U)	Glycine (G)	Proline (P)	Alanine (A)
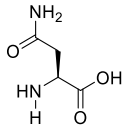	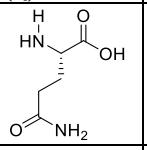	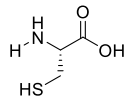	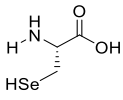	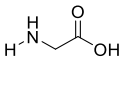	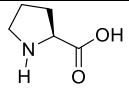	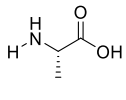
Valine (V)	Isoleucine (I)	Leucine (L)	Methionine (M)	Phenylalanine (F)	Tyrosine(Y)	Tryptophan(W)
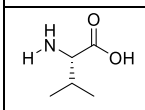	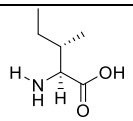	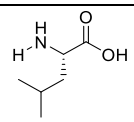	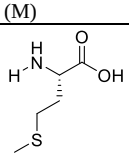	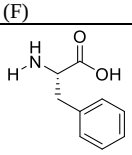	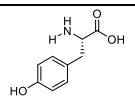	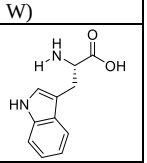

To fathom the utility and possibility of peptides a knowledge of the amino acids and their interaction is necessary. One possible way to categorize amino acids is by the chemical functionality of their R-group. The three categories are hydrophobic, hydrophilic or "other" amino acid. The hydrophobic amino acids are further separated into aliphatic residues (A, I, L, M, V) and aromatic residues (F, W, Y). The aliphatic groups are interesting for creating a hydrophobic environment with their hydrocarbon R-groups, which enable the peptide to self-assembly *via* hydrophobic and van der Waals interactions. The aromatic residues allow the peptide in which they are incorporated to participate in π-π-stacking. This describes the process of overlapping conjugated π-electron-systems. The opposing category, the hydrophilic amino acids are further categorized into the charged and uncharged amino acids. The charged amino acids can be classified as positively charged (H, K, R) and negatively charged (D, E). These charged amino acids can be used to support the self-assembly of the peptides by engineering attracting charge interactions between opposing charges. They can also hinder the self-assembling by engineering repulsive charge interactions using amino acids with the same polarity of charge. The subcategory of hydrophilic uncharged amino acids is comprised of the ones with a hydroxyl group (S, T) and the ones with a carboxamide group (N, Q) in the residue. The last category contains the "other" amino acids. These are amino acids with an individual behavior which is not defined by being grouped in one of the above categories or show behavior not explained by the category they are in (C, G, H, P, and Y). Cysteine has an uncommon chemical reactivity due to the thiol side chain. This allows crosslinking *via* disulfide bridging and unique chemical modifications. Glycine is an excellent example of controlling peptide behavior by engineering of the sequence. It is the amino acid with the smallest steric hindrance and can therefore be used to produce more flexible peptide chains. The exact opposite in control over the architecture of peptide structures provides proline. It has a very rigid structure due to its distinctive cyclic form. Accordingly, the incorporation of proline into the sequence produces a more rigid peptide. The other amino acids in this category (H, and Y) give the peptide a higher chance for binding to metals or allowing for the possibility of enzymatic modification in their side chains. The amino acids form peptides through amid bonds shown in **Figure 4**. These peptides' structures are inherently dependent on the sequence of amino acids and the interaction of their R-groups. Then, these peptide chains can interact

with complementary peptide chains *via* intermolecular self-assembly. Hence, supramolecular structures are formed by the interacting of several peptide chains.[28]

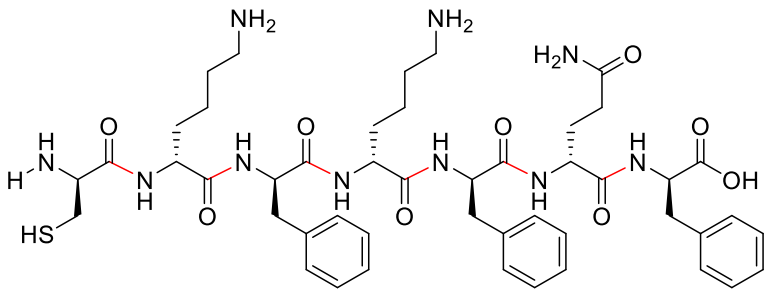

Figure 4: Peptide with the amino acid sequence CKFKFQF and the amide bonds (peptide bond) in red.

The self-assembly behavior and the resulting supramolecular structures depend on these processes and systems which can broadly be categorized as natural or non-natural. In the category of natural processes are systems involved in the self-assembling and folding of proteins. These natural processes can be observed and studied, leading to a broader and more in-depth understanding of these natural systems. Examples include β-sheets, turns, α-helices, coiled coils, and π-π interactions. Peptide amphiphiles (PA) are an example of a non-natural system.

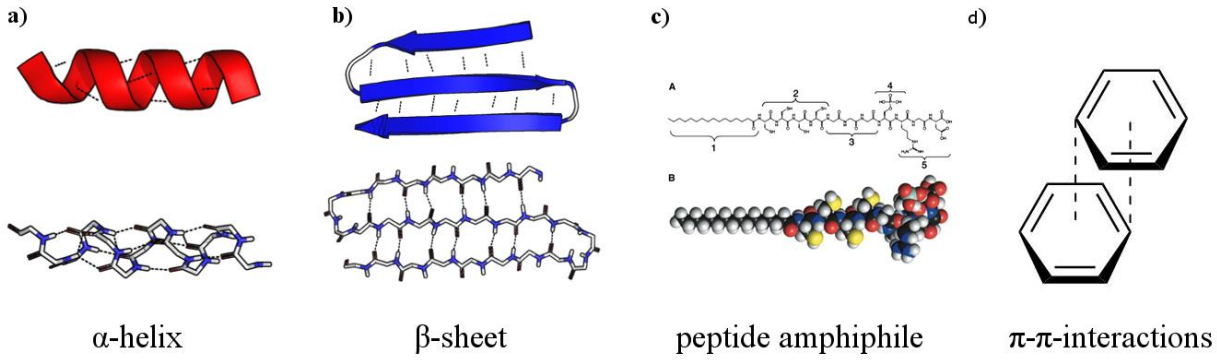

Figure 5: Samples of natural and non-natural systems and phenomes involved in the self-assembly of supramolecular structures. a) α-helix as cartoon (top) and as stick model (bottom).[49] b) β-sheet as cartoon (top) and as stick model (bottom); c) peptide amphiphiles as skeletal formula (top) and as space-fill model (bottom); d) skeletal formula of π-π-interactions between aromatic rings.

The β-sheet like interactions are of great importance in this work, hence they will be discussed in more detail. The first concept of β-sheets was proposed by W. Astbury and others in the 1930s but they could not describe an accurate structural model.[50-51] This was accomplished by L. Pauling and R. Corey in 1951.[52] A key feature of β-sheets is their ability to self-assemble into fibrous structures, this makes them so important for the control of self-assembling processes but also gives them a potentially destructive potential, demonstrated by their role in the amyloid diseases Alzheimer and Parkinson.[53] The first demonstration of the structural engineering possibilities offered by β-sheets was discovered by Zhang *et al*.[54] In their work, they created peptides which, upon the addition of salt, self-assembled into macroscopic membranes. The motif of the β-sheet has a pleated structure because of the side chains of the amino acids. The links between the peptide chains in a β-sheet can be parallel, antiparallel or a combination of both. In the parallel configuration, an amino acid in one chain forms hydrogen bonds with two different amino acids in the next peptide chain. It forms one hydrogen bond *via* its carbonyl-group with the amine-group of one amino acid in the next peptide chain and the second hydrogen bond *via* its amine-group with the carbonyl-group of the next amino acid in that chain. Consequently, every amino acid is bonded to two amino acids in the other peptide chain, and as a result, the atoms of the sheet are parallel to each other. In the antiparallel configuration the amine- and carbonyl-group of one amino acid form hydrogen bonds with the respective counterparts of one amino acid in the other chain. For this reason, the atoms are antiparallel to each other. In the third configurational option, there is a mixture of both parallel and antiparallel bonding.

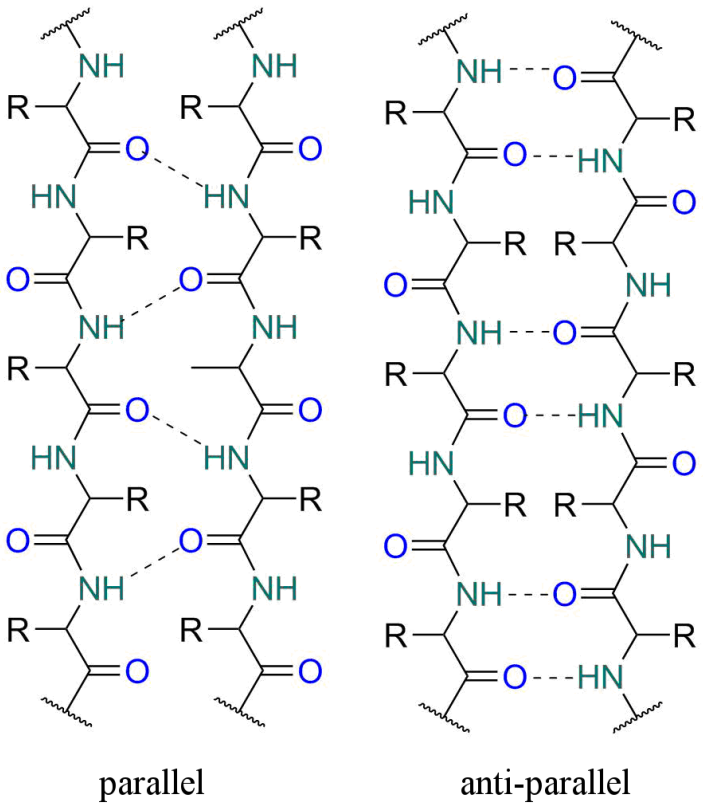

Figure 6: Comparison of parallel and anti-parallel β-sheet interaction.

A very common motif in *β*-sheets is a chain of amino acids with alternating hydrophobic and hydrophilic residues; therefore, the self-assembled *β*-sheets are facially amphiphilic. As a result in the emerging supramolecular structure, the *β*-sheets may combine to shelter the hydrophobic face from surrounding water.[41] *β*-Sheets can form different hierarchical structures depending on the number of *β*-sheets involved, the possibilities include tapes, ribbons fibrils, and fibers.[55] N. Boden *et al.* postulated that the peptide monomers can be regarded as rod-like structures which self-assemble into long twisted tapes, as shown in **Figure** 7. The twisting of tapes is a result of the chirality of the amino acids. Furthermore, the tapes have faces with two different chemical environments which results in a helical conformation. One face of the tapes should be less soluble, to overcome this chemical anisotropy the tapes form dimers. The dimers are the so-called ribbons, contrary to their building blocks the ribbons have no chemical difference in their faces. The structure of the ribbons forms a saddle curve, as a result, the ribbons are straight. The faces of the ribbons are equally attractive, and they can

stack on every side. Consequently, this stacking forms the fibrils which have a homogenous chemical environment at their edges. If the concentration of the monomer is high enough fibrils entwine themselves around each other to assemble into fibers.

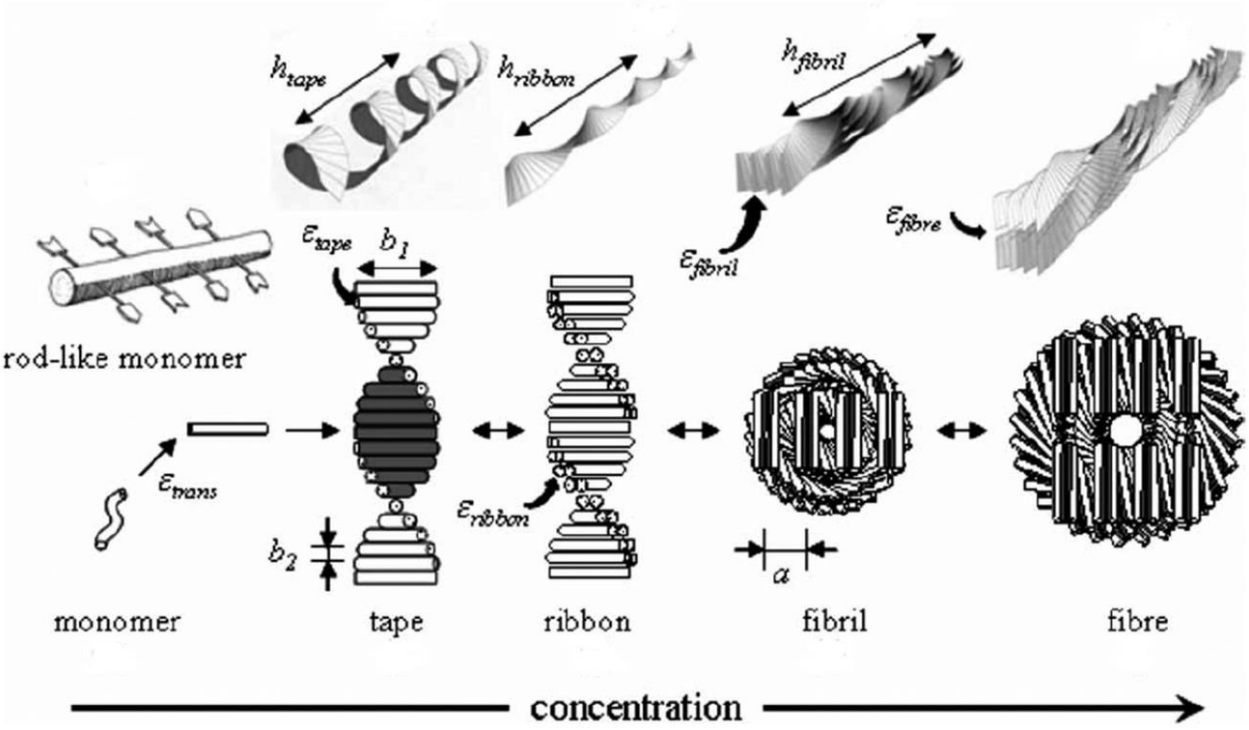

Figure 7 Theoretical model of concentration dependent hierarchical self-assembly from rod-like monomer.[55]

Lateral stacking of β-sheet like structures results in a width growth of the structure. This stacking follows a laminated pattern, which was categorized by Eisenberg *et al.* in eight types, shown in **Figure 8**.[56] This stacking interaction is dominated by the side chains of the amino acids, because it occurs along the direction of the side chains.[57] The width growth follows a hierarchical pattern, which is driven by the competition between so-called elastic energy penalty and the attraction of the neighboring sheets.[55] The elastic energy penalty describes the strain on the widening structure, caused by the attempt to decrease the exposure of the hydrophobic β-sheet to the surrounding water. If the elastic energy penalty becomes larger than the attraction between β-sheet the fibrils do not grow any wider.[57]

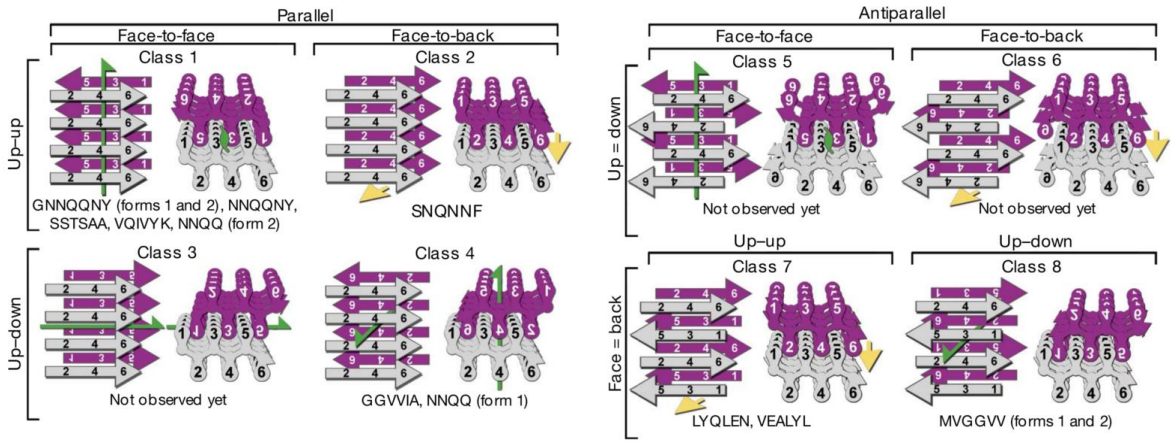

Figure 8: The eight classes of laminated stacking in β-sheet like structures classified by Eisenberg et al.[56]

The resulting width is detrimental to the resulting supramolecular structure formed by the peptide.[57] There is a critical value of width, if the structure gets broader the stable morphology of lamination with *β*-sheet structures is generally the α-helical ribbon, but if it is smaller the stable structure will be twisted fibrils.[58]

2.1.2. Controlled Supramolecular Structures

The main challenge of controlling self-assembling processes into supramolecular structures lies in the achieving of uniformity and reproducibility of these structures. Even minor differences in the balance between repulsive and attractive interactions can have major implications on the resulting structure, or their dynamics. There are many different factors which influence these attractive and repulsive forces and thereby the self-assembling process and its outcome, as amino acid sequence, solvents, pH-value, salt concentration and more. The obvious one is the sequence of amino acids in the peptide, which was discussed in **chapter 2.3**. Also, the group of D. A. Lauffenburger *et al.* investigated the influence of the variation of amino acids on the self-assembly of the peptide.[59] Another factor is the concentration of the peptide. This factor is represented by the critical concentration which is needed to assemble into supramolecular structures. This concentration can be lowered by increasing the side chain hydrophobicity in the peptide.[59] By the comparison of the peptides I_3K and L_3K, it was

discovered that the first forms β-sheet like structures while the later forms random coils, because of the higher hydrophobicity of isoleucine compared to lysine.[27]

2.1.2.1. Non-covalent Interactions and their Influence on the Peptide Self-Assembly.

To better understand these parameter and their impact on the self-assembly behavior of the investigated peptides, the underlying non-covalent interactions and their synergism and cooperativity will be described in more detail.[60] Self-assembled systems often have a careful balance between attractive and repulsive forces giving rise to a plethora of different structures. The hierarchical process and the resulting nanostructures change when this balance is disturbed.[58] The attractive forces are the hydrogen bonds, the hydrophobic, the π-π-, the van der Waals and the coulomb interactions. On the repulsive side are the coulomb repulsion, steric hindrance, and the solvation.

Hydrogen Bonds

Hydrogen bonds are formed by a hydrogen atom and a strongly electronegative atom like oxygen or nitrogen. In the peptide this occurs at the peptide backbone and the carboxyl and amino groups in the residues.[61] The formation of the hydrogen bonds is responsible for the formation of secondary structures as β-sheet. This non-covalent interaction is probably the most important one for peptide self-assembly, as its controls with high selectivity and directionality the 3D structure of the peptide self-assembly.[61]

π-π Stacking

The π-π stacking is important for the self-assembling behavior of peptides containing conjugated electron systems. Phenylalanine with its aromatic ring is a good example of introducing π-π stacking interactions into a peptide. The π-π stacking induces a directional growth of the supramolecular structure.[61] This π-π interactions are also tolerant towards water because of the bad solubility of the aromatic groups.[62]

Electrostatic Interactions

These interactions can work both attractive and repulsive. In the case of coulomb attraction between two opposite charges the formation of ion pairs influences the self-assembling. These interactions are stronger than hydrogen bonds, with ~500 kJ mol^{-1} against ~20 kJ mol^{-1}, but have nonetheless more specific effect on the self-assembly.[63] The opposing repulsive coulomb interaction between equivalent charges also effect the self-assembly of peptides and can hinder the formation of supramolecular structures. The electrostatic interactions are directly affected by the pH value, this makes it possible to incorporate pH responsiveness into the peptide.

Hydrophobic Interaction

These interactions are driven by the hydrophobic parts of the peptides which try to minimize their exposure to water by aggregating. This is a strong factor in the self-assembly of peptide amphiphiles, compared to peptides with aromatic groups where the π-π-interactions are the dominating forces.[61] If the self-assemble is salt-triggered the influence of the hydrophobic interactions is increased, because of the shielding of the charges through the salt ions.[64]

Van der Waals Interactions

The van der Waals interactions are one of the weaker attractive forces that play a role in the self-assembling of peptides. They are highly dependent on the number of aliphatic parts within the peptide.[61] With ~5 kJ mol^{-1} they are weaker than the hydrogen bond and therefore it is only in a few cases a predominant force in the self-assembling process.[65]

Steric Hindrance

The steric hindrance results from the incapability of molecules to come close enough together to interact. Therefore, it is a clear antagonist to the attractive force described in this chapter.

2.1.2.2. Solvent

The peptide is seldom solved in the solvent it will self-assemble in. The established practice is to solve the peptide in a so-called good solvent, which easily dissolves it. After this a portion of this stock solution is dilution into the so-called bad solvent. The solvent in which the supramolecular structures can equilibrate in.[66] In most cases the good solvent is an organic solvent like DMSO and the bad solvent is some kind of water. It is this mixture of solvents that allows a manipulation of the self-assembling process. The point at which the good solvent has a high enough proportion of the mixture that the self-assembled structures start to be molecularly dissolved, is the critical good/poor solvent ratio.[67] The fundamental role of the solvent mixture is visible in the effect it has on the stability of the supramolecular structures and even their architecture can be controlled with this ratio.[68] In **Figure 9** the results of different ratios of good/bad solvent investigated by S. I. Stupp *et al.* are shown. The SEM images are taken after the peptide amphiphiles were freeze dried and are therefore not representative for the structure in solution, but they can give an idea of the effect of solvent ratio on the self-assembling behavior. The good solvent in this experiment was HFIP and the bad one water. PA1 (palmitoyl-V3A3E3-NH2) with 10% HFIP yields fibrous structures after freeze drying, with 50% and 100% of the formed structures are ill defined. On the other hand PA2 (palmitoyl-E(ALAE)3W) forms fibrous structures at 10% and 50%, given ill-defined ones, while in 100% HFIP it forms flak like structures.[69]

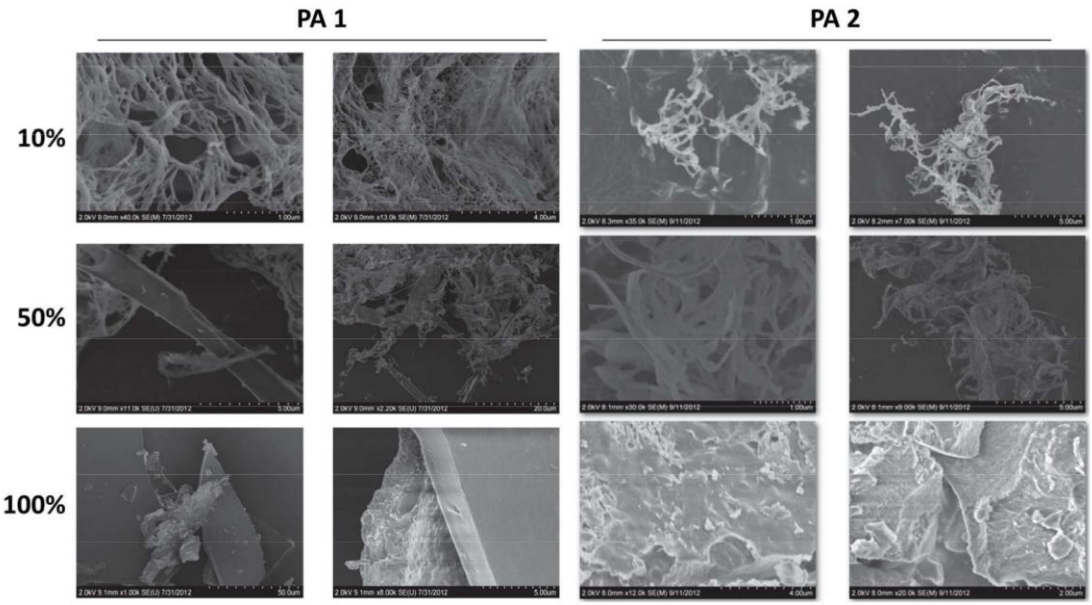

Figure 9: SEM images of different ratios of good/poor solvent. The figures shows SEM images after freeze drying of the peptide amphiphiles PA1 (palmitoyl-V3A3E3-NH2) and PA2 (palmitoyl-E(ALAE)3W). The peptide amphiphiles were solved in 3 different ratios of good/bad solvent, in this case HFIP/water. The portion of HFIP increases in the mixtures from 10%, to 50% and in the last one to 100%.[69]

2.1.2.3. pH Value

The pH value is one of the easier levers that can be used to change the conformation of the self-assembled structures. The change in the pH value has a direct influence on the charged amino acids in the peptide. Therefore, it is possible to implement a pH switch into the design of a peptide sequence. In the case of β-sheets, for which the charge interaction plays an essential role in the hierarchical self-assembly processes, shifts in the pH value can have huge impacts. β-Sheets, for example, form hydrogen bonds and maintained by hydrophobic and electrostatic interactions.[70-72] It could be shown that in some peptide sequences a decline in electrostatic interaction facilitates the self-assembly into fibers.[59, 73] In the work of S. Zhang and P. Chen, the peptide EAK10-IV showed different self-assembly behaviors under changed pH value. At a neutral pH (~7) it self-assembles into a globular architecture, is the pH lowered (pH value of 4) or elevated (pH value of 11) it self-assembles into fibrillar structures. They postulated that the reduction of the electrostatic interactions by neutralization of the ionizable side chains of the amino acids (E, K), which are the reason for the bending of the chains (globular structure), results in the straight peptide molecules from fibrils.[74] In **Figure 10** the

results of the group of V. Subramaniam *et al.* are shown.[75] They investigated the self-assemble behavior of the protein α-synuclein under different pH conditions. They could show that the aggregation at pH value 7.0 and 6.0 resulted in fibrillar structure. At the lower pH value the aggregation was ill defined. These results depict clearly the influence the pH value of the surrounding solution can have on the self-assembling behavior.

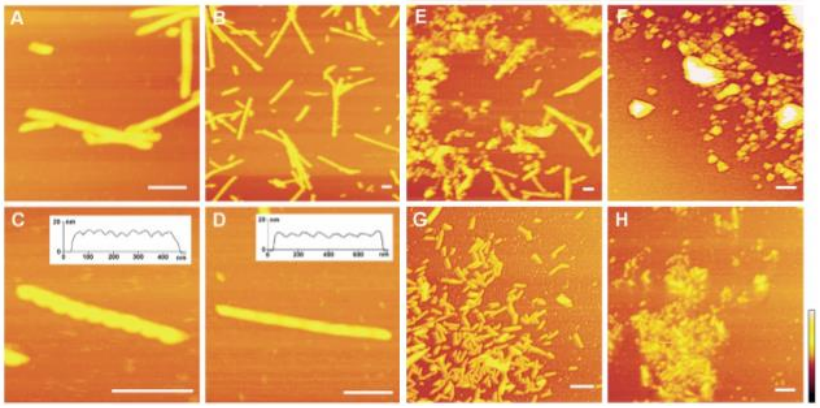

Figure 10: AFM images of a-synuclein aggregates, on the effect of pH value on the self-assembling behavior of peptides.[75] A and H at a pH value of 7.0, B – D at a pH value of 6.0, E at a pH value of 5.0, and F and G at a pH value of 4.0.

2.1.2.4. Salt Concentration

The salt concentration is an interesting parameter in the self-assembly of peptides, because of the implication for *in vivo* applications. The main effect of ionic strength in the solution on the peptide self-assembly seems to be the shielding of the peptide charges resulting in a reduction of repulsive interactions.[76] In their work, M. Lopez de la Paz *et al*. investigated the influence of different NaCl concentrations on the self-assembly of β-sheets forming peptide sequences.[77] The concentration was between 0 M and 1.0 M NaCl. At low concentrations up to 0.1 M NaCl, an increase of fibrillation with the increase in ionic strength was observed, this change was attributed to the reduction in charge-repulsion effects. At higher salt concentration only short fibrils and amorphous aggregates were formed. The group of P. Chen *et al*. observed a similar behavior. They could define a critical NaCl concentration for their system under which the equivalent radius of their peptide fibrils with the salt concentration increased, but the opposite happened when the NaCl concentration was over the critical concentration.[76]

2.1.2.5. Formation Pathway Dependence

In their work, F. Tantakitti *et al.* showed the possibility to trap thermodynamic metastable supramolecular structures depending on the pathway of the self-assembling.[78] They used the amphiphilic peptide $V_3A_3K_3$-R which has two pathway dependent supramolecular architectures. The thermodynamically stable configuration assembles into long bundled fiber and the metastable one into short monodisperse fibers. The conditions in both pathways were the same, namely the peptide concentration, the pH value or others. But the positions of some of the preparation steps in the pathway are swapped which leads to a different outcome, as shown in **Figure 11**. If the *β*-sheets are switched off by dilution and the solution is annealed, the thermodynamically favored product forms, *i.e.* monodisperse short fibers. Addition of salt produces the metastable short fibers with *β*-sheets. If the solution is fist annealed and afterwards diluted, the kinetically trapped product is formed, long *β*-sheets containing fibers. Addition of salt has no effect within this pathway.

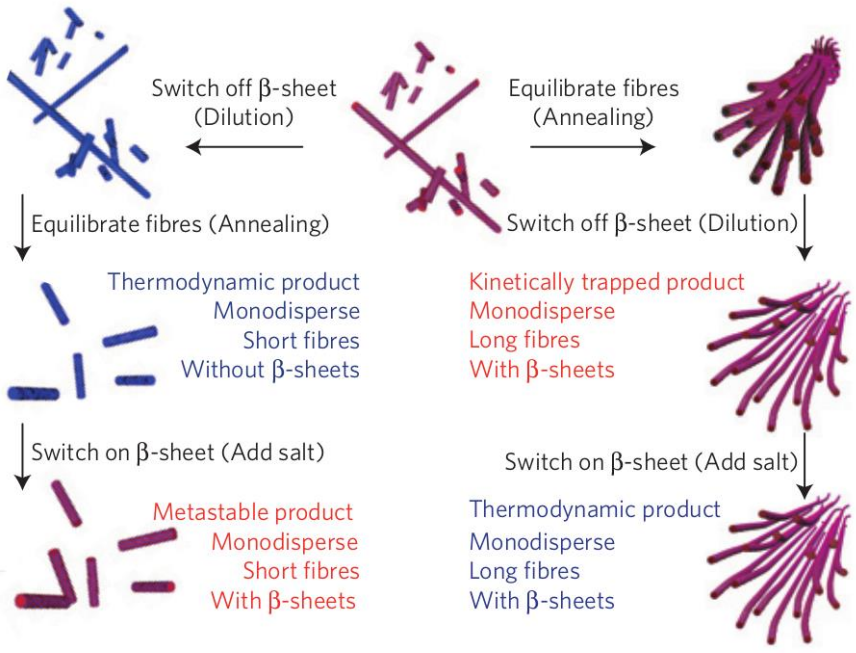

Figure 11: Two preparation pathways for the peptide amphiphile $V_3A_3K_3$-R with different outcomes for the supramolecular morphology. The left one shows the switching of, of the β-sheets with dilution. Followed by the equilibrating of the assemblies (annealing), which results in the thermodynamically favored product, short monodisperse fibers. In the last step, salt is added to switch the β-sheets on again. This produces short metastable fibers with internal β-sheets structure. In the other pathway the fibers ate first equilibrated by annealing and then diluted. This results in kinetically trapped fibers with internal β-sheet structure. The addition of salts has no influence on the supramolecular structure. The fibers with internal β-sheet structure are in red and the ones with internal coil-like structure in blue.[78]

In **Figure 12** the corresponding energy landscape of two different peptide systems are shown. In the system with the low charge repulsion, high salt concentration, the long β-sheet fibers are the thermodynamically stable product. In the system with high charge repulsion, low salt concentration, the short coil-like fibers. It depicts the energy barriers which trap the morphologies of the peptide assembly. In the example of the dilution before the annealing, the annealing produces the metastable product of the high charge energy landscape, the short fibers. With the addition of the salt the charges are shielded and the charge repulsion decreases. The β-sheet containing short fibers are formed but now they are trapped and don't transform into the long variant.

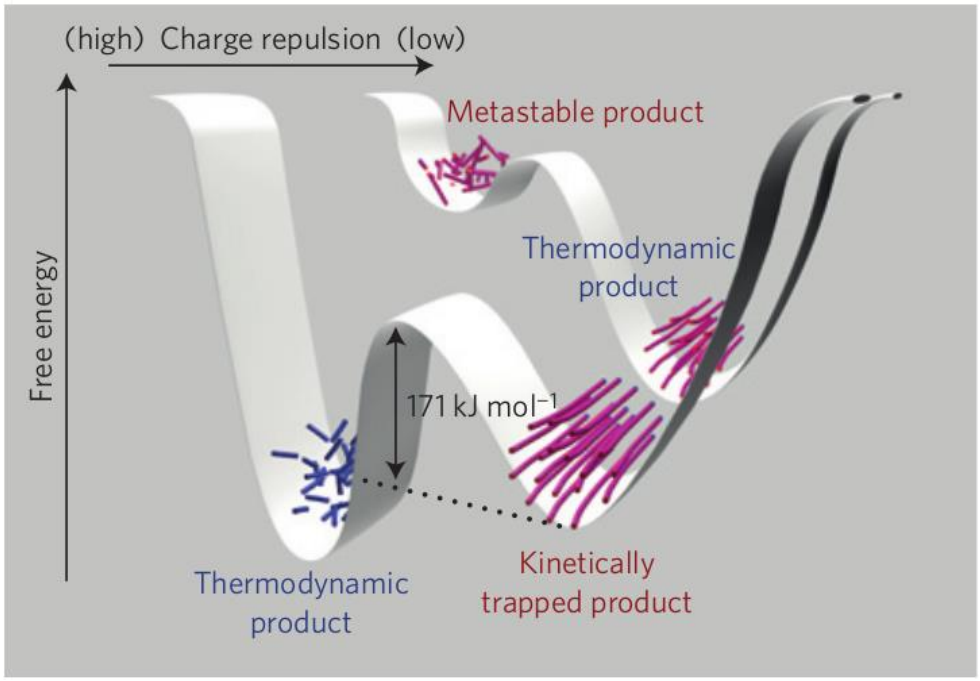

Figure 12: Energy landscape of different supramolecular structures. With the representation for high charge repulsion at the front and the representation of the low charge repulsion in the back of the picture. At high charge repulsion the kinetically trapped and the thermodynamically favored product were found and low charge repulsion only the long fibers with β-sheet are found. The fibers with internal β-sheet structure are in red and the ones with internal coil-like structure in blue[78]

The effect of this change is enormous, the stable configuration is able to promote biological cell adhesion and survival. The metastable configuration, on the other hand, hindered cell adhesion and can lead to cell death.

S. I. Stupp *et al.* investigated the idea that entrapped configurations could be freed if the temperature was elevated. The fast dynamics of this process should allow the monomer to equilibrate.[69] They compared three samples of their peptide (PA1), alternating different solvent mixtures (water with 10%, 15% or 20% HFIP). The samples were prepared at 50 °C, cooled to 0 °C and then heated with a ramp of 1 °C/min until they reached a temperature of 50 °C. In 10% HFIP the peptides self-assembled into *β*-sheets at 50 °C and showed no change after that. A similar behavior could be observed with the peptides in 20% HFIP, they self-assembled into coiled coils and showed throughout the temperature annealing little change in their morphology. The peptides in 15% HFIP, on the other hand, displayed rather different behavior. At 50 °C, they self-assembled into coiled coils. But when cooled, at 40 °C they started to switch to the *β*-sheet structure and even after the temperature annealing finished they kept the *β*-sheet configuration. These examples show how temperature annealing enables trapping the peptide in metastable configuration, which they would not self-assemble into otherwise.

2.1.2.6. Polymer Corona

The synthesis of peptide-polymer conjugates has two potential goals, either to create a system in which peptide and polymer profit from synergetic behavior or to overcome intrinsic drawbacks of the individual components.[13] The polymer can provide the peptide with higher stability against pH, temperature or give it the capability to respond to such parameters in the case of responsive polymers.[14-15] L. Noirez *et al.* described in their work that the peptide they PEGylated still self-assembled into *β*-sheets and with high enough concentration into fibrils. Further, they showed that the fibril length could be shortened when the PEG component was increased.[14]

2.1.2.7. Oxidation

The oxidation of the residue of one of the peptide chains, to influence the self-assembling behavior, is a more demanding parameter. Its effect is highly dependable on the availability of a residue which can be selectively oxidized, like methionine. In this case it is the oxidation of the methionine amino acid with H_2O_2. The group of P. Besenius *et al*. used this process to regulate the supramolecular polymerization of their dendritic peptide.[79] The methionine residue is changed during the oxidation from a thioether-group into a sulfoxide-group. This increases the hydrophilicity of the peptide, which interferes with the supramolecular polymerization.

2.2. Reversible-Deactivation Radical olymerization (RDRP)

Reversible-deactivation radical polymerization (RDRP), also known as controlled radical polymerization or living free-radical polymerization, is the cornerstone of modern polymerization in material and medical science applications of radical polymerizations. There are different approaches for RDRP and in this work two of them, namely, ATRP and RAFT will be described in more detail in the following sections. First, the common attributes of an RDRP will be discussed. To understand the need for the RDRPs, knowledge about the shortcomings of the free radical polymerization (FRP) and its upsides are necessary. Free radical polymerization is the most used polymerization method in industrious processes, because of its high tolerance towards water, oxygen, and impurities.[80] In the big scale of industrial chemistry these factors are much more important than the drawbacks of poor dispersity control, incapability of block copolymerization and the lack of control over the macromolecular architecture.[80] Free radical polymerization is classified as a chain reaction. The mechanism of the FRP is the textbook example to explain the chain reactions. The reaction is divided into 3 steps, the initiation, the propagation, and the termination. The first step is the initiation in which the radical initiator is activated, and one or two radicals are produced. The so produced radicals can then react with monomer molecules and form the first active monomer radicals. In the next step this can add new monomer molecules to them and so the chain starts to grow. This propagation has two possible ways to end. The first one is the

termination in which the radical activity is terminated, and the radical reaction stops. The second possibility is the chain transfer reaction in which the radical transfers its activity to another molecule, be it a monomer, a solvent molecule or any other in the reaction. This does not stop the radical reaction but makes any meaningful control over the outcome impossible. In the following **Scheme 1** some the described steps a schematically depict.

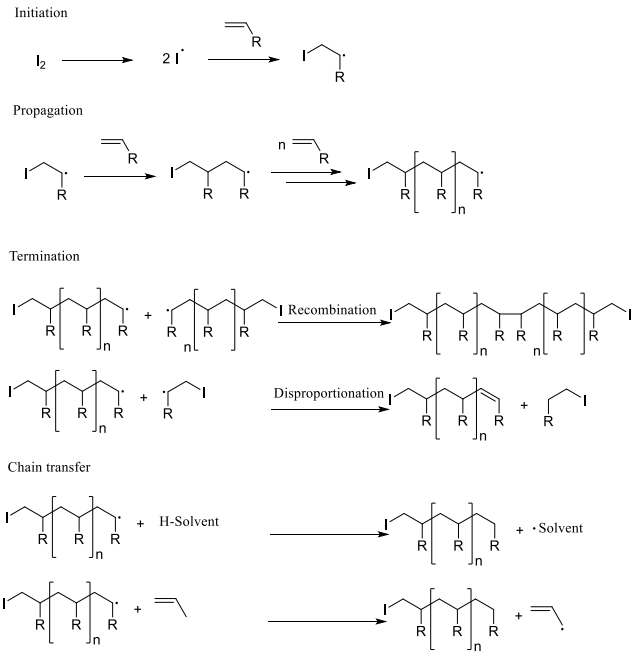

Scheme 1: Steps in the FRP process.

These different terminations and chain transfer reactions make any meaningful control of the reaction, for example dispersity- or architecture-control, elusive. The solution to overcome this problem was inspired by the anionic living polymerization (ALP). ALP is a truly living polymerization and makes the synthetization of polymers with precise length and dispersity possible. It is the gold standard for polymerizations. The ALP was discovered by Szwarc *et al.* in 1956.[81-82]

In radical polymerization, a pseudo-living polymerization could be achieved with the discovery of RDRP reactions such as the NMP reaction.[83-84] These reactions bypass the problems of the free radical polymerization with the persistent radical effect (PRE). The effect was first described by Bachmann and Wiselogel in 1936. They discovered the existence of

persistent radicals, which do not undergo termination reactions. In the RDRP these persistent radicals make a controlled “living” radical polymerization possible.[85]

The PRE means the formation of one radical that is excessively more stable (Y) than the other formed radicals (R). The stable radical (Y) will not be terminated in self-coupling and only react in cross-coupling with the less stable radical (R). This, on the other hand, will react with itself and over time the concentration of R becomes smaller and smaller. This leads to a higher and higher concentration of Y until the most likely reaction product will be the coupled form (R-Y).[86]

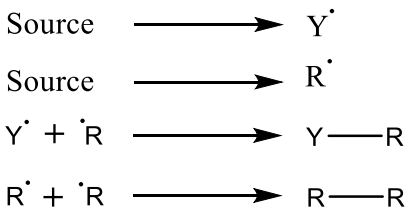

Scheme 2: Schematic representation of the persistent radical effect.[86]

In the NMP, for example, the nitroxide species is the more stable radical and over time the concentration of this species will increase until the other radical, mostly a carbon species can only react with the nitroxide radical. The so formed cross-coupling product will be reversible with the equilibrium on the side of the coupled species. With time most of the radicals will be in the coupled form and any “released” radical will most likely react with a monomer and not in a termination reaction. But this process is not a complete one and there will always be a small number of termination reactions in the NMP and other RDRP reactions, because of this they cannot be called living reactions.

2.2.1. Atom-Transfer Radical Polymerization (ATRP)

Atom-transfer radical polymerization (ATRP) is an RDRP like the NMP and was discovered independently by the group of M. Sawamoto *et al.* and by J. S. Wang and K. Matyjaszewski.[87-88] ATRP has the advantages of a simple experimental setup combined with the easy commercial availability of most reactants.[17] The propagating radical (P) is created in

an inner sphere electron transfer between an alkyl haloalkane and a transition metal complex.[89] The persistent radical in the case of the ATRP is the metal complex formed in this reaction.

The ATRP process can be used to polymerize from peptide macroinitiators.[90] It is even possible to synthesize a wide range of polymer architectures.[91] But for all its virtues the ATRP has a few drawbacks when used to synthesize peptide-polymer conjugates. One drawback is the incapability to prevent interactions between the copper catalyst and the peptide[92] Another complication arises because some of the amino acid residues display inherent ligating properties and allow the peptide to function as a multidentate ligand for the copper ions[93]

2.2.2. Reversible Addition-Fragmentation Chain Transfer (RAFT)

The first reversible addition-fragmentation chain transfer (RAFT) polymerization as it is understood today was carried out in 1998 by the group of Rizzardo *et al.* in the CSIRO Institute.[94]

Since then RAFT polymerization had an enormous impact, far beyond the boundaries of polymer science. The fast pace of new scientific discoveries is evident in the repeated updating of the review about RAFT polymerization, from the group of G. Moad, E. Rizzardo, and S.H. Thang.[95-97] RAFT polymerization allows the synthesis of complex architectures of polymers like stars, multiblock copolymers and many others.[98-100] It can be used in modern fields like green chemistry or impending industrial applications.[101-102] More in line with this thesis are the developments in self-assembling polymers or bioapplications.[103-105] The mechanism of the RAFT polymerization, is shown in **Scheme 3**. In the RAFT polymerization the key role is played by the chain transfer agent (CTA).[106]

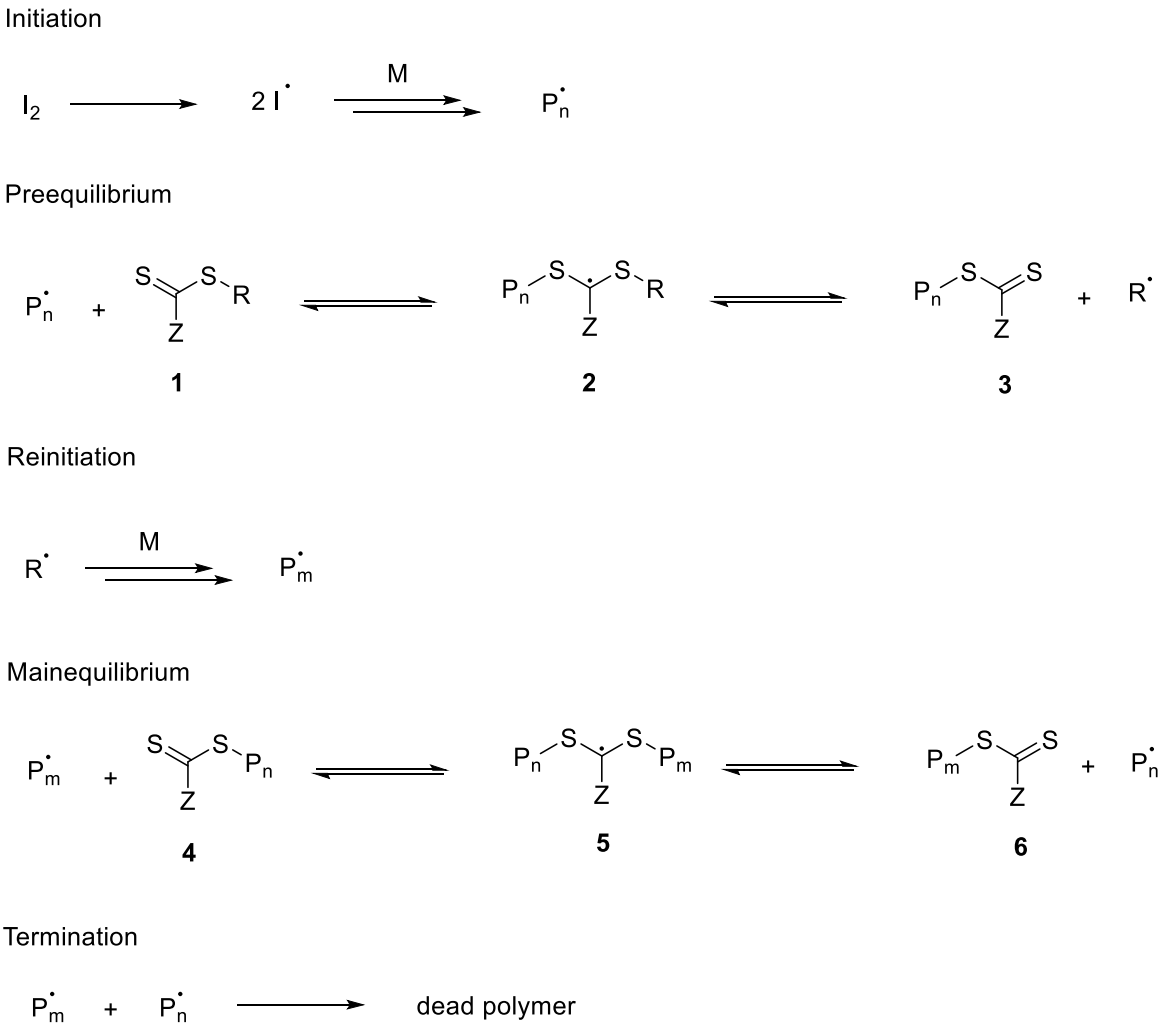

Scheme 3: Mechanism of the RAFT polymerization.

The initiation step is the same as in conventional FRP. But in the propagation step, the growing radical chain will react with a thiocarbonylthio compound, at this stage this is the CTA. This forms the first addition fragmentation equilibrium when the fragmentation occurs a polymeric thiocarbonylthio compound is formed and a new radical created. With inactive monomer, this radical can form a new growing polymer chain. This polymer chain can then react in an addition-fragmentation equilibrium. This equilibrium between growing polymer chains and the inactive polymeric thiocarbonylthio compounds produces an equal probability for each individual chain to grow at the same rate. This results in a low dispersity of the RAFT polymerization

2.3. Origin of the Sequence

The foundation of the work in this thesis was provided by S. Sieste and other members of the group of T. Weil at the University of Ulm. She developed a peptide library to investigate the connection between molecular and supramolecular structure with the potential to enhance the transduction of viruses. As part of that study, the peptide sequence CKFKFQF was identified as having a strong ability to form one-dimensional nanofibers in solution and strongly enhance the transduction of viruses *in vitro*. In contrast, the removal of the cysteine group resulted in a peptide, KFKFQF that has a poor ability to form fibers and does not significantly enhance viral transduction. It is hypothesized that the cysteine group improves the formation of β-sheets and therefore support the self-assembly into fibrils, which in turn are necessary for efficient transduction.

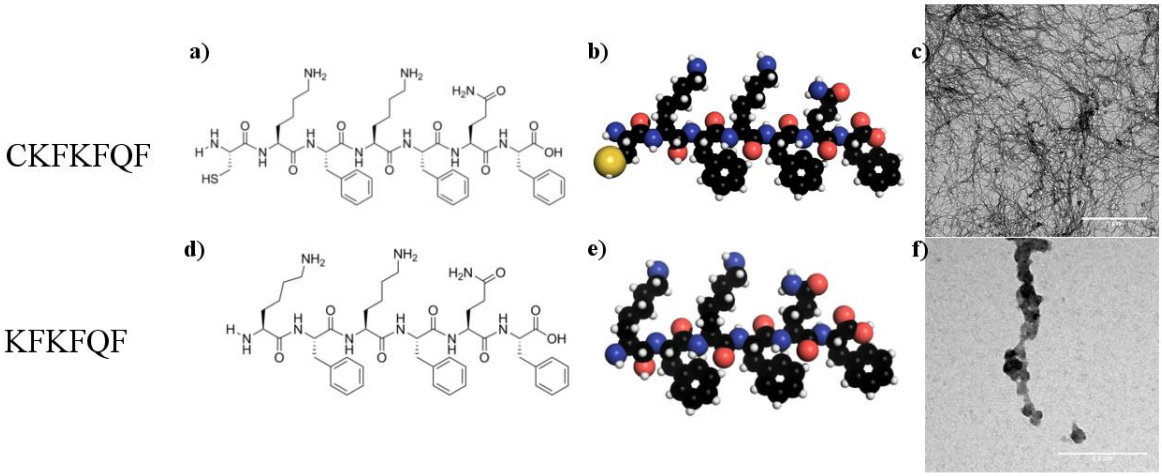

Figure 13: A) chemical structure, space fill model and TEM image (sample solved in DMSO, then transferred to PBS puffer at a pH of 7.4) of the peptide CKFKFQF (from left to right); B) chemical structure, space fill model and TEM image (sample solved in DMSO, then transferred to PBS puffer at a pH of 7.4) of the peptide KFKFQF(from left to right).

2.4. SPPS Theory

One of the standard routes of the synthesis of peptide chains is the solid-phase peptide synthesis (SPPS) developed by R. B. Merrifield in 1963.[107] In this approach, a solid resin bead is used as a solid substrate for the synthesis. The resin has a cleavable linker, this linker has an amine ($-NH_2$) and a hydroxyl group (H_2O) at the terminus. On this fictional group the peptides can be coupled step wise. The method has the main upside, that thanks to the protecting group (Fmoc or Boc) great excesses of the added amino acid can be used, which results in a near completed coupling reaction. The danger of multiple couplings on the same chain is inhibited by the protecting groups. Another big upside of the SPPS is the simple separation of the reactants and product. This is simply achieved by washing, because the product is fixated on the solid base. As a result after every step, it is possible to wash the excess reagent and byproducts away.[36] This makes the SPPS ideal for automatization and the production of many different peptide chains quite effortless.

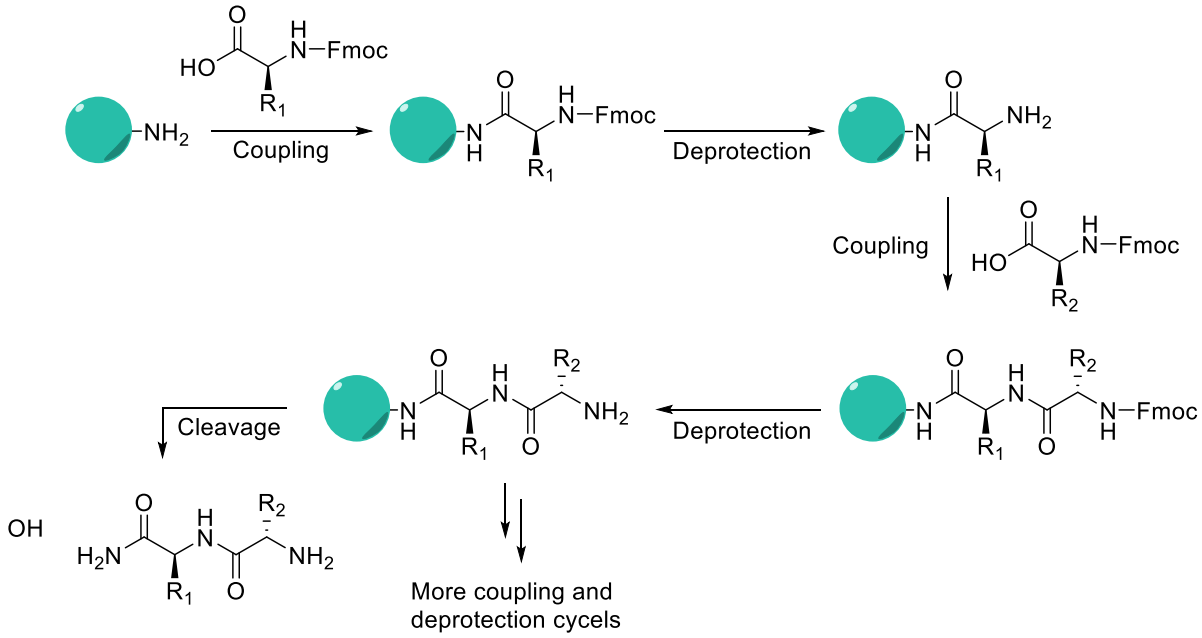

Scheme 4: Schematic depiction of the SPPS cycle.

The mechanism of SPPS can be divided into different steps. In the first step the amino acid is coupled to the resin bead. In the second step the inactivated amino acid on the resin is deprotected. There a two common routes of protection in SPPS the Fmoc- and the Boc-route, because the SPPS used in this thesis worked with the Fmoc-route, it is the one depicted in Error! Reference source not found.. The third step is the coupling step. In this step, the next amino acid is coupled to the N-terminus of the first amino acid. After this, the second and third step are repeated until the desired peptide chain is complete. Then in the final step, the peptide is cleaved from the resin support and the SPPS is finished.

3. Results and Discussion

3.1. Peptides

The peptides used in the self-assembling study are the result of the work of S. Sieste. The first peptide synthesized was the CKFKFQF but its solubility in aqueous media was rather low. This led to the loss of significant amounts of material during the filtration step with the syringe filters (0.2 µm), prior to injection into the HPLC. In order to improve the solubility of the peptide, different sequences that either replaced the cysteine with a methionine or completely removed it, were tested. In the previous work by S. Sieste, the presence of a terminal cysteine was found to strongly enhance fiber formation. These peptide sequences had the same meager yield after injection into the HPLC. In another attempt to increase the yield the use of different syringe filter was explored. But change from PTFE (0.2 µm) to PES (0.2 µm) syringe filter made no difference to the poor yields. Only when the filtration step was replaced by a centrifugation step, to sediment larger aggregates, the yields of pure peptide increased to values around 73%.

3.1.1. CKFKFQF

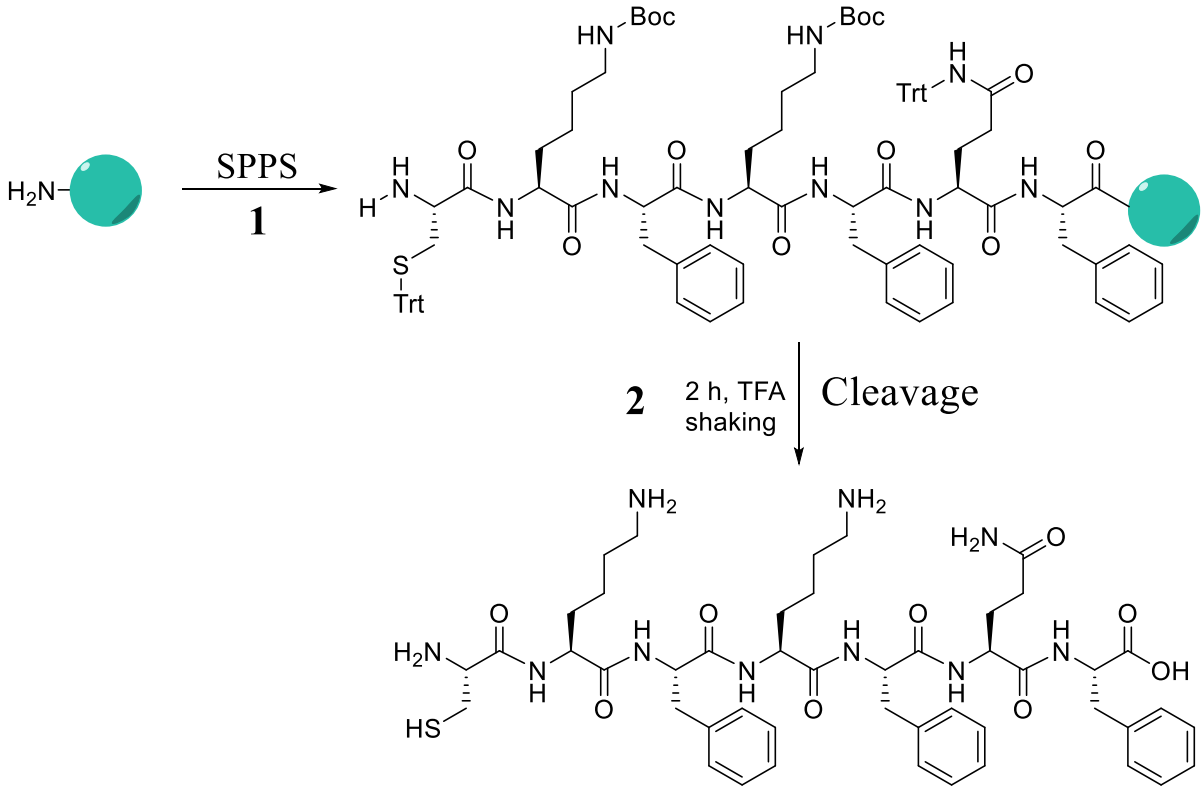

Scheme 5: The synthetic pathway to the peptide CKFKFQF. The 1st step of the reaction is the SPPS. The 2nd step is the cleavage of the peptide from the solid base with TFA.

For the synthesis of CKFKFQF the SPPS method was chosen, it facilitates a fast synthesis and an easy separating of the peptide from excess reactants. For this reason an excess of the different amino acids could be used to assure a high yield of the product. In the next step the peptide was cleaved form the resin and deprotected at the same time. After freeze drying peptide was then purified with the preparative HPLC.

The first reparations of this reaction pathway yielded a meager yield (theoretical yield of 95 mg, achieved yield of 5 mg). This is a result of the good aggregation behavior of the peptide. The cysteine residue in the peptide can form disulfide bridges and therefore enhance the self-assemble of the peptide. The eluent in the preparative HPLC was predominantly water and therefore an ideal self-assembly medium for the peptide. The first evidence for this aggregation was the clogging of the syringe filters in the sample preparation of the peptides. It was

impossible to use one syringe filter for more than 1 mL of the peptide solution (7 mg/mL). The change from PTFE (0.2 µm) to PES (0.2 µm) syringe filter made no difference in the poor yields. The upscaling of the synthesis from 0.1 mmol to 0.5 mmol brought no significant improvement of the yields ether. The solution was letting go of the syringe filter step in the sample preparation and supplementing it with an extra step of centrifuging of the sample. This made it possible to achieve yields up to 73% of the theoretical yield.

The LC-trace in **Figure 14 b)** shows the success of the purification *via* the preparative HPLC. The corresponding mass spectrum in **Figure 14 c)** proves the success of the synthesis pathway in **Scheme 5**.

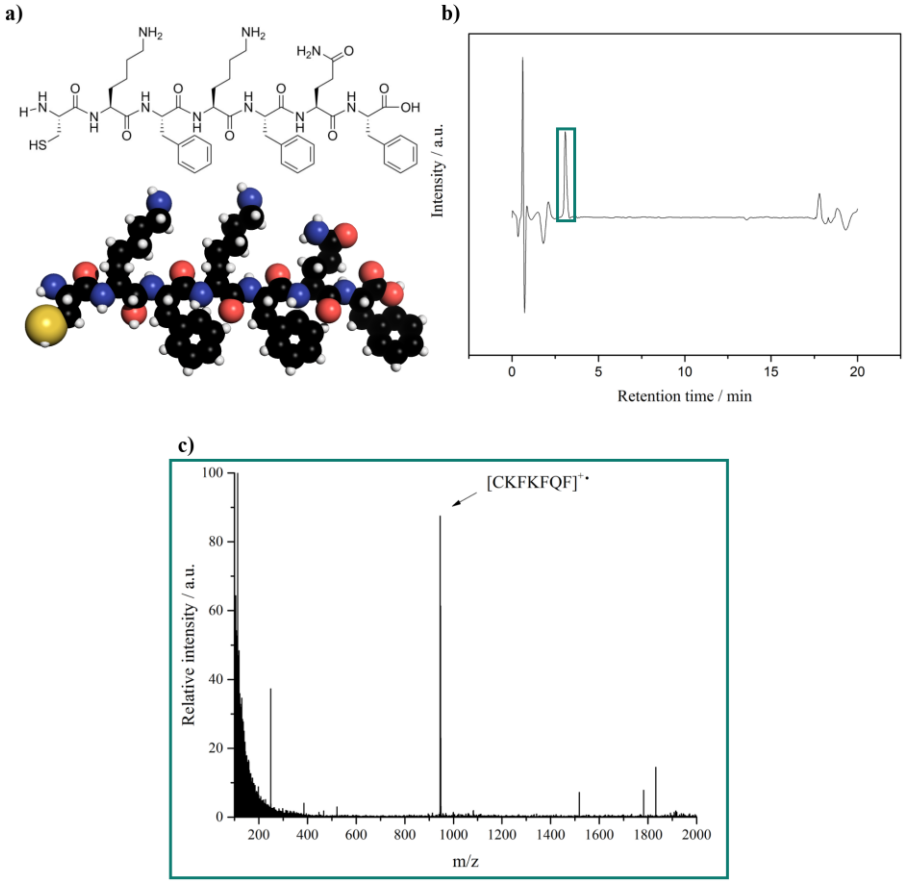

*Figure 14: a) On the top the skeletal formula of CKFKFQF and on the bottom the space-fill model. b) The LC-trace of the LC-MS measurement after the purification of the peptide with the preprative HPLC. c) the corresponding mass spectrum to the LC-trace in a). The corresponding data to the mass spectrum is in **Table 5** in the Appendix.*

3.1.2. KFKFQF

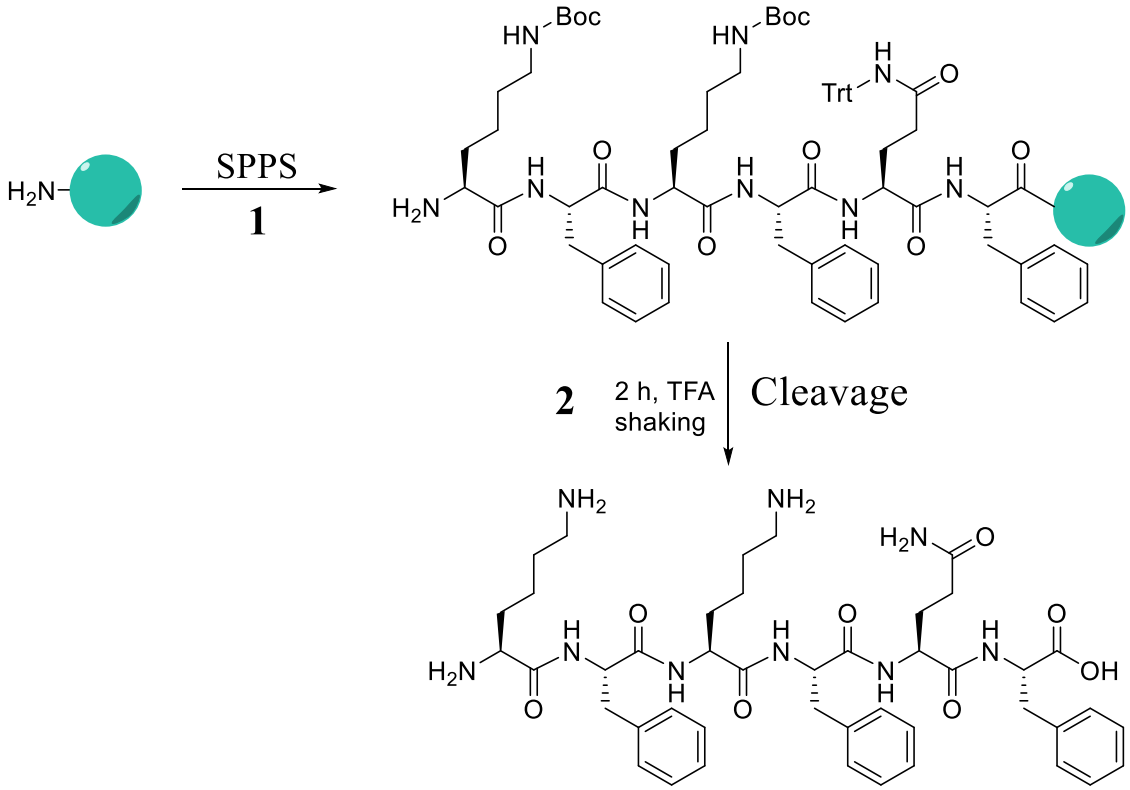

Scheme 6: The synthetic pathway to the peptide KFKFQF. The 1st step of the reaction is the SPPS. The 2nd step is the cleavage of the peptide from the solid base with TFA.

The sequence KFKFQF was also the result of S. Sieste work and was known to self-assemble, albeit not as strongly as CKFKFQF. The synthesis pathway for this peptide is similar to the one for CKFKFQF and shown in **Scheme 6**, of course with one amino acid coupling step less. This peptide also exhibited a very low yield in the single digits. This disproved the theory that the cysteine was responsible for the meager yield by aggregation *via* disulfide bonds. After the switch in sample preparation for the preparative HPLC the yield of KFKFQF also improved dramatically.

After the purification *via* preparative HPLC and freeze drying of the fractions containing product, samples were analyzed with the LCMS. The results are presented in **Figure 15 b)** and **c)**. The LC-trace proves the successful purification of the peptide and the mass spectrum confirms the synthesis of the KFKFQF peptide.

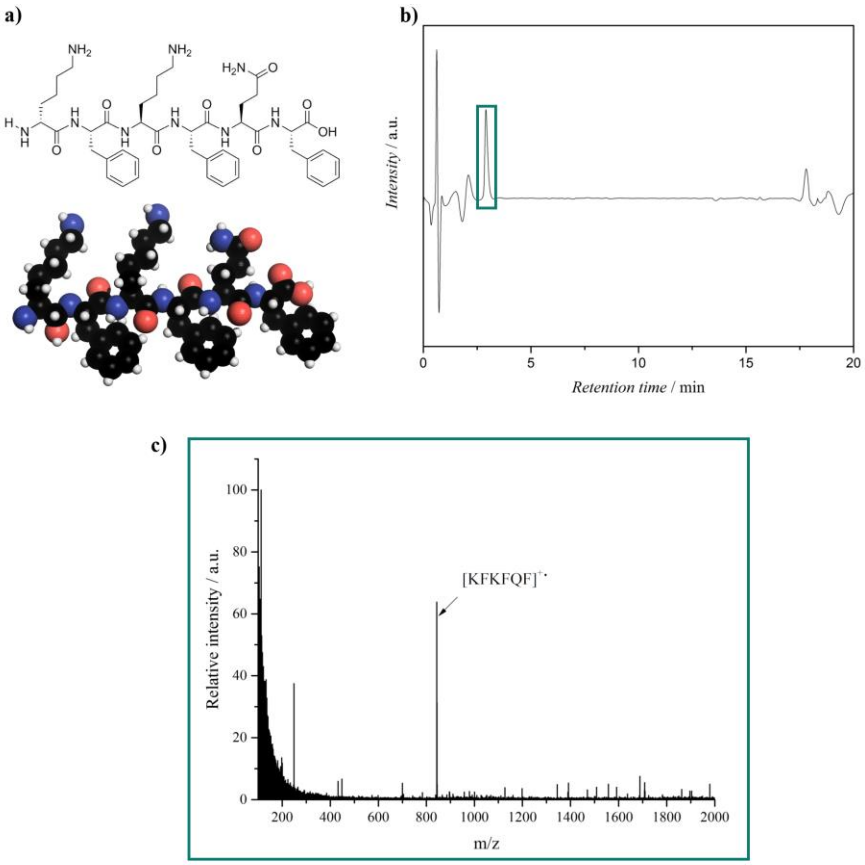

Figure 15: a) On the top the skeletal formula of KFKFQF and on the bottom the space-fill model. b) The LC-trace of the LC-MS measurement after the purification of the peptide with the preparative HPLC. c) The corresponding mass spectrum to the LC-trace in a). The corresponding data to the mass spectrum is in ***Table 6*** *in the Appendix.*

3.1.3. MKFKFQF

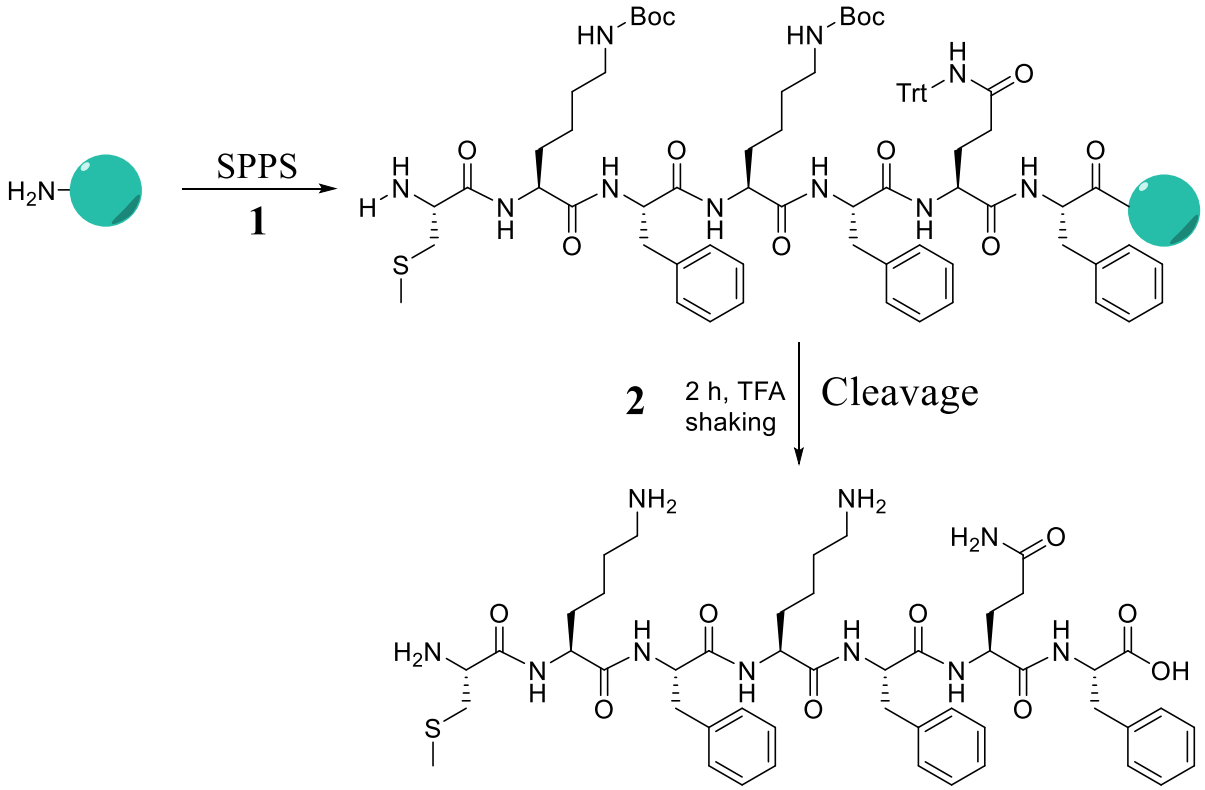

Scheme 7: The synthetic pathway to the peptide MKFKFQF. The 1st step of the reaction is the SPPS. The 2nd step is the cleavage of the peptide from the solid base with TFA.

This sequence is also the result of the group from Ulm but was not as thoroughly investigated as the two others (CKFKFQF and KFKFQF). It was picked because of the more stable thioether group in the methionine, which should not react as a transfer agent during the polymerization. Also, in line with the theory of the aggregation of the cysteine, this sequence should achieve the predicted yields and show a better self-assembly behavior than the KFKFQF peptide.

The synthesis pathway is nearly identical with the one of CKFKFQF, as shown in **Scheme 7**. The synthesis of the peptide was successful as shown in the **Figure 16 c)**, where the mass spectrum is shown. The corresponding table with theoretical predicted m/z values compared to the experimentally found m/z values is shown in the APPENDIX. The **Figure 16 b)** also shows the success of the purification method *via* HPLC. As in the cases before, after the new

preparative HPLC purification method was implemented, the yield began to match the predicted results.

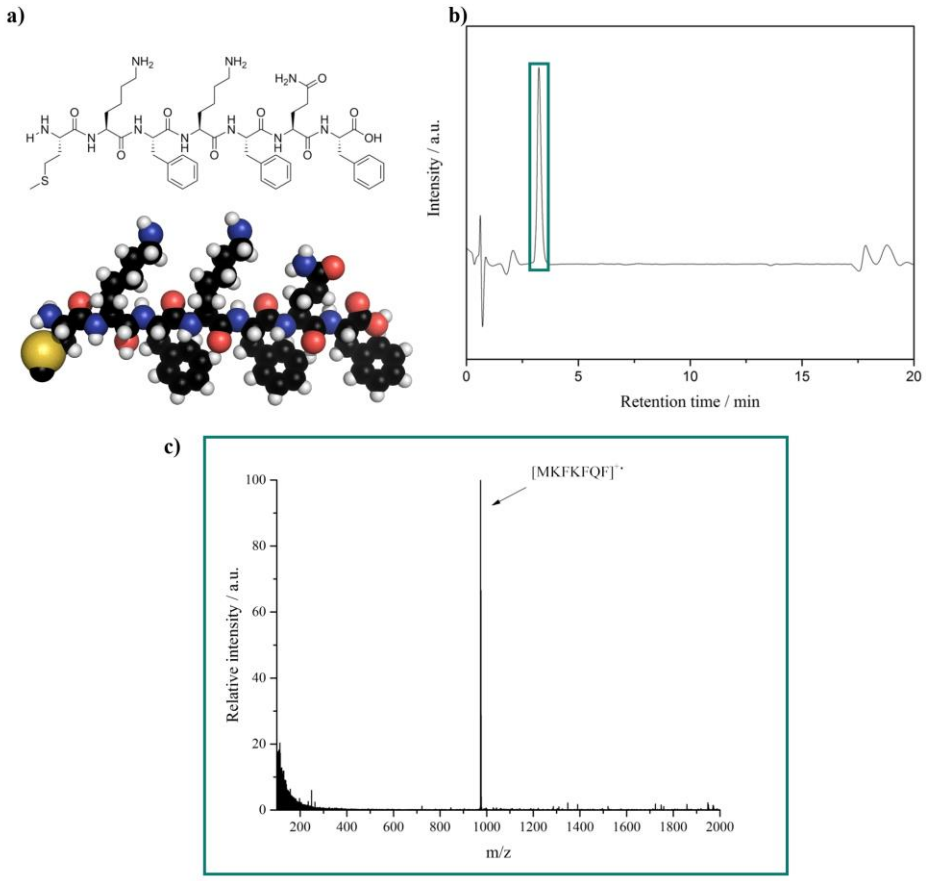

Figure 16: a) On the top the skeletal formula of MKFKFQF and on the bottom the space-fill model. b) The LC-trace of the LC-MS measurement after the purification of the peptide with the preparative HPLC. c) The corresponding mass spectrum to the LC-trace in a). The corresponding data to the mass spectrum is in ***Table 7*** *in the Appendix.*

3.2. Self-Assembly Studies

The self-assembly is precisely the behavior, which makes these peptide sequences interesting for gene transfer applications.[8] It offers a wide range of possible structures and the outcome of the self-assembling can be effected by minor changes to the preparation pathway or the environmental conditions. Therefore it is of utmost importance to develop an understanding of the effects the different parameters have on the self-assembling behavior of the peptides. At the moment very little is known about how changing certain parameters define the resulting structure. In order to better understand the underlying principles governing the self-assembly of selected peptides, a systematic investigation is necessary. This accumulated knowledge will ultimately make it possible to engineer the perfect preparation pathway for any desired use of self-assembled supramolecular peptide structures. The parameters that were chosen in this project are peptide sequence, polymer corona, pH value, and others. The experiments and results are discussed in the following chapters.

TEM was used to qualitatively evaluate the morphology of the sample from a given preparation condition. TEM is a qualitative method and has certain limitations, however, it can be used to directly compare the effects of the changed conditions. Further, to minimize wrong interpretation, any sample gird was thoroughly scanned to control that the presented structure is the absolutely dominating one.

3.2.1. Peptide Sequence

The first analyzed parameter was the structure of the peptides. The peptide sequences of KFKFQF, MKFKFQF and CKFKFQF were compared. The samples shown in **Figure 17** were prepared by creating a stock solution in MilliQ water (**Figure 17 a)** – **c)**) and in DMSO (**Figure 17 d)** – **f)**) with 1 mg in 100 µL. They were then diluted by taking 10 µL of this stock solution into 90 µL in MilliQ water (**Figure 17 a)** – **c)**) or PBS buffer (DPBS (1X)) (**Figure 17 d)** – **f)**). It was expected that the CKFKFQF would show the strongest self-assembly tendency and KFKFQF would show a clearly weaker one, because of the by S. Sieste postulated aggregation enhancing formation of disulfide bridges. For MKFKFQF a higher tendency for self-assembling behavior compared to KFKFQF was predicted, because of addition an aliphatic amino acid residue. This will enhance the van der Waals attraction, but it was not clear, how much.

The results are shown in **Figure 17Error! Reference source not found.**. It is visible that the CKFKFQF has a strong tendency to self-assemble into supramolecular fibrils. KFKFQF on the other hand has a very low self-assembling tendency, in pure water no formation of fibrous supramolecular structures could be witnessed. If the three observed peptide sequences form a spectrum, CKFKFQF would be on the end of highest probability for supramolecular architecture and KFKFQF on the end with the lowest. On this spectrum MKFKFQF could be found in the middle. This matches the results produced by S. Sieste in Ulm. It seems highly likely that the incorporation of a sulfur containing amino acid into the peptide increases the self-assembly tendency. As postulated by S. Sieste and others, the high self-assembly behavior of the cysteine containing peptide is rooted in the possibility to form disulfide bonds between the different supramolecular structures.[108] This cannot explain the behavior of the methionine containing peptide because methionine cannot form disulfide bonds. The heightened self-assembly behavior could be explained by the hydrophobic effect.[109] Another possibility is the already mentioned enhanced van der Waals attraction by addition of the methionine. It could be shown that the incorporation of methionine enhances the building of supramolecular structures.[110]

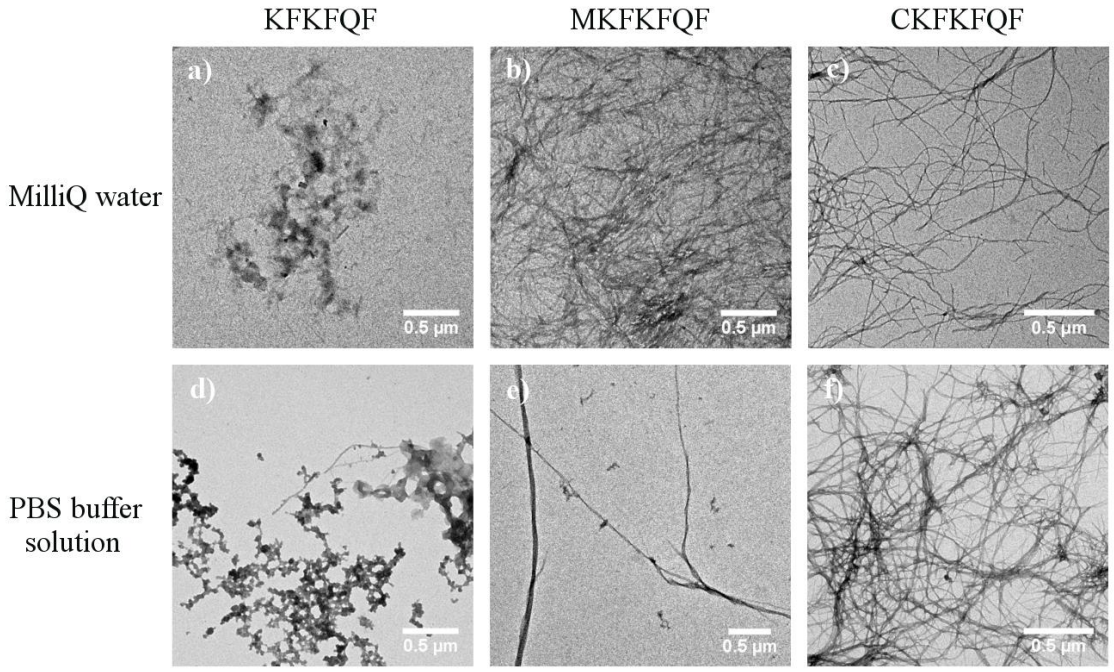

Figure 17: Effect of the peptide sequence on the supramolecular structure of different peptides. Top: Peptides stock solution in MilliQ than diluted into MilliQ, a) KFKFQF, b) MKFKFQF, and c) CKFKFQF. Bottom: Peptides stock solution in DMSO than diluted into PBS buffer solution, d) KFKFQF, e) MKFKFQF, and f) CKFKFQF.

3.2.2. Preparation Pathway and Solvent Ratio

The second varied parameter was the preparation pathway. Therefore the behavior of the same peptide sequence prepared by different pathways was investigated. With the lyophilized peptides stock solutions with 1 mg of the peptide in 100 µL of ether, MilliQ water or DMSO were prepared. In both cases 10 µL of the respective stock solution were then diluted into 90 µL MilliQ water.

The established pathway is to solve the peptide in the good solvent and then transfer it into the poor solvent for self-assemble. In this context good solvent means a solvent in which the peptide is completely solved and does not form aggregates. Consequently poor solvent means a solvent which enables the aggregation of the peptides. MilliQ water can be classified as the poor solvent compared to the DMSO, which can be classified as the good solvent.[67] A reasonable prediction is that the pathway using a stock solution in poor solvent leads to ill-defined structures, because the lyophilized peptide was never completely solved. Therefore the

structures formed during the freeze drying process are disturbing the self-assembly. Further is it possible that the pathway with the poor solvent leads to a less dynamical self-assembly process and thus it has a lesser chance of correcting defects in the forming structures. The pathway with the good solvent in the stock solution on the other hand starts with completely solved peptides, which can "slowly" assemble into more homogeneous materials and have fewer tendencies to aggregate. The results are shown in **Figure 18**.

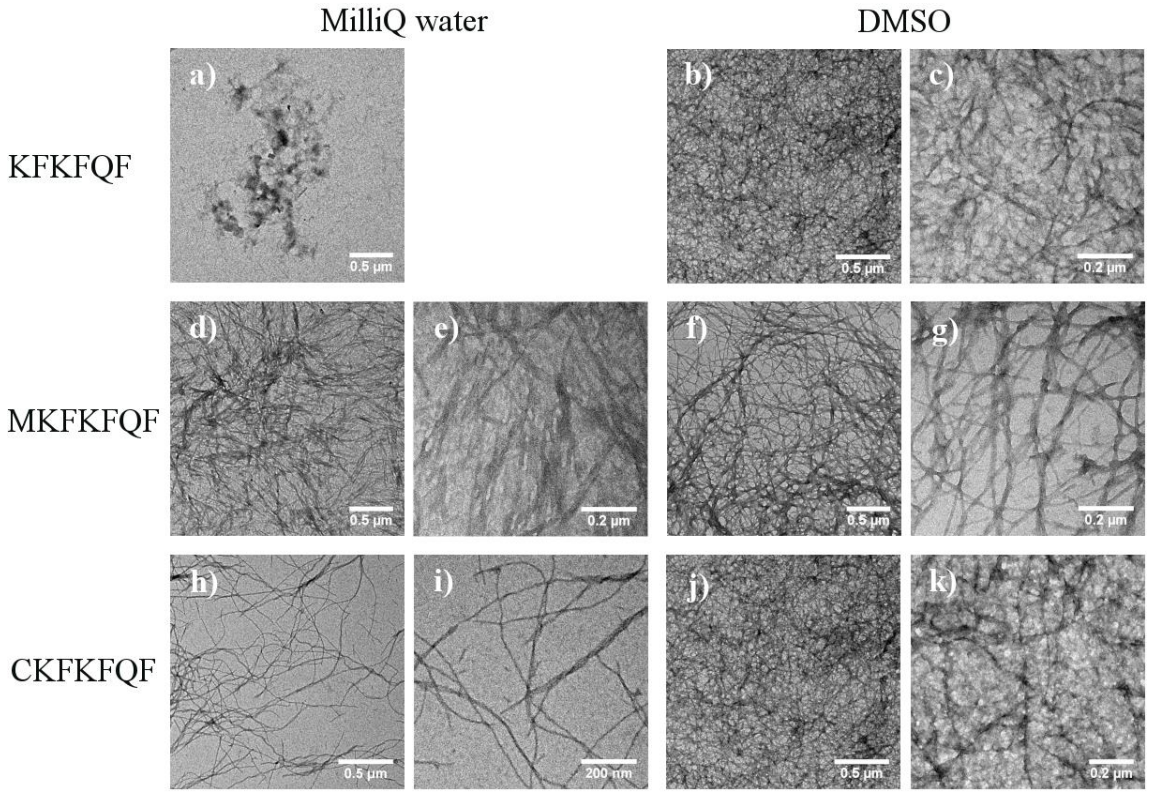

Figure 18: Effect of different preparation pathways on the peptide self-assembly. The samples for a), d), e), h), and i) were prepared by solving the respective peptide in MilliQ water and then diluting it into MilliQ water. The samples for b), c) f), g), j), and k) were prepared by solving the respective peptide in DMSO and then diluting it into MilliQ water. The images are in pair, for example b) has a scale bar of 0.5 µm and c) one of 0.2 µm.

For the peptide KFKFQF there was no visible fibrils if the stock solution was MilliQ water. This corresponds with the expectations, that the peptide itself has the least promising self-assembly behavior and MilliQ is a poor solvent for the stock solution. Correspondingly, the

established pathway *via* DMSO stock solution yielded ill-defined structures. Compared to the other peptide sequences this shows again the lower self-assembly tendency of KFKFQF.
On the other hand, the results of the peptides MKFKFQF and CKFKFQF show qualitatively little difference between both pathways of preparation. The difference between 0% and 10% good solvent could be too little to have a strong effect on the self-assembly behavior of the peptides. Like discussed, S. I. Stupp *et al*. compared the behavior of three ratios of good/poor solvents.[69] They had 10%, 20 %, 50% and 100% good solvent (HFIP) in their mixtures. They could demonstrate, that samples at 10% and 20% formed β-sheet structures and at 50% and 100% samples formed random coils. This clearly shows that for future experiments a higher difference in good/poor solvent ratio is worth investigating.

3.2.3. pH Value

Another parameter which was varied in the studies was the pH value of the solution. The peptides were compared at final pH values of 7.4, 5, and 3. The samples were prepared by first dissolving the peptide in DMSO to create a stock solution. Then subsequently diluted 10fold into MilliQ water to a final concentration of 0.01 mg/mL. Then, the pH value was adjusted through the addition of small amounts of 0.1 M HCl or NaOH solution. Directly after pH adjustment samples were prepared for TEM analysis. Because the KFKFQF peptide did not form fibers at neutral pH, this peptide was excluded from this study. For both peptides the expectation was that the form of the structures would be more ill-defined. The lysine amino acid, which they both have in their backbone has an amine residue which can be protonated at the lowered pH value. This enhances the charge repulsion between the β-sheet like structures and therefore hinders the self-assembling. In **Figure 19** a selection of the corresponding TEM images is given.

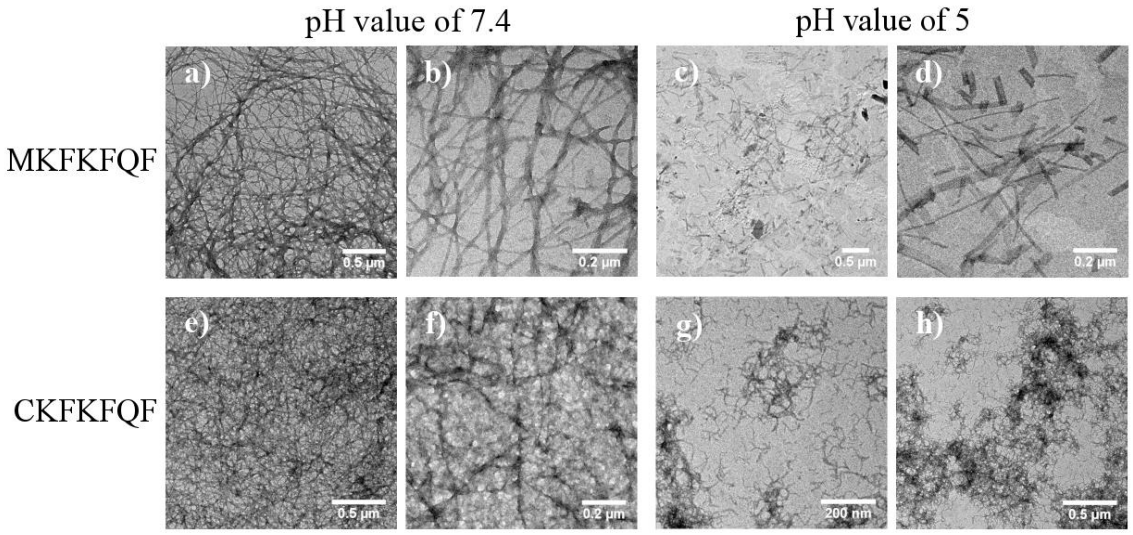

Figure 19 : The influence of the pH value of the solution on the self-assembly tendency of the peptides MKFKFQF and CKFKFQF. a), b), e), and f) show the supramolecular fibrous structure at a pH value of 7.4. c), d), g), and h) depict the supramolecular structure of the respective peptides at a pH value of 5. The images are in pair, for example a) has a scale bar of 0.5 µm and b) one of 0.2 µm.

As expected the pH value clearly has a great impact on the self-assembly behavior. The results of the peptide CKFKFQF fulfil the expectations completely. At a pH value of 7.4 they show long fibril structures, but at a pH value of 5 they form short fibrils. This is the result of the predicted protonation of some of the lysine residues. Through the added positive charges the charge repulsion is enhanced and the interaction of the β-sheet like structures is hindered.

The peptide MKFKFQF on the opposite defies the expectations. At a pH value of 7.4 it assembles into long well-defined fibrils, but at the pH value of 5 it forms a mixture of fibrils and ribbons of different length. At first that contradicts the predicted increase in charge repulsion between the β-sheet like structures. But the added charge could enhance the hydrophily of the structures which lessens the elastic energy penalty as a results of the strain of the supramolecular structure to minimize the contact of its hydrophobic parts with the aqueous medium. This results in a growth in width of the supramolecular structure. If a fibril gets wider at some point it starts to transform into twisted ribbons and if it gets even wider it transforms into helical ribbons and in the end into nanotubes.[58]

3.2.4. Salt Concentration

Another parameter investigated was the salt concentration of the solution. For these experiments different lyophilized peptides were all solved in DMSO. Then two different preparation pathways were compared. In one the peptides were diluted into MilliQ water and in the other they were diluted into PBS buffer solution (DPBS (1X)), both with an end concentration of 0.01 mg/mL. The pH was adjusted in both pathways to the same value. The salt ions should in theory shield the charge repulsion between the β-sheet like structures and therefore lead to an increased self-assembly behavior. The results of some chosen experiments a shown in **Figure 20**.

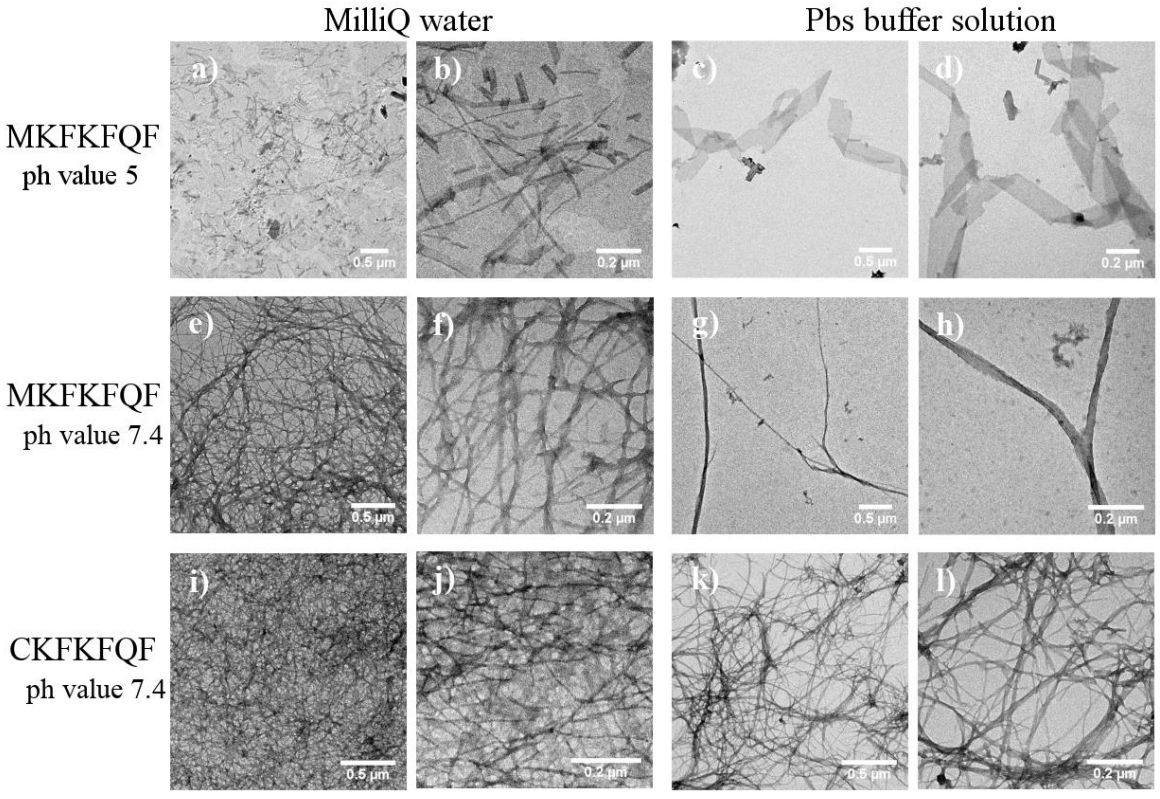

Figure 20: The influence of the salt concentration on the self-assembly behavior of the peptides CKFKFQF and MKFKFQF. a) – b) show the peptide MKFKFQF at a pH value of 5, in the images a) and b) the peptide was diluted in MilliQ water in c) and d) in PBS buffer solution. e) – h) show the same peptide at the pH value of 7.4. e) and f) diluted in MilliQ water and g) and h) in PBS buffer solution. i) – l) show the peptide CKFKFQF at the pH value of 7.4 in i) and j) the dilution was in MilliQ water and k) and l) in PBS buffer solution.

In all preparation pathway a growth in width of the supramolecular structures is visible. In the case of the **Figure 20 i)** – **l)** the fibrils get wider and begin to form bundles. This is a result of the decrease in charge repulsion through the shielding influence of the salt ions. In **Figure 20 e)** – **h)** the fibrils begin to entwine and form fibers.[55] This also is the result of the salt ions shielding the charges and decreasing the repulsion between the structures. It seems possible that this effect lowers the critical concentration for the formation of fibers from fibrils. The peptide MKFKFQF at a pH value of 5 is shown in **Figure 20 a)** – **d)**, the higher salt concentration clearly changes the morphology of the supramolecular structures. The effect of the pH value onto the peptide lowered the elastic energy penalty which allowed for a wide growth and the transformation of fibrils into twisted ribbons. The shielding of positive charges increases the inter structure attraction, as a result the twisted ribbons grow wider until they become helical ribbons.[58] The next step would be to try and further increase the width growth and to produce nanotubes.

3.2.5. Oxidation

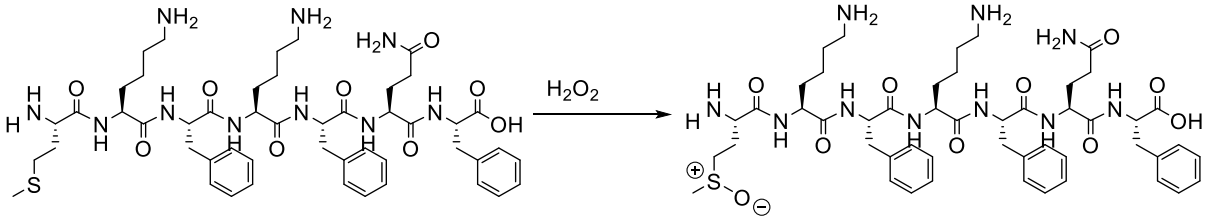

Scheme 8: Synthesis pathway oxidation reaction of the peptide MKFKFQF with H_2O_2 to the oxidized MKFKFQF.

In this experiment the effect of oxidation on the methionine amino acid in the peptide was investigated. The oxidation reaction is shown in **Scheme 8** the reaction was ended after 5.5 h. Samples were taken at 0 min, 5 min, 1.5 h, 3 h, and 5.5 h. The samples were directly analyzed by LCMS. In **Figure 21** the results of the sample after 1.5 h is shown, the LC-trace in **a)** shows two peaks, the first is the oxidized peptide. It elutes first because of the oxidation. It becomes more hydrophilic and therefore interacts less with the column. In **b)** and **c)** the mass spectra for the respective peaks are shown and demonstrate that the peaks truly represent the peptide and its oxidized form.

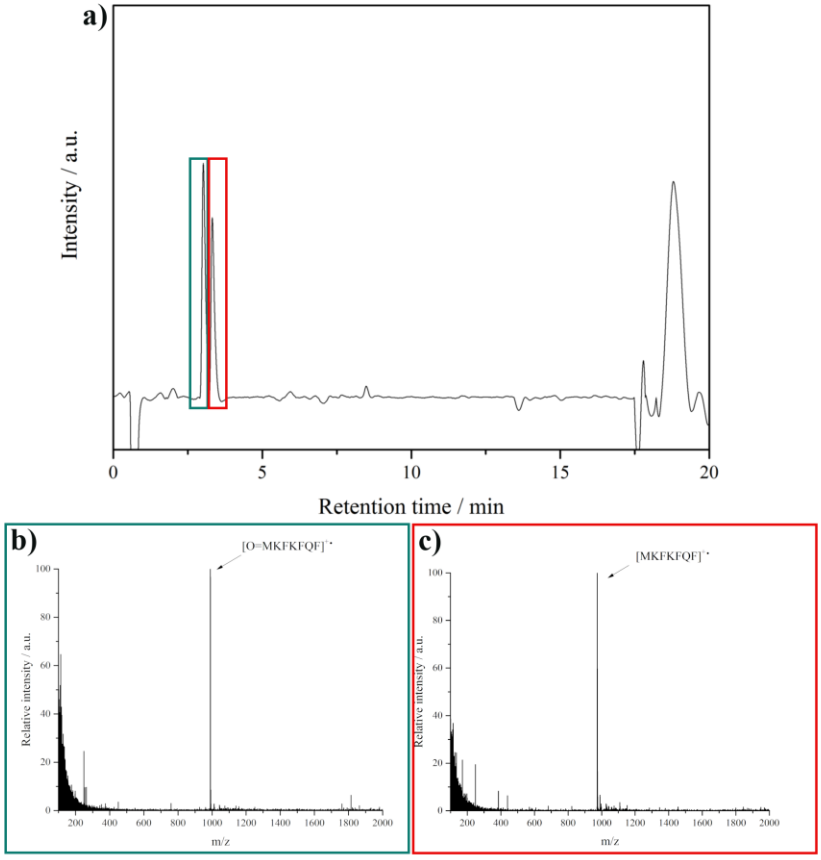

Figure 21: Example of a) the LC-trace of the kinetic study and b) and c) the corresponding mass spectra of the peaks in the LC-trace.

The LC-traces of the different samples were then compared with Origin (9.1) and put in the graph in **Figure 22**. This demonstrates that the first peak increases with the reaction time and the second one decreases with the reaction time. The longer the reaction continues the more peptide is oxidized. The LC-traces used in this graph are shown in the Appendix of this thesis.

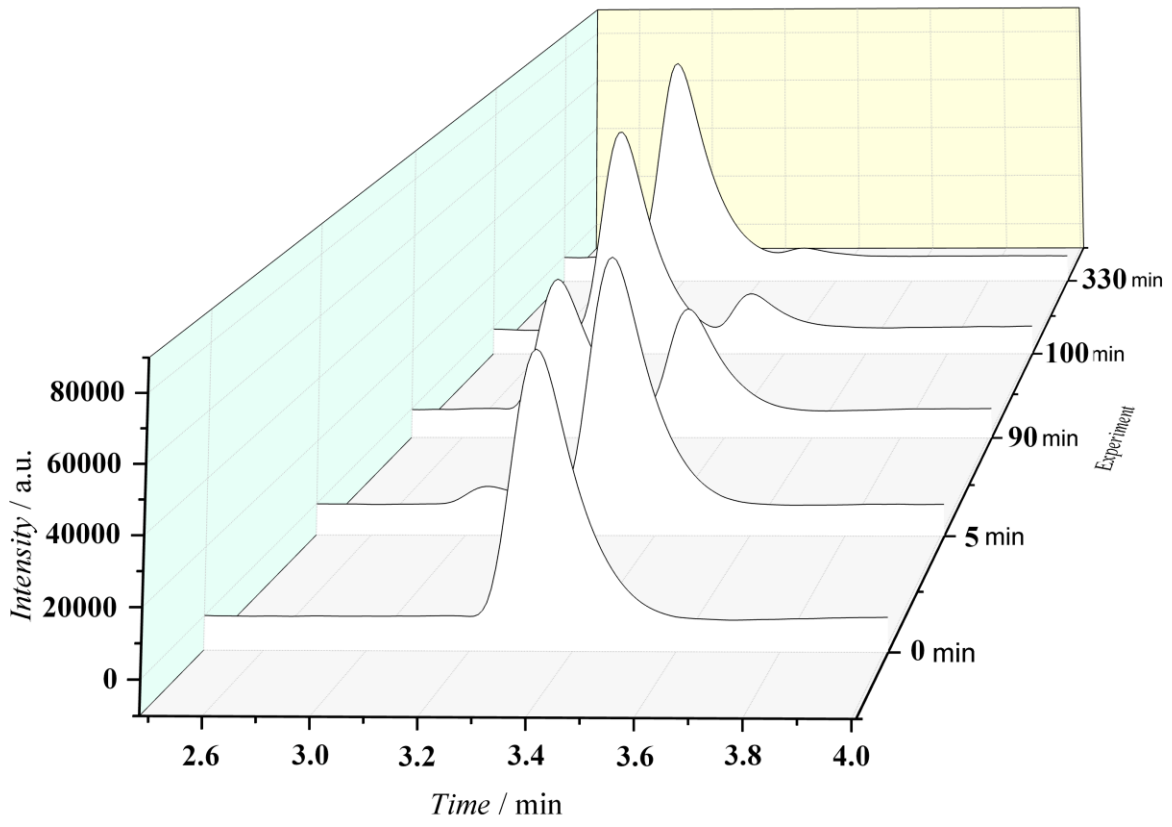

Figure 22: LC-traces of the samples for the kinetic studies of the oxidation reaction of MKFKFQF.

The LCMS measurements produced quantitative LC-traces. Therefore, it was possible to integrate the peaks with Origin (9.1) and calculate the percentual share of oxidized peptide in the reaction mixture at the time the corresponding sample was taken. The results were put into a graph, which is shown in **Figure 23**. With these results it was possible to predict the reaction time for 25%, 50% and 75% conversion of the peptide to its oxidized form. These reactions were then done with the same synthesis pathway as shown in **Scheme 8** and stopped at the respective time. The resulting lyophilized peptides were then solved in DMSO to make a stock solution, then diluted into MilliQ water and the pH value adjusted to 7.4. The corresponding TEM images and the graph are shown in **Figure 23**.

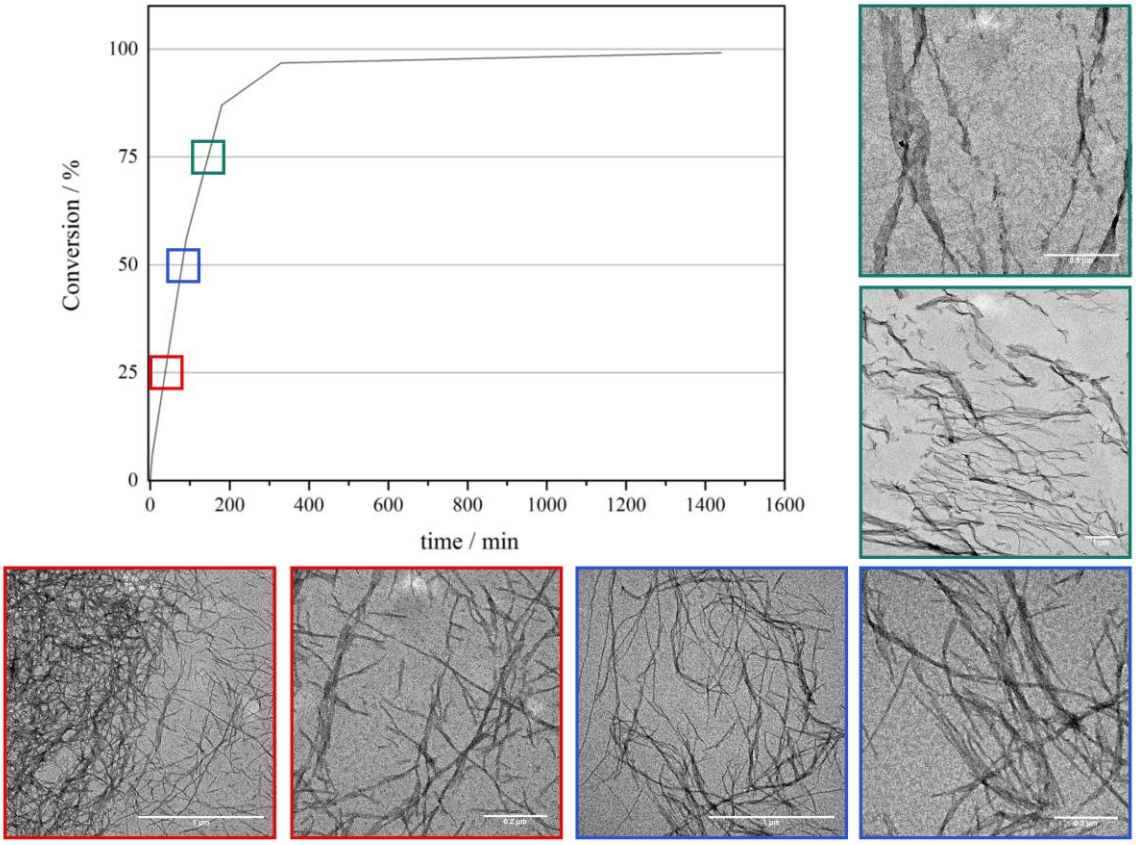

Figure 23: a) Graph depicting the conversion of peptide MKFKFQF to its oxidized form. The points 25%, 50% and 75% are color-coded. b) – g) TEM images of the self-assembled structures corresponding to the point in the graph coded in the same color.

Figure 24 shows the TEM images of the different reactions producing peptide mixtures with 25%, 50% and 75% share of the oxidized peptide. Between the 25% and the 50% point there is no clear difference in the morphology of the supramolecular structures. In both cases they can be described as fibrils, possibly a little longer at the 50% mark. But the difference between the 50% and 75% mark in morphology is huge. At the 75% point the structure resembles twisted ribbons, this indicates a growth in width over the critical point between fibril and ribbon.[58] This could be the result of the increase in hydrophilicity of the oxidized peptide, as a result of transforming a hydrophobic thioether in a hydrophilic sulfoxide. That decreases the elastic energy penalty of the structures and allows for width growth. This results in the transformation of the fibrils into twisted ribbons.[58]

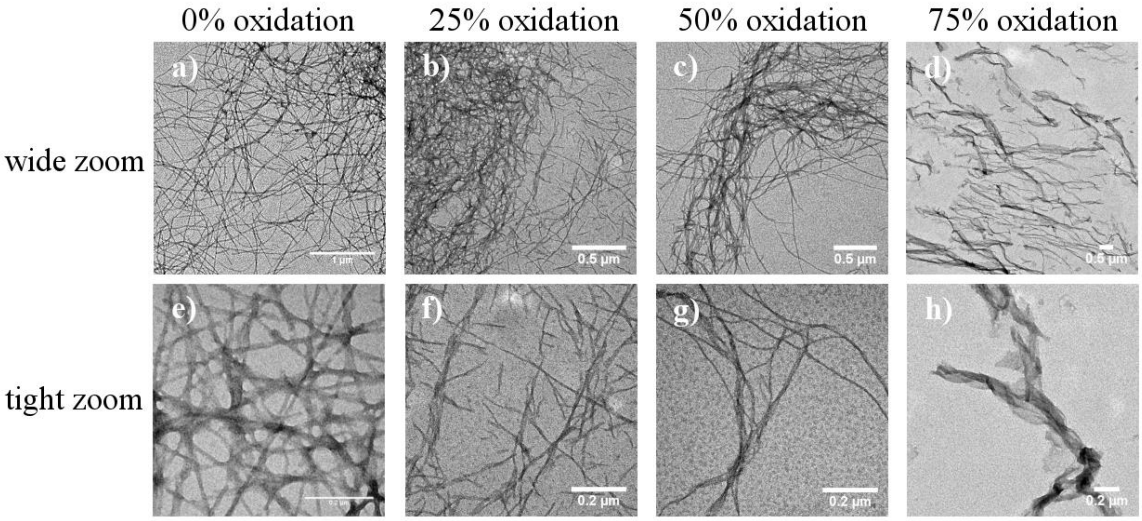

Figure 24: Influence of oxidation of the methionine residue on the self-assembly of the peptide MKFKFQF. The images show different proceduale shares of oxidized peptide mixed with MKFKFQF.

3.2.6. Thermal Annealing

Thermal annealing is supposed to get structures that were kinetically trapped before the annealing step to convert to the energetically favorable structure, without having to wait for long periods of time. It was also supposed to help homogenize samples that have potentially heterogeneous populations.

In these experiments the influence of a thermal annealing on the self-assembly was investigated. The respective samples were prepared by the same pathway. One was thermal annealed for 30 min at 80 °C and then cooled for 1 h to 20 °C with a gradient of -1 °C/min. After annealing the sample was put on the grid. The corresponding sample that was not annealed was put on the grid directly after pH adjustment.

In **Figure 25** six different preparation pathways are compared. As S. I. Stupp *et al.* discovered, not every pathway responded to temperature annealing. All the samples were chosen because they showed at least a little change through the annealing process.[69]

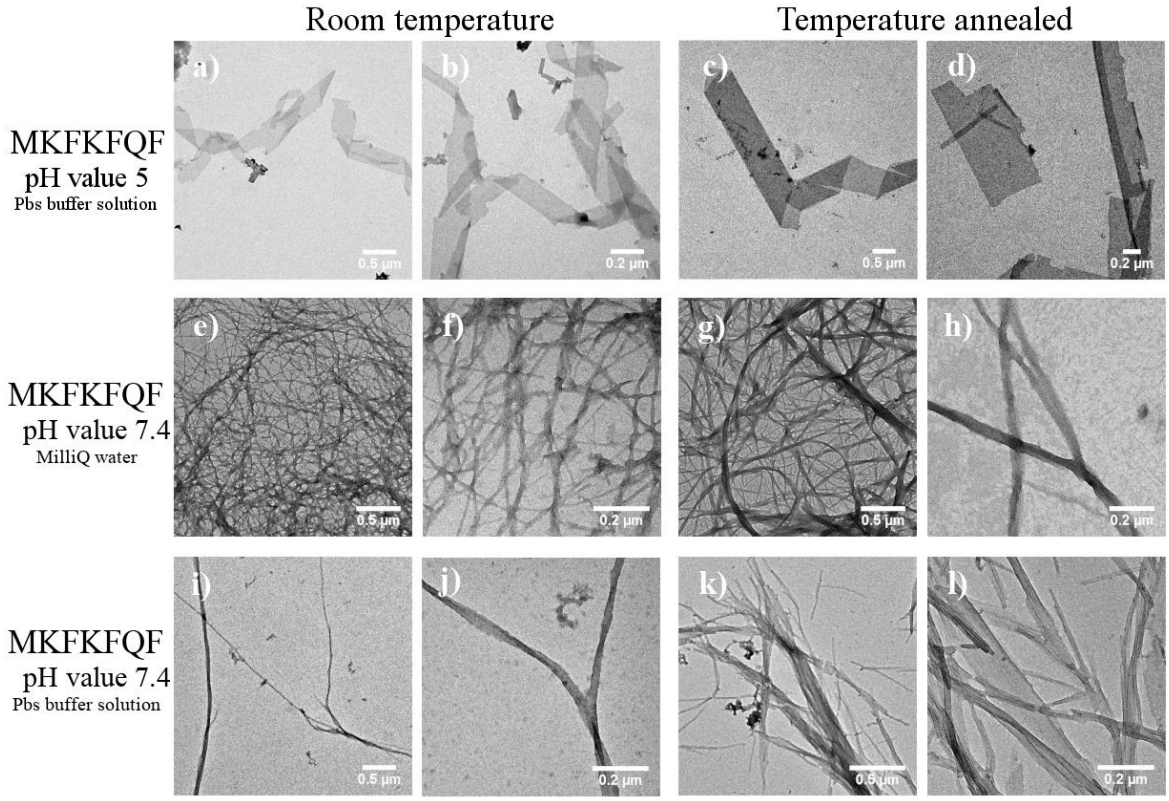

Figure 25: Influence of the thermal annealing on the peptide self-assembly. a) – b) show the peptide MKFKFQF at a pH value of 5 diluted into PBS buffer solution, in the images a) and b) the peptide was not annealed c) and d) it was annealed. e) – h) show the same peptide at the pH value of 7.4diluted in MilliQ water. e) and f) it was not annealed and in g) and h) it was annealed. i) – l) show also MKFKFQF at the pH value of 7.4, put diluted in PBS buffer solution, in i) and j) without annealing and in k) and l) with annealing.

Temperature annealing of the different samples did not induce any major changes in the morphology of any of the tested samples. All comparisons show a slight increase in the diameter of the structures. This could be a result of the temperature annealing processes. The samples at a pH value of 5 exhibits no structural changes except a possible growth in thickness, but a trapped state of the energy landscape shows more morphological difference. Like the difference between the short fibers and the long bundled fibers in the work of F. Tantakitti *et al.*[78] This change in thickness could also be the result of the slightly longer time interval between sample preparation and TEM grid preparation, caused by the temperature annealing processes. The difference in the samples in **Figure 25 k)** and **l)**, besides the growth in thickness, speaks more for a trapped supramolecular state. The fibrils in the pathway without temperature annealing are longer and the process of entwining to form fibers is visible. On the contrary

samples after temperature annealing seem to be shorter and their aggregation is more a stacking of short fibrils. The samples in **Figure 25 e)** – **h)** show the growth in thickness again, this could be the result of the next stage in hierarchical self-assembly of the *β*-sheets: the entwining of fibrils to fibers. It remains unclear, if this process is in any way the result of the temperature annealing.[55]

3.2.7. Polymer Corona

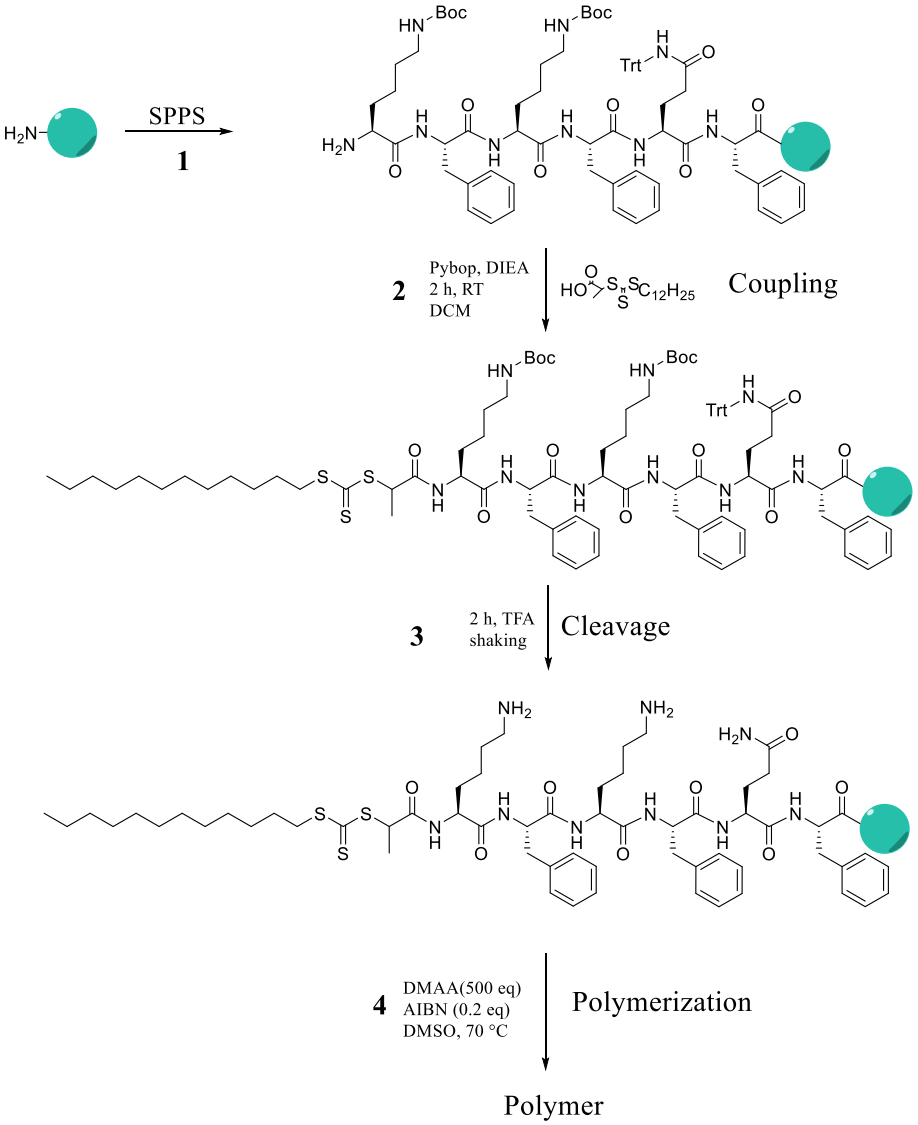

Scheme 9: The synthetic pathway for the RAFT polymerization. The 1st step of the reaction is the SPPS. In the 2nd step the Raft-Agent is coupled to the N-terminus of the peptide KFKFQF. In the 3rd step is the cleavage of the peptide from the solid base with TFA. The 4th step shows the polymerization of DMAA with the RAFT-macroinitiator.

The first experiments to incorporate a polymer corona into the supramolecular structures were attempted using the ATRP technique. As described in the **chapter 3.3.1** the coupling of the ATRP-Initiator onto the CFKFQF peptide was successfully achieved and the presence of the initiator group did not influence the self-assembly behavior of the peptide. Unfortunately, the following polymerization proved difficulties and no monomer conversion could be detected. The reason could be in the chain transfer capability of the Cysteine or in a competing complexion of the copper catalyst by the peptide rather than the bipyridyl ligand. The attempt to achieve a polymerization with a higher Cu concentration also failed.

Because of the problems of synthesizing the peptide and the inability to successfully use the ATRP technic for polymerization a switch in polymerization technique was tried. The first step was to change from ATRP to RAFT polymerization. To minimize the risks the next goal was to prove the concept with a less difficult peptide. For this reason, the peptide KFKFQF was chosen for functionalization with a RAFT moiety. The coupling of the RAFT-agent onto the peptide and the polymerization worked as shown in **Scheme 9** . The TEM images in **Figure 26** show that the peptide with RAFT-agent forms less defined structures than the unaltered peptide. This could be the result of the added hydrophobic aliphatic chain at the RAFT-agent.

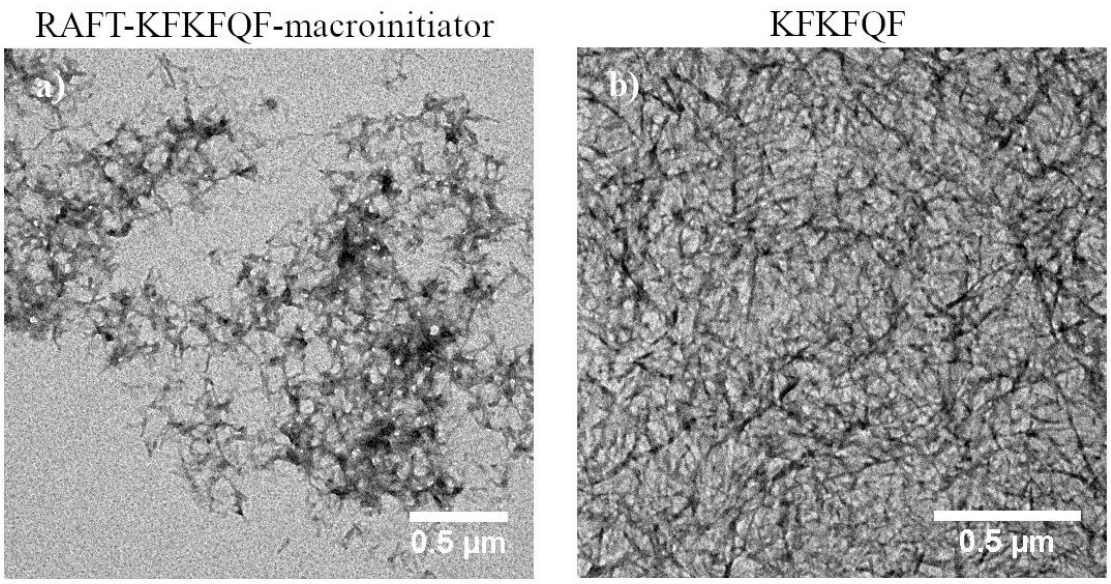

Figure 26: Compared self-assembly behavior of a) the RAFT-macroinitiator and b) the peptide KFKFQF.

3.3. Polymer-Peptide Hybrid

The synthesis of a polymer-peptide hybrid followed two synthesis pathway, one utilized the ATRP method the other one the RAFT polymerization method.

The challenge was the production of purified peptide. It was not possible to achieve a yield in the two-digit margin. The source of the meager results was identified as the HPLC purification after solid phase peptide synthesis. The crude peptide initiator (Bib-CKFKFQF) had a rather low solubility in aqueous media, with large aggregates being present. As with the pure peptides this led to a significant amount of lost material during the filtration step with the syringe filters (0.2 µm), prior to injection into the HPLC. As a result, only very small amounts of pure peptide initiator could be prepared, which significantly hindered the optimization of the polymerization conditions in the following step.

3.3.1. ATRP-Macroinitiator

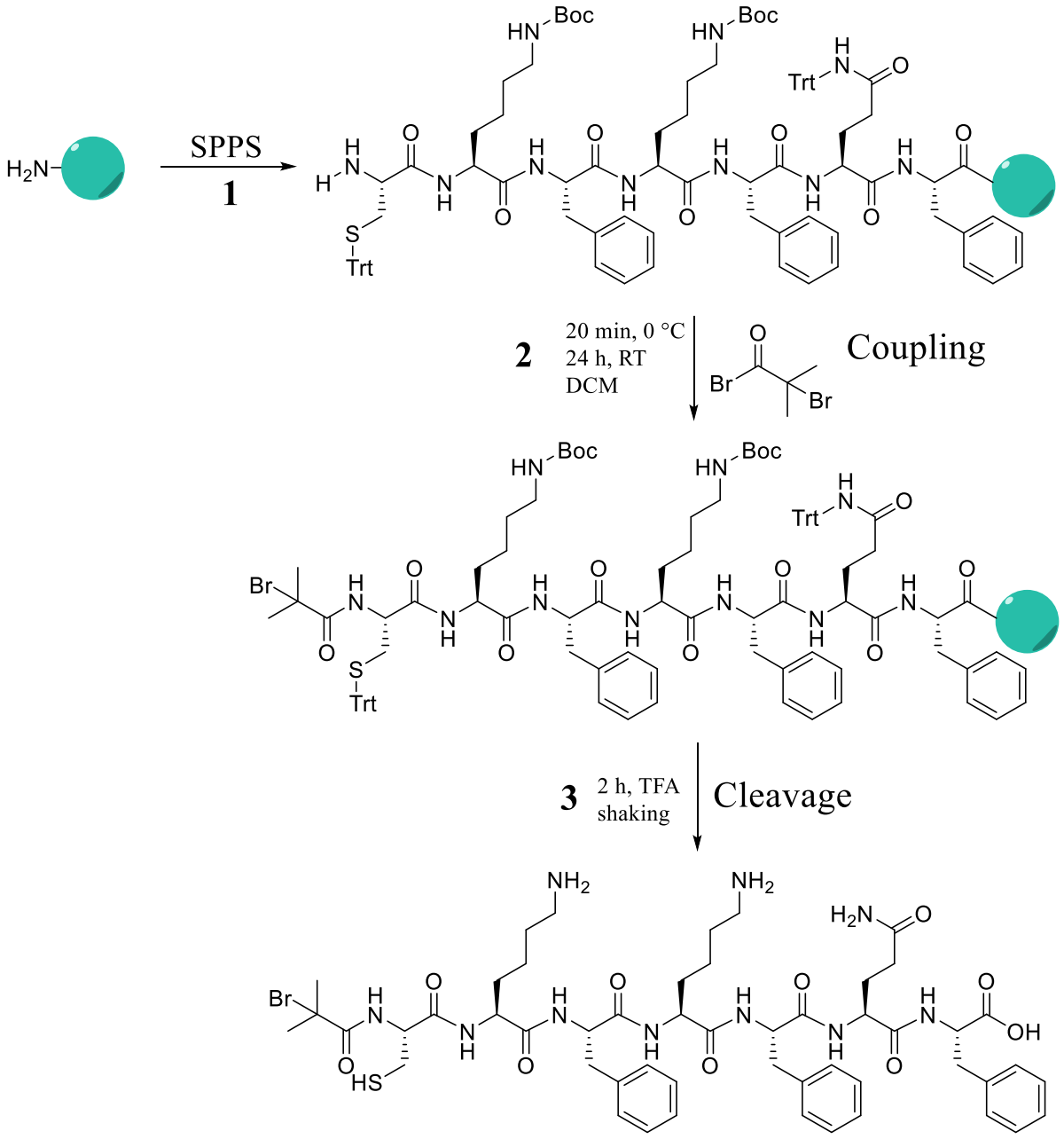

Scheme 10: The synthetic pathway to the ATRP-macroinitiator. The 1st step of the reaction is the SPPS. The 2nd the α-Bromoisobutyryl bromide is coupled to the N-terminus of the peptide CKFKFQF. In the 3rd step is the cleavage of the peptide from the solid base with TFA.

For the ATRP-macroinitiator the peptide CKFKFQF was chosen, because of its excellent self-assembly behavior. The reaction pathway for the synthesis of the ATRP-macroinitiator is

shown in **Scheme 10**. In this synthesis the strength of the SPPS were used again. The peptide was synthesized in the peptide synthesizer and only the Fmoc protective group was cleaved. This way the protective groups of the residues were intact and there were no risk of side reactions. The peptide was also still on the solid base for the coupling reaction to the ATRP-initiator (the α-Bromoisobutyryl bromide), therefore the ATRP-initiator could be used in excess without problems of separating it from the product after the reaction. This excess also guaranteed a nearly completed coupling. The ATRP-macroinitiator than was cleaved and deprotected with TFA.

However, very little material was obtained after freeze drying, complicating comprehensive characterization (~ 5 mg). The results of the LCMS are shown in **Figure 27**, confirming the purity of the ATRP-CKFKFQF peptide. The results of the corresponding mass spectrum prove the success of the coupling of the ATRP-initiator and the peptide CKFKFQF.

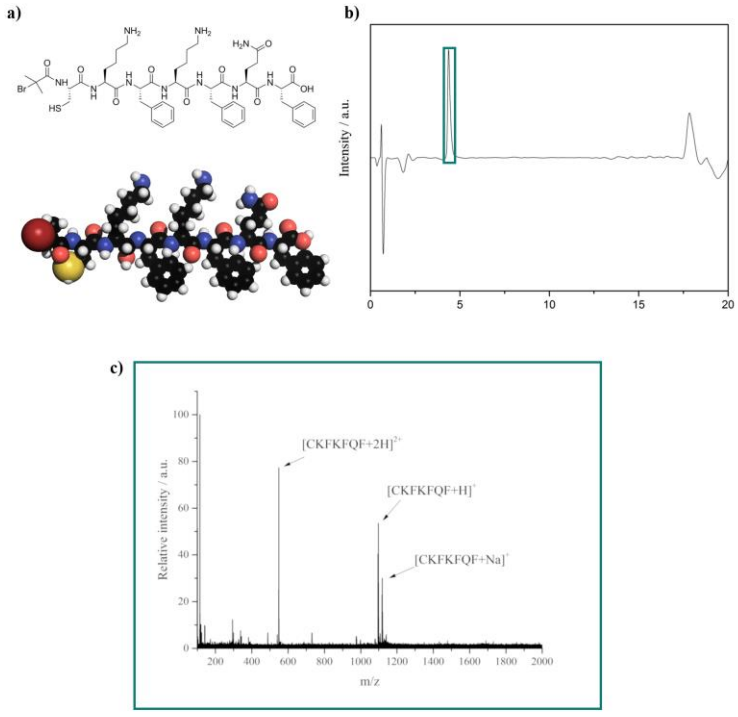

*Figure 27: a) On the top the skeletal formula of Bib-CKFKFQF and on the bottom the space-fill model. b) The LC-trace of the LC-MS measurement after the purification of the peptide with the preparative HPLC. c) The corresponding mass spectrum to the LC-trace in a). The corresponding data to the mass spectrum is in **Table 8**Table 4 in the Appendix.*

3.3.2. ATRP-Polymerization

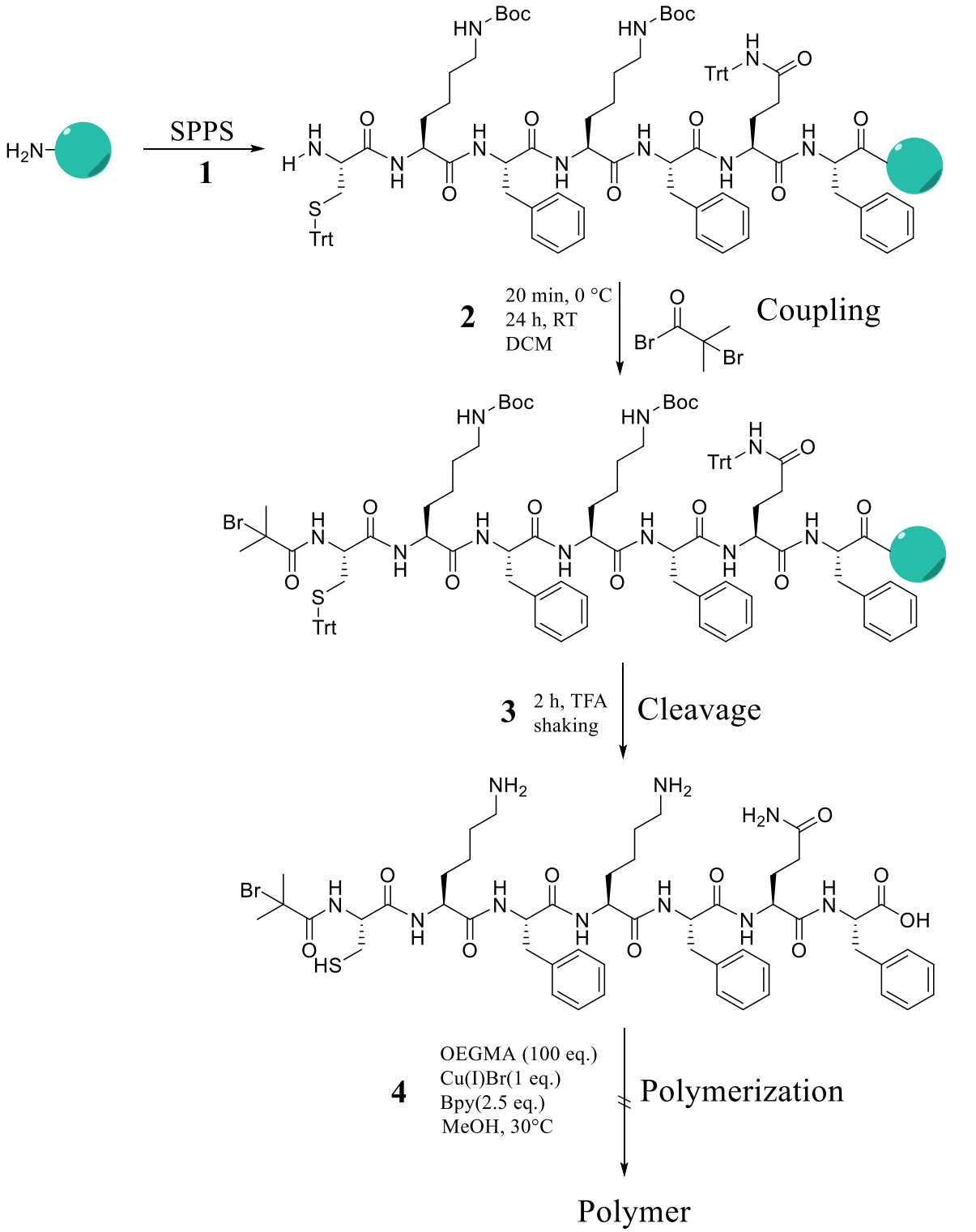

Scheme 11: The synthetic pathway for the ATRP. The 1st step of the reaction is the SPPS. The 2nd the α-Bromoisobutyryl bromide is coupled to the N-terminus of the peptide CKFKFQF. In the 3rd step is the cleavage of the peptide from the solid base with TFA. 4th Step shows the polymerization of the monomer OEGMA with the ATRP-macroinitiator.

To optimize the reaction conditions for the polymerization, without wasting precious ATRP-CKFKFQF initiator, a series of test polymerizations using commercially available ATRP initiator (Ethyl α-bromoisobutyrate) were performed. After conditions with a promising outlook were found the polymerization of the ATRP-macroinitiator was undertaken. Unfortunately, no polymer formation was found both in GPC (no polymer signal), and in NMR, shown in **Figure 28**, where the intensity of the vinyl peaks at 6.12 and 5.70 ppm remained unchanged throughout the whole reaction time.

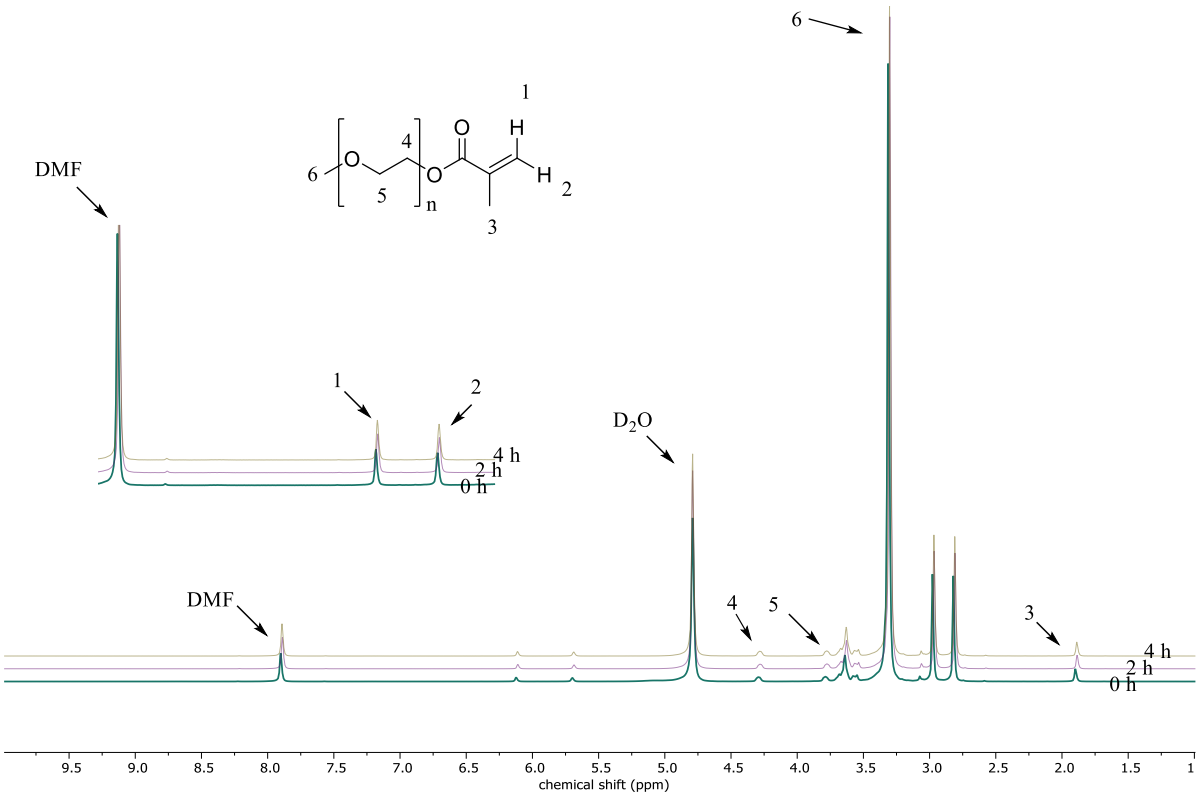

Figure 28: [1]H-NMR spectra of the kinetic measurments of the ATRP. The spectra is compounded from samples taken at 0 h, at 2 h, and as 4 h. The [1]H-NMR spectra were measuret in deuterium oxide (D2O).

It is possible, that the peptide can act as a multidentate ligand for the copper catalyst during the reaction.[93] To compensate for this possible complexation of copper ions, an excesses (3 eq) of copper(I) bromide was used. This reaction also showed no monomer consumption and the GPC also showed no polymer signal. A further increase of copper(I)bromide could be an option but the precious stock of ATRP-macroinitiator was depleted at this point. Furthermore the cysteine in the peptide chain could negatively interact with the ATRP-agent and hinder the

polymerization.[92] For example it is possible that the cysteine acts as a chain transfer agent and possible interfere with the polymerization.[111] For this reasons alternative pathways for the synthesis of polymer-peptide conjugates should be investigated.

3.3.3. RAFT-Macroinitiator

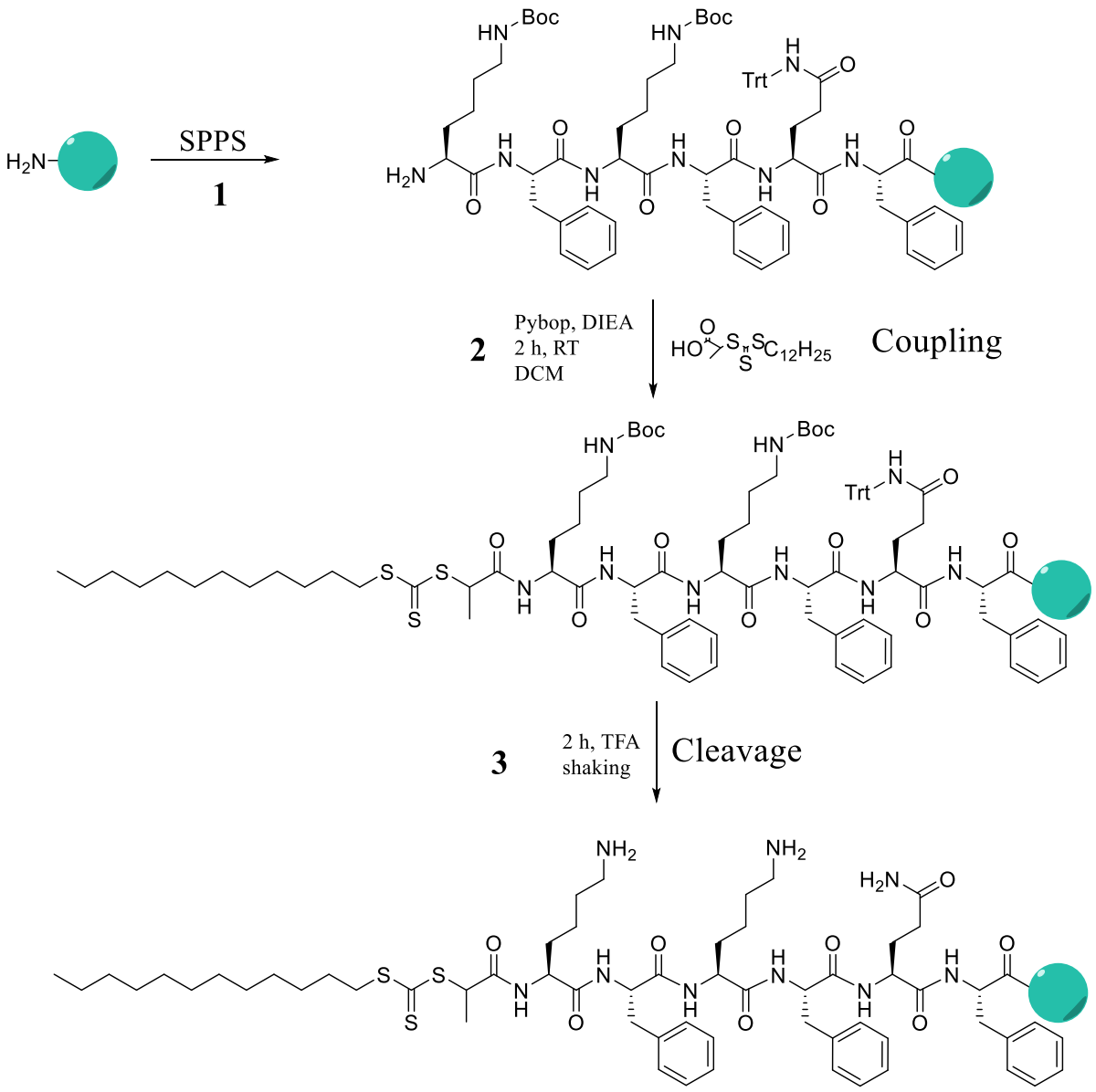

Scheme 12: The synthetic pathway to the RAFT-macroinitiator. The 1st step of the reaction is the SPPS. The 2nd the Raft-Agent is coupled to the N-terminus of the peptide KFKFQF. In the 3rd step is the cleavage of the peptide from the solid base with TFA.

After the challenges with the ATRP synthesis of the polymer peptide conjugate the RAFT polymerization was a promising alternative. The RAFT polymerization offers several potential advantages compared to the ATRP. Its components have a strong tolerance towards air and water and can therefore be measured out under atmospheric conditions. Oxygen can be removed in the final step before polymerization is started. This speed up in reaction preparation alone justifies the switch in RDRP system. Further, the use of the RAFT without a copper ion dependent PRE solves the problem of peptide backbone metal interaction.[112] To prevent any side reactions between the sulfur atom the cysteine (CKFKFQF) the peptide KFKFQF was chosen as peptide for the RAFT-macroinitiator.

The synthesis was done as shown in **Scheme 12** and after quenching of the reaction the Kaiser test showed that stoichiometric coupling had occurred. The micro cleavage and following ESI-MS showed that the desired product had formed and therefore the preparative HPLC purification was done. After freeze drying the product containing fractions from HPLC, purity was confirmed by LCMS, as shown in **Figure 29.**

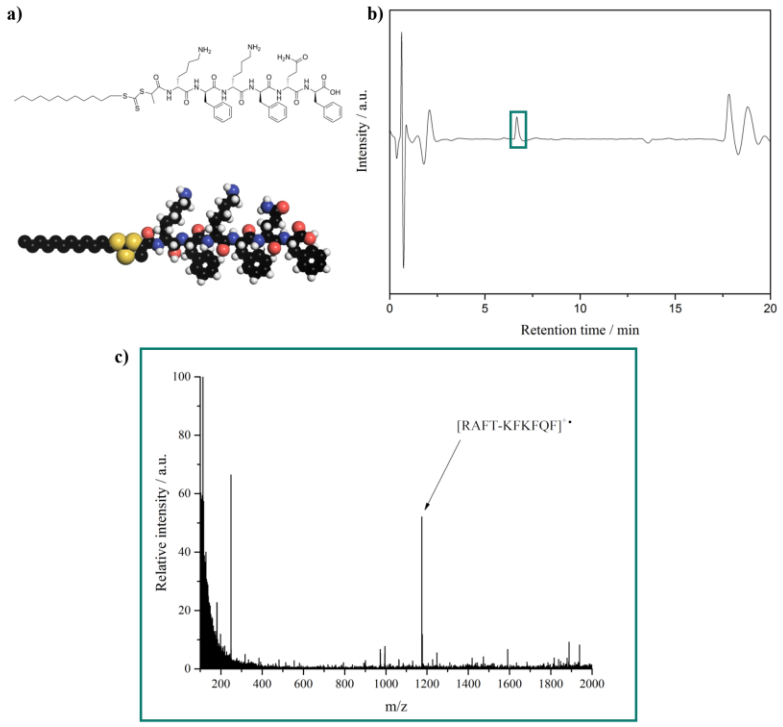

Figure 29: a) On the top the skeletal formula of RAFT-KFKFQF and on the bottom the space-fill model. b) The LC-trace of the LC-MS measurement after the purification of the peptide with the preparative HPLC. c) the corresponding mass spectrum to the LC-trace in a). The corresponding data to the mass spectrum is in ***Table 9****Table 4 in the Appendix.*

3.3.4. RAFT-Polymerization

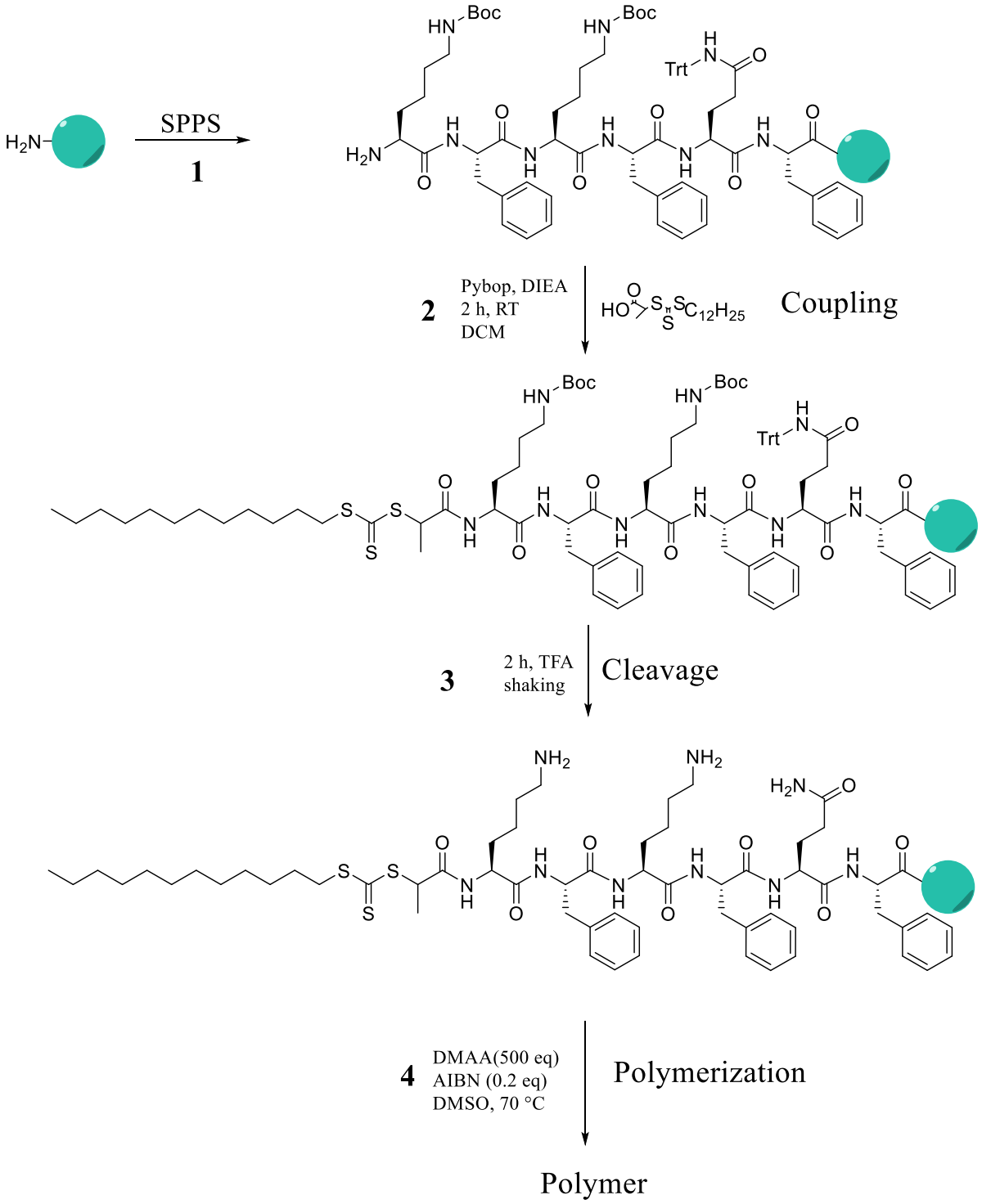

Scheme 13 The synthetic pathway for the RAFT polymerization. The 1st step of the reaction is the SPPS. The 2nd the Raft-Agent is coupled to the N-terminus of the peptide KFKFQF. In the 3rd step is the cleavage of the peptide from the solid base with TFA. The 4th step shows the polymerization of DMAA with the RAFT-macroinitiator.

The last step to prove the feasibility of the RAFT polymerization with the peptide based macroinitiator, was of course polymerization. DMAA was chosen as monomer because of its fast polymerization rate in radical polymerizations. The reaction media, DMSO, was chosen for its capability to easily solve the RAFT-macroinitiator, but of course for later application in living organisms a water based polymerization has to be the goal.[113] The polymerization experiment was carried out as shown in **Scheme 13**, the sample taken for 1H-NMR and GPC at 1 h were promising because of its visible viscosity. The NMR results were analyzed and a nearly complete consumption (over 90 %) of the monomer can be shown in **Figure 30**, the intensity of the vinyl peaks at 7.50, 6.07 and 5.65 ppm decreased nearly complete. The GPC results prove a successful RAFT polymerization, after nearly complete consumption of the monomer, the dispersity is with 1.33 in the margin of a RDRP. The results of the GPC are shown in **Table 2**.

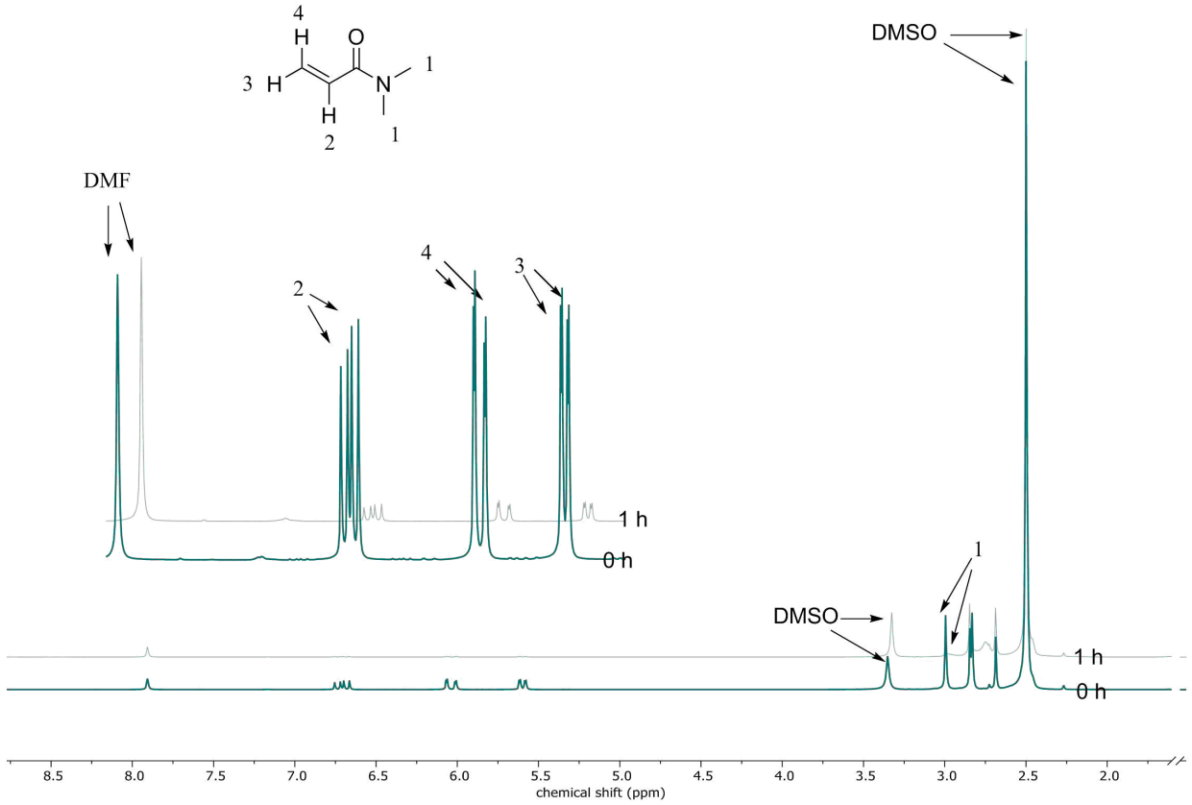

Figure 30: ^{1}H-NMR spectra of the kinetic measurements of the RAFT polymerization. The spectra compared are from samples taken at 0 h and 1 h. The ^{1}H-NMR spectra were measured in deuterated dimethyl sulfoxide (DMSO-d6).

Table 2: Analytical data of the RAFT-polymerization with the KFKFQF peptide-macroinitiator.

Monomer consumption after 1 h		96.1%
GPC Data 1h		
M_n	M_w	D
50636.70	67384.40	1.33

4. Summary

Over the course of this diploma thesis, a deeper understanding of the self-assembly behavior of the investigated peptides could be achieved. It was possible to show how the balance between attractive and repulsive forces involved in the self-assembling process could be actively influenced, to change the resulting supramolecular structures.

Of the investigated parameters the peptide sequence, the pH value and the salt concentration showed the strongest influence on the self-assembling behavior. The addition of the methionine or the cysteine onto the sequence KFKFQF greatly improved the self-assembly behavior of the peptide, leading to the robust formation of fibrous structures. As shown in **Figure 17** on samples solved in MilliQ water and PBS buffer solution. The addition of cysteine to the peptide sequence most likely enables the assembled supramolecular structures to form disulfide bridges, which enhance the aggregation. In the case of the added methionine the peptide backbone of alternating hydrophobic and hydrophilic amino acids is extended by a hydrophobic one, which may be is responsible for the increase in self-assembly tendency. The pH value had a great impact on the self-assembly behavior of the peptides, because it directly impacts the attractive and repulsive interactions within the supramolecular structure. An example is the peptide MKFKFQF in **Figure 19**, where switching the pH value from 7.4 to 5, increases the hydrophilic character of the peptide. Fibril-like structures at pH 7.4 were observed to further grow further in width and transform into twisted ribbons. By increasing the salt concentration this effect can be further enhanced as shown in **Figure 20**. The salt ions shield the charges and as a result the repulsive charge interaction decreases further. As a consequence, the twisted ribbons grow wider and form helical ribbons.

To investigate the effect of the polymer corona on the self-assembly behavior of the peptides different polymerization methods were tested. The RAFT polymerization pathway, shown in **Scheme 13**, proved to be the most successful. A RAFT-agent was coupled to the peptide KFKFQF and a polymerization with the monomer DMAA was achieved. Unfortunately, due to difficulties in sample preparation, the resulting morphology could not be analyzed during the final stages of this thesis. But now with the pathway for polymerization known it is possible

to produce more of the modified peptide and optimize the TEM sample preparation for the polymer-peptide hybrid.

To build further on the results of this thesis, other parameters capable of influencing self-assembly, should be investigated. Especially, the incorporation of a polymer corona promises enhanced control over the properties of the resulting supramolecular structures. The result will enable future research into the application as gen transfer agent, as for this application the fibrillar structure is needed. Therefore, the gained information about the influencing parameter will be helpful.

5. Experimental

5.1. Materials

All organic solvents were obtained from Fisher Scientific. They had HPLC grade or analytical grade and were used without further purification. MilliQ water used was produced with the Millipore purification system.
Reagents used in the syntheses were acquired from Fisher Scientific, Alfa Aesar and Sigma Aldrich and were used without further purification.

5.2. Characterization Methods

5.2.1. Nuclear Magnetic Resonance (NMR) Spectroscopy

NMR analysis was performed on a Bruker Avance 300 (^{1}H-NMR: 350 MHz). All spectra were collected using 32 scans. The chemical shift (δ) are reported in parts per million (ppm) and the scale is referred to the standard of tetramethylsilane (TMS). The solvents used were either deuterium oxide (D_2O) or deuterated dimethyl sulfoxide (DMSO-d6) and are assigned with the respective spectra.
All resulting spectra were analyzed using MestReNova (Verson: 12.0.3-21384).

5.2.2. Mass Spectrometry (MS)

Mass spectra for the reaction control of the micro cleavage were measured with an electrospray ionization (ESI) device from Advion (expression CMS). The injection method was per syringe driver directly into the chamber.
The mass spectra to control the success of the purification, as well as the corresponding LC-trace were taken on a Shimadzu (LC-MS 2020) equipped with an electrospray ionization (ESI) source, a SPD-20A UV-Vis detector and a Kinetex EVO C18 column (2.1x 50 mm, 2.6 µm).

5.2.3. Transmission Electron Microscopy (TEM)

TEM images were measured on the JEOL JEM1400 transmission electron microscope, the emission source was a tungsten needle cathode operating at 120 kV. The samples were prepared on commercially available grids. The images were recorded with a 2k CCD camera (Gatan US1000).

5.2.4. High Performance Liquid Chromatography (HPLC)

High performance liquid chromatography (HPLC) was carried out using Shimadzu Analytical HPLC system for purification of the peptides and their derivatives. The column used was a Phenomenex® (Gemini® 5 µm NX-C18 11 Å) (150 x 30 nm). The flow rate used were 25 mL/min and the eluent was a mixture of acetonitrile (ACN, HPLC Grade) and MilliQ water.

5.2.5. Solid Phase Peptide Synthesis (SPPS)

SPPS was carried out on a Liberty Blue^{TM} peptide synthesizer (CEM Corporation.). HPLC-grade solvents were used in the reactions.

5.3. Synthetic Procedures

5.3.1. Peptide-Synthesis

5.3.1.1. Standard Micro Cleavage for Reaction Control

A few beads of resin with coupled peptide were put into a 1.5 mL Eppendorf tube and 200 µL TFA are was added, after a few minutes the liquid turned yellow. The reaction mixture was then shaken for 2 h at room temperature. Subsequently, the TFA was evaporated *via* air stream in the fume hood.

To the solid residue, a mixture of MilliQ water (100 µL) and Acetonitrile (100 µL) was added. This mixture was shaken for a few minutes before being centrifuged to separate solid residue and supernatant. The supernatant was carefully extracted and then subjected to ESI-MS analysis

5.3.1.2. Standard Cleavage Procedure Peptides

The peptide cleavage method was adapted from a technical bulletin which combined the work of different groups to create a manual for different cleavage pathways.[114-116] All the peptides and derivatives were cleaved following the same procedure with only little deviation for the CFKFQF peptide. To cleave the peptide from the resin a cleavage cocktail from TFA, MilliQ and TIPS was mixed as described in their work, with a ratio of 95:5:5. The cleavage cocktail was shaken for a few minutes and then the resin and the cocktail were united in a snap cover vial. The reaction mixture was shaken for 2 h. The mixture was then filtered using a fritted glass (POR 3, 16 – 40 µm) and the resin globes were washed once with TFA.
The filtrate was partly evaporated with a rotary evaporator. In the case of the peptides KFKFQF, MKFKFQF, and the derivatives, the partly evaporated filtrate was put in cooled diethyl ether (-20 °C), so that the peptide could precipitate. This didn't work in the case of CKFKFQF and therefore the crude peptide was obtained after total evaporation of the TFA with the rotary evaporator.

5.3.1.3. Standard Preparative HPLC Method for Peptides Purification

The solid sample mixed in water, dissolution was assisted with the Horn Sonicator (Branson Digital Sonifier®, 250-D). If this procedure did not work ACN was added in steps until the sample could be dissolved. In the case of KFKFQF and MKFKFQF pure MilliQ water was enough to dissolve the solid complied. In the case of CKFKFQF and the ATRP-macroinitiator, the mixture of 30:75 ACN to MilliQ water was used. In the case of the RAFT-macroinitiator a mixture of 25:70 ACN to MilliQ water was used, as described in the literature.[117] After this step the solution was centrifuged (Beckman Coulter), at 4000 RPM for 10 min. The residue

and solution were then separated by decantation. Directly before the sample was put into the auto sampler of the HPLC it was filtered with a syringe filter (Fischerbrand, PTFE 0.2 µm).
For every new peptide the HPLC elution program needed to be adjusted starting from a standard method. Therefore, the HPLC would run the first 5 min with the mixture the sample was solved in, then the ACN percentage was ramped up to 100% over 70 min, to be sure every significant LC-peak could be collected. After the eluent reached 100% ACN, the method would ramp down the eluent mixture to the parameter of used, to solve the sample and run it for 5 min. After the collected fractions were analyzed by ESI-MS, the HPLC method could be optimized for every individual sample.
It turned out, that the use of the syringe filter was removing large quantities of product, which is why in the second half of this project an optimized method for sample preparation of the preparative HPLC was used. To avoid clogging the column with large particles the syringe filter step in the sample preparation was supplemented with an extra step of centrifuging of the sample.

5.3.1.4. KFKFQF (JJA6)

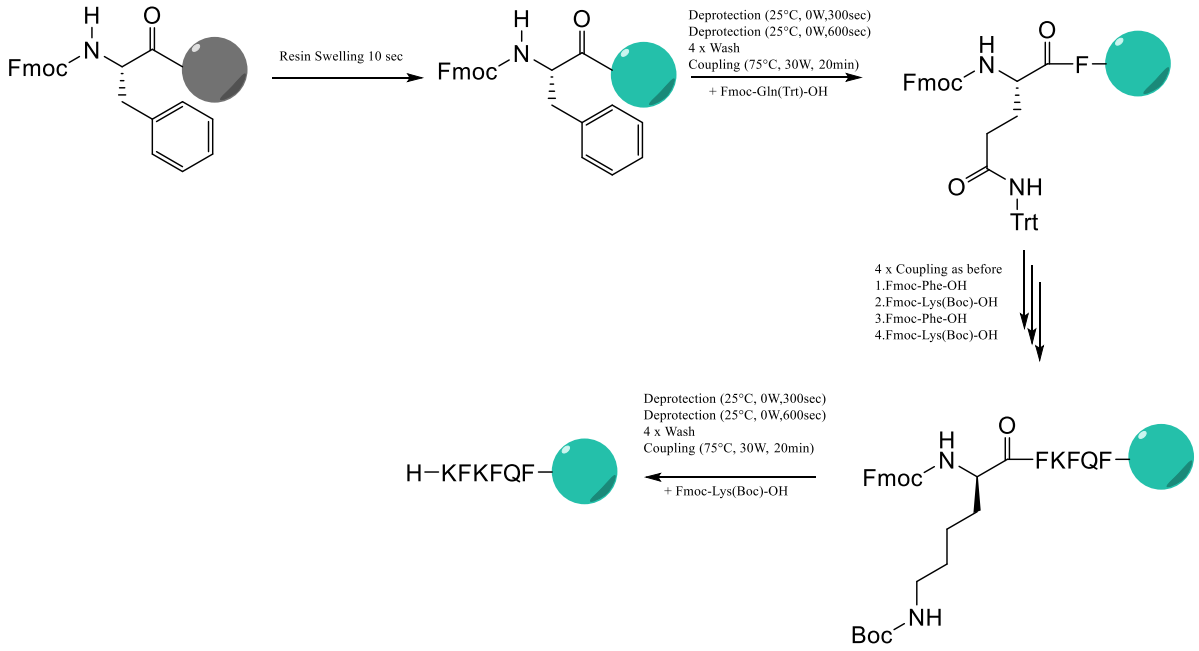

Scheme 14: Reaction scheme of the automated microwave peptide synthesis using the Liberty Blue™ program for the synthesis of the peptide sequence KFKFQF. The amino acids were protected the complete time, lysine with Boc and glutamine with Trt.

The syntheses were carried out using an automated microwave peptide synthesizer (Liberty Blue™). The Fmoc-Phe-Wang-resin (0.65 mmol/g) (0.5 mmol, 769 mg, 1 eq) was allowed to swell for 1h in DMF in a snap cover vial. During this time, the synthesizer was equipped with the amino acids, glutamine (Fmoc-Gln(Trt)-OH) (0.5 mmol, 1470 mg, 1 eq in mL 12 DMF), (lysine Fmoc-L-Lysin-(Boc)) (1 mmol, 2250 mg, 2 eq in 24 mL DMF), and phenylalanine (Fmoc-Phe-OH) (1 mmol, 1860 mg, 24 eq in 2 mL DMF), necessary for synthesis. Then, the synthesizer was filled with DMF (solvent, 400 mL), piperidine (40 mL 160 mL in DMF), PyBOP (6245 mg in 24 mL DMF) and DIEA (4.2 mL in 7.8 mL DMF). After the swelling was completed, the resin was filled in the reaction chamber of the synthesizer and the snap cover vial was washed three times with DMF. Then, the synthesizer program was started which is shown in **Scheme 14**, which describes the program used in the syntheses. After the program finished, the resin was transferred to a snap cover vial and the reaction chamber was washed with DCM. The resin was washed several times with DCM over a fritted glass (POR 3, 16 – 40 µL). For reaction control a micro cleavage was done of every batch, followed by an ESI-

MS measurement, as described in the **chapter 5.3.1.1**. Then, the resin was vacuum dried on the Schlenk line. The resin was put under argon and stored at -20 °C.

In preparation for the purification of the peptide, a cleavage procedure was done as described in **chapter 5.3.1.2**. Then, the peptide was purified *via* preparative HPLC with the method described in the **chapter 5.3.1.3**.

5.3.1.5. MKFKFQF (DF5)

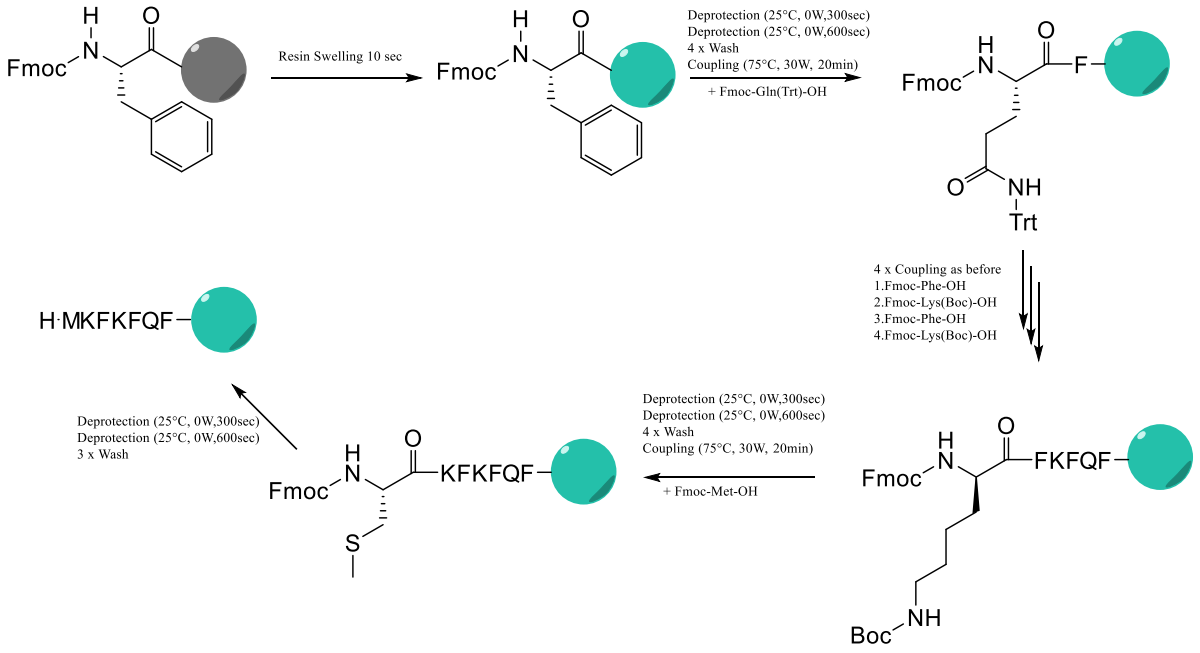

Scheme 15: Schema of the automated microwave peptide synthesizer from Liberty Blue™ program for the synthesis of the peptide sequence MKFKFQF.

The syntheses were carried out using an automated microwave peptide synthesizer from Liberty Blue™. The Fmoc-Phe-Wang-resin (0.65 mmol/g) (0.5 mmol, 769 mg, 1 eq) was allowed to swell for 1 h in DMF in a snap cover vial. During this time, the synthesizer was equipped with the amino acids, glutamine (Fmoc-Gln(Trt)-OH) (0.5 mmol, 1470 mg, 1 eq in mL 12 DMF), (lysine Fmoc-L-Lysin-(Boc)) (1 mmol, 2250 mg, 2 eq in 24 mL DMF), methionine (Fmoc-Mer-OH) (0.5 mmol, 900 mg, 1 eq in 12 mL DMF), and phenylalanine (Fmoc-Phe-OH) (1 mmol, 1860 mg, 2 eq in 24 mL DMF), necessary for synthesis. Then the synthesizer was filled with DMF (solvent, 400 mL), piperidine (40 mL in 160 mL DMF),

PyBOP (7550 mg in 29 mL DMF) and DIEA (5.2 mL in 9.8 mL DMF). After the swelling was completed, the resin was filled in the reaction chamber of the synthesizer and the snap cover vial was washed three times with DMF. Then the synthesizer program was started which is shown in **Scheme 15**Error! Reference source not found., which describes the program used in the syntheses. After the program was finished, the resin was transferred to a snap cover vial and the reaction chamber was washed with DCM. The resin was washed several times with DCM over a fritted glass (PRO 3, 16 – 40 µL). Of every patch a micro cleavage with following ESI-MS was done for reaction control, as described in the **chapter 5.3.1.1**. Then, the resin was vacuum dried on the Schlenk line. The resin was put under argon and stored at -20 °C.
In preparation for the purification of the peptide cleavage procedure was done as described in **chapter 5.3.1.2**. Then, the peptide was purified *via* preparative HPLC with the method described in the **chapter 5.3.1.3.**

5.3.1.6. CKFKFQF (BL4)

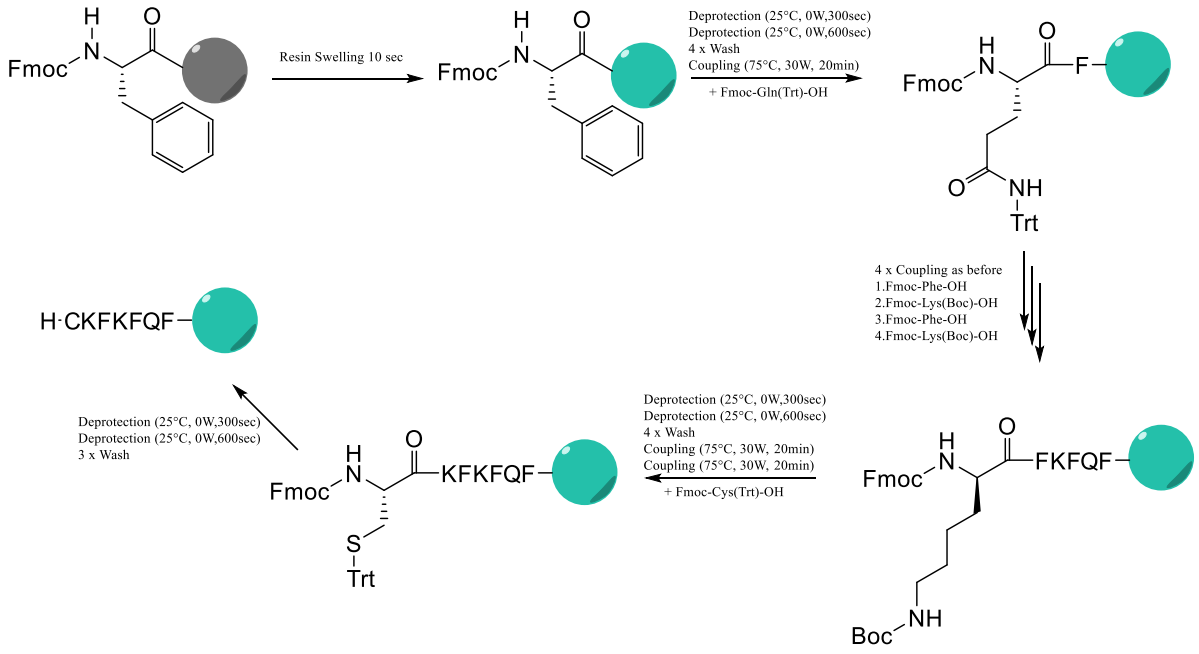

Scheme 16: Schema of the automated microwave peptide synthesizer from Liberty Blue™ program for the synthesis of the peptide sequence CKFKFQF.

The syntheses were carried out using an automated microwave peptide synthesizer (Liberty Blue™). The Fmoc-Phe-Wang-resin (0.65 mmol/g) (0.5 mmol, 769 mg, 1 eq) was allowed to swell for 1 h in DMF in a snap cover vial. During this time, the synthesizer was equipped with the amino acids, cysteine (Fmoc-Cys(Trt)-OH) (1 mmol, 2820 mg, 2 eq in 24 mL DMF,) glutamine (Fmoc-Gln(Trt)-OH) (0.5 mmol, 1470 mg, 1 eq in mL 12 DMF), (lysine Fmoc-L-Lysin-(Boc)) (1 mmol, 2250 mg, 2 eq in 24 mL DMF), and phenylalanine (Fmoc-Phe-OH) (1 mmol, 1860 mg, 2 eq in 24 mL DMF), necessary for synthesis. Then the synthesizer was filled with DMF (solvent, 400 mL), piperidine (40 mL in 160 ml DMF), PyBOP (8847 mg in 34 mL DMF) and DIEA (5.9 mL in 11.1 mL DMF). After the swelling was completed, the resin was filled in the reaction chamber of the synthesizer and the snap cover vial was washed three times with DMF. Then the synthesizer program was started which is shown in **Scheme 16** and describes the program used in the syntheses. After the program finished, the resin was transferred to a snap cover vial and the reaction chamber was washed with DCM. The resin was washed several times with DCM over a fritted glass (POR 3, 116 – 40 µL). Of every patch a micro cleavage with following ESI-MS was done for reaction control, as described in the **chapter 5.3.1.1**. Then, the resin was vacuum dried on the Schlenk line. The resin was put under argon and stored at -20 °C.

In preparation for the purification of the peptide, a cleavage procedure was done as described in **chapter 5.3.1.2**. Then, the peptide was purified *via* preparative HPLC with the method described in the **chapter 5.3.1.3**.

5.3.2. Peptide-Initiator Synthesis

5.3.2.1. ATRP-Initiator

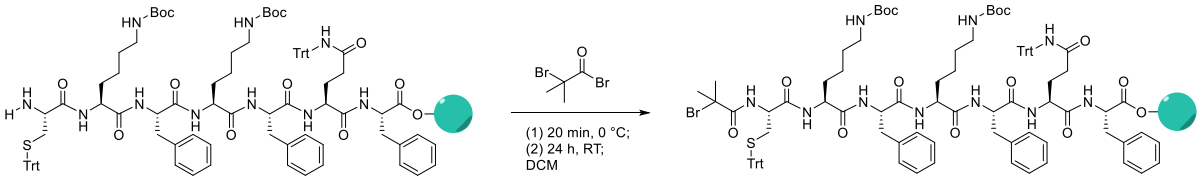

Scheme 17: Schematic representation of the coupling reaction of the peptide CKFKFQF with the ATRP-agent (α-Bromoisobutyryl bromide) in DCM, resulting in the ATRP-macroinitiator (Bib-CKFKFQF).

The peptide on resin beads (0.22 mmol) was transferred into a 250 mL two-necked flask with DCM (60 mL, solvent). Then the reaction mixture was cooled with an ice bath. Into the cooled mixture DIEA (2.2 mmol, 383 µL, 10 eq) was added. The α-Bromoisobutyryl bromide (1.1 mmol, 136 µL, 5 eq) was slowly and dropwise added into the reaction mixture, which was then stirred still for 20 min. under cooling of the ice bath. The ice bath was removed and after 40 min the solution started to turn light red. A second dosage of α-Bromoisobutyryl bromide (50 µL) was added and the reaction mixture stirred for 24 h. On the next day the reaction mixture had turned to a clear red color. The mixture was filtered over fritted glass and the solid washed with DCM.

The resin was dried under reduced pressure using the Schlenk line and a few beads of resin were used for a standard micro cleavage. Then the product was purified with the respective HPLC method.

5.3.2.2. RAFT-Initiator

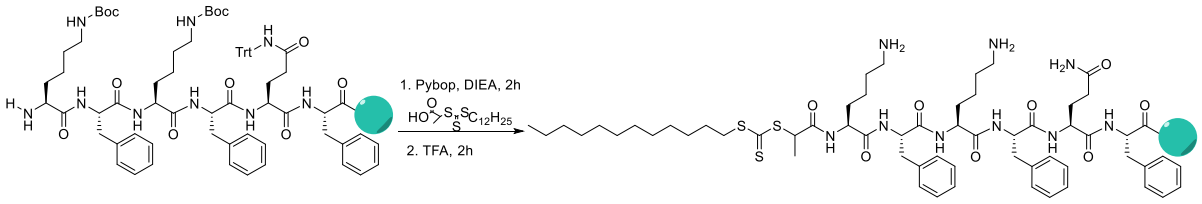

Scheme 18: Schematic representation of the coupling reaction of the peptide KFKFQF with the RAFT-agent (2-(Dodecylthiocarbonothioylthio)propionic acid) in DCM, resulting in the RAFT-macroinitiator (RAFT-KFKFQF).

The RAFT-initiator was synthesized according to the literature procedure.[117] The peptide sequence KFKFQF was used which was still linked to the resin during initiator coupling. It was filled into a snap cover vial (0.35 mmol, 940 mg, 1 eq) and allowed to swell in DCM for 1 h. In a second snap cover vial the RAFT-Agent (2-(Dodecylthiocarbonothioylthio)propionic acid) (1.4 mmol, 491 mg, 4 eq), PyBop (1.33 mmol, 692 mg, 3.8 eq) and DCM (50 mL, solvent) were combined. The swelled resin was added to the second snap cover vial and DIEA was added (4.9 mmol, 853 µL, 14 eq). The reaction mixture was stirred for 2 h at room temperature. The reaction was then stopped by filtration. The residue was cleaned by washing several times with DCM. A few resin beads were taken for micro cleavage and Kaiser Test.

The peptide was then cleaved from the resin by standard procedure and then purified by HPLC according to the literature procedure.[117]

5.3.3. Peptide-Hybrid Polymerization

5.3.3.1. Peptide-Hybrid Synthesis *via* ATRP-Polymerization

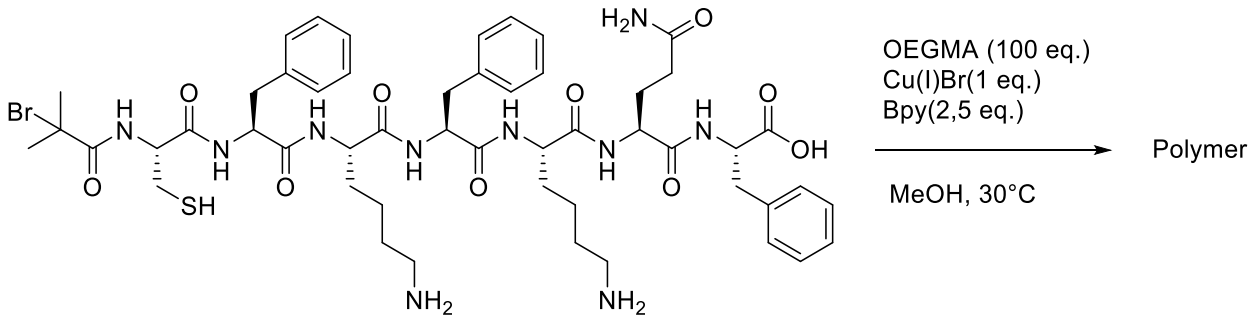

Scheme 19: Schematic representation of the ATRP of the Bib-CKFKFQF-macroinitiator with the monomer OEGMA and the catalyst system cupper bromide and bipyridin in methanol.

Two Schlenk flasks were dried and degassed using the Schlenk line. The ATRP-Peptide-Initiator (0.005 mmol, 5,47 mg, 1 eq), Cu(I)Br (0.005 mmol, 0.718 mg, 1 eq) and Bpy (bipyridin) (0.0125 mmol, 1.95 mg, 2,5 eq) were put under argon counterstream in one of the Schlenk flasks. Vacuum was drawn on the Schlenk flask and then again an argon atmosphere was established. $OEGMA_{300}$ (0.5 mmol, 150 mg, 100 eq) was separated from its inhibitor by means of an alox-flash-column. The $OEGMA_{300}$, DMF (200 µL, NMR-standard) and methanol (1 mL, solvent) were put into the second Schlenk flask and were degassed *via* three freeze thaw cycles. Then under argon atmosphere the solution from the second flask was transferred *via* syringe to the first flask. The reaction mixture changed the color to brown. After the combination of these two the mixture immediately was degassed again *via* two freeze thaw cycles. The reaction mixture was then stirred for 4 h at 30 °C. Samples were taken at 0 h, then at 2 h and at 4 h for analyzation with NMR and GPC.

5.3.3.2. Peptide-Hybrid synthesis *via* RAFT-Polymerization

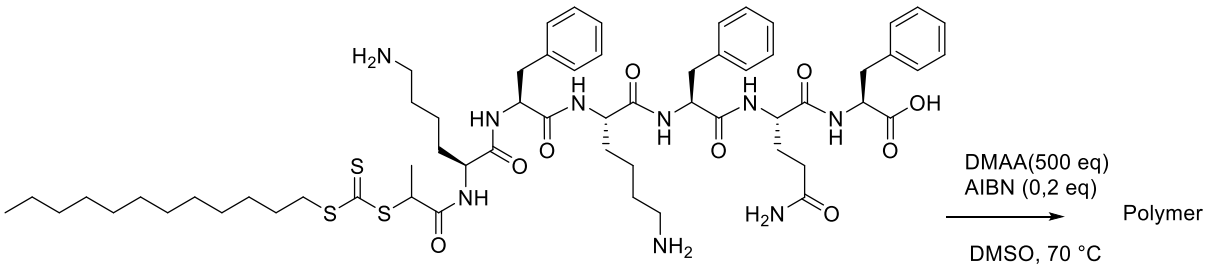

Scheme 20: Schematic representation of the RAFT polymerization of the RAFT-KFKFQF-macroinitiator with the monomer DMAA and the initiator AIBN in DMSO.

The reaction was carried out under argon atmosphere. The RAFT-peptide-initiator (0.0025 mmol, 2.94 mg, 1 eq) was put into a small Schlenk flask with a micro stirrer. DMAA (1.25 mmol, 124 mg, 0.2 eq), DMSO (322 µL, solvent) and DMF (50 µL, NMR, standard) were added to the mixture. An AIBN stock solution was made and the AIBN was added (0.0005 mmol, 0.082 mg, 0.2 eq). The reaction mixture was degassed *via* three freeze thaw cycles. The solution was then stirred for 2 h by 70 °C and quenched by exposure to atmosphere.

5.3.4. Standard Preparation Pathway and Preparation of the TEM Samples

The samples for the TEM measurement were prepared using the following procedure. At first a stock solution was prepared with 1 mg of the respecting peptide in 100 µL DMSO or MilliQ water. In the second step 10 µL of the stock solution was added to 90 µL MilliQ water or PBS solution. Then the pH value was adjusted, in the case of lowering it by adding 0.1 M HCl solution and elevated through adding of 0.1 M NaOH solution. Some samples were further treated using temperature annealing in a thermal cycler (MyCycler^{TM} thermal cycler). The same procedure was repeated for each trial, the samples were heated for 30 min at 80 °C and then over 60 min cooled 1 °C per min.

The samples were then put onto to a TEM grid (S 162-3) after 4 min the excess solution was carefully removed. The TEM grid was put for 2 min on a droplet of a 4 % Uranyl acetate

solution for staining. After that the grid was put on a droplet of MilliQ water to remove excess Uranyl acetate solution, this step was repeated 3 times.

5.3.5. TEM: Oxidation for Kinetic Study

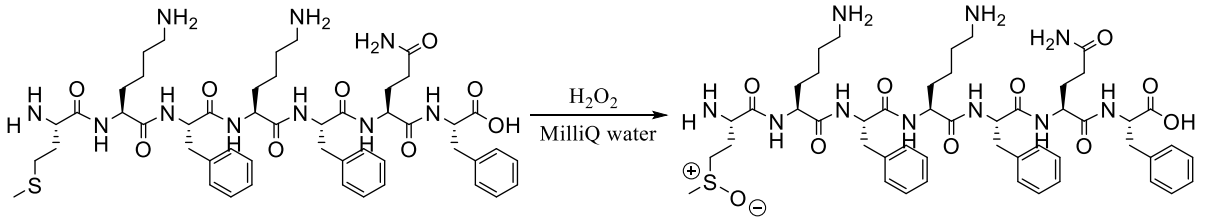

Scheme 21: Schematic representation of the oxidation reaction of the peptide MKFKFQF with H_2O_2 in MilliQ water. Yielding the oxidized form of the peptide.

The reaction was adapted from the literature procedure.[79] The peptide (0.003 mmol, 2.29 mg, 2 eq) and MilliQ water (3 mL, solvent) were added to a snap cover vial. The mixture was then shaken until the peptide was completely dissolved. Then the H_2O_2 (0.210 mmol, 6.44 µL, 70 eq) was added to the solution. The reaction mixture was stirred at room temperature for 5.5 h. During this time, samples were taken (at 0 min, 5 min, 90 min, 180 min and 330 min) and directly measured with the LCMS. The sample volume was 20 µL and the samples were diluted fortyfold and submitted for the LCMS analysis.

With the resulting data the conversion rate was calculated and then the time was calculated to have a conversion of approximately 25%, 50% and 75%. The corresponding times are listed in **Table 3**. The reaction in **Scheme 21** was then repeated 3 times and quenched at the respective time for the desired conversion. The crude mixture was the freeze dried. The resulting solid samples were then prepared with the standard partway for self-assembling and investigated in the TEM.

Table 3: With Origin (9.1) calculated reaction times to achieve the desired conversion of peptide into oxidized peptide.

Time /min	Percent oxidized product /%
23	~25
76	~50
236	~75

A. APPENDIX

A.1. Additional Experimental Data

A1.1. ATRP-Initiator

Table 4: Experimental and theoretical data from the mass spectrum of the LCMS analysis of the ATRP-CKFKFQF-macroinitiator.

	experimental		theoretical		
	m/z	I/ %	m/z	I/ %	Δm/z
Peak1[CKFKFQF+2H]2^{+}	548.3	32.7	548.2	100	0.1
Peak2[CKFKFQF+2H]2^{+}	549.0	100.0	548.7	55.2	0.3
Peak3[CKFKFQF+2H]2^{+}	549.6	16.4	549.2	97.3	0.4
Peak1[CKFKFQF+H]$^{+}$	1095.5	75.4	109.4	100	0.1
Peak2[CKFKFQF+H]$^{+}$	1096.5	57.1	1096.5	55.2	0.1
Peak3[CKFKFQF+H]$^{+}$	1097.5	100.0	1097.4	97.3	0.1
Peak4[CKFKFQF+H]$^{+}$	1098.5	52.2	1098.4	53.7	0.1
Peak5[CKFKFQF+H]$^{+}$	1099.5	24.3	1099.4	14.7	0.1
Peak1[CKFKFQF+Na]$^{+}$	1117.5	76.1	1117.4	100	0.1
Peak2[CKFKFQF+Na]$^{+}$	1118.5	47.3	1118.4	55.2	0.1
Peak3[CKFKFQF+Na]$^{+}$	1119.4	100.0	1119.4	97.3	0.0
Peak4[CKFKFQF+Na]$^{+}$	1120.5	51.5	1120.4	53.7	0.1
Peak5[CKFKFQF+Na]$^{+}$	1121.5	25.7	1121.4	14.7	0.1
Peak6[CKFKFQF+Na]$^{+}$	1122.5	11.3	1122.4	9.8	0.1

A1.2. CKFKFQF

Table 5: Experimental and theoretical data from the mass spectrum of the LCMS analysis of the peptide CKFKFQF.

	experimental		theoretical		
	m/z	I/ %	m/z	I/ %	Δm/z
Peak1 [CKFKFQF]$^{+\cdot}$	945.5	100	945.5	100	0.0
Peak2 [CKFKFQF]$^{+\cdot}$	946.4	70	946.5	51	0.1
Peak3 [CKFKFQF]$^{+\cdot}$	947.4	26	947.5	13	0.1

A1.3. KFKFQF

Table 6: Experimental and theoretical data from the mass spectrum of the LCMS analysis of the peptide KFKFQF.

	experimental		theoretical		
	m/z	I/ %	m/z	I/ %	Δm/z
Peak1 $[KFKFQF]^{+\cdot}$	842.7	100	842.46	100	0.24
Peak2 $[KFKFQF]^{+\cdot}$	843.7	49	843.46	48	0.24
Peak3 $[KFKFQF]^{+\cdot}$	844.7	8	844.46	11	0.24

A1.4. MKFKFQF

Table 7: Experimental and theoretical data from the mass spectrum of the LCMS analysis of the peptide MKFKFQF.

	experimental		theoretical		
	m/z	I/ %	m/z	I/ %	Δm/z
Peak1 $[MKFKFQF]^{+\cdot}$	973.5	100	973.50	100	0
Peak2 $[MKFKFQF]^{+\cdot}$	974.5	66	974.50	53	0
Peak3 $[MKFKFQF]^{+\cdot}$	975.5	29	976.50	14	0

A1.5. ATRP-Macroinitiator

Table 8: Experimental and theoretical data from the mass spectrum of the LCMS analysis of the ATRP-CKFKFQF-macroinitiator.

	experimental		theoretical		
	m/z	I/ %	m/z	I/ %	Δm/z
Peak1$[CKFKFQF+2H]2^{+}$	548.3	32.7	548.2	100	0.1
Peak2$[CKFKFQF+2H]2^{+}$	549.0	100.0	548.7	55.2	0.3
Peak3$[CKFKFQF+2H]2^{+}$	549.6	16.4	549.2	97.3	0.4
Peak1$[CKFKFQF+H]^{+}$	1095.5	75.4	109.4	100	0.1
Peak2$[CKFKFQF+H]^{+}$	1096.5	57.1	1096.5	55.2	0.1
Peak3$[CKFKFQF+H]^{+}$	1097.5	100.0	1097.4	97.3	0.1
Peak4$[CKFKFQF+H]^{+}$	1098.5	52.2	1098.4	53.7	0.1
Peak5$[CKFKFQF+H]^{+}$	1099.5	24.3	1099.4	14.7	0.1
Peak1$[CKFKFQF+Na]^{+}$	1117.5	76.1	1117.4	100	0.1
Peak2$[CKFKFQF+Na]^{+}$	1118.5	47.3	1118.4	55.2	0.1
Peak3$[CKFKFQF+Na]^{+}$	1119.4	100.0	1119.4	97.3	0.0
Peak4$[CKFKFQF+Na]^{+}$	1120.5	51.5	1120.4	53.7	0.1
Peak5$[CKFKFQF+Na]^{+}$	1121.5	25.7	1121.4	14.7	0.1
Peak6$[CKFKFQF+Na]^{+}$	1122.5	11.3	1122.4	9.8	0.1

A1.6. RAFT-Macroinitiator

Table 9: Experimental and theoretical data from the mass spectrum of the LCMS analysis of the peptide RAFT-macroinitiator.

	experimental		theoretical		
	m/z	I/ %	m/z	I/ %	Δm/z
Peak1 [RAFT-KFKFQF]$^{+\cdot}$	1176.8	100.0	1176.6	100.0	0.2
Peak2 [RAFT-KFKFQF]$^{+\cdot}$	1175.6	22.7	1175.6	61.9	0.0
Peak3 [RAFT-KFKFQF]$^{+\cdot}$	1176.7	22.6	1176.6	20.7	0.1

A1.7. Oxidation Studies

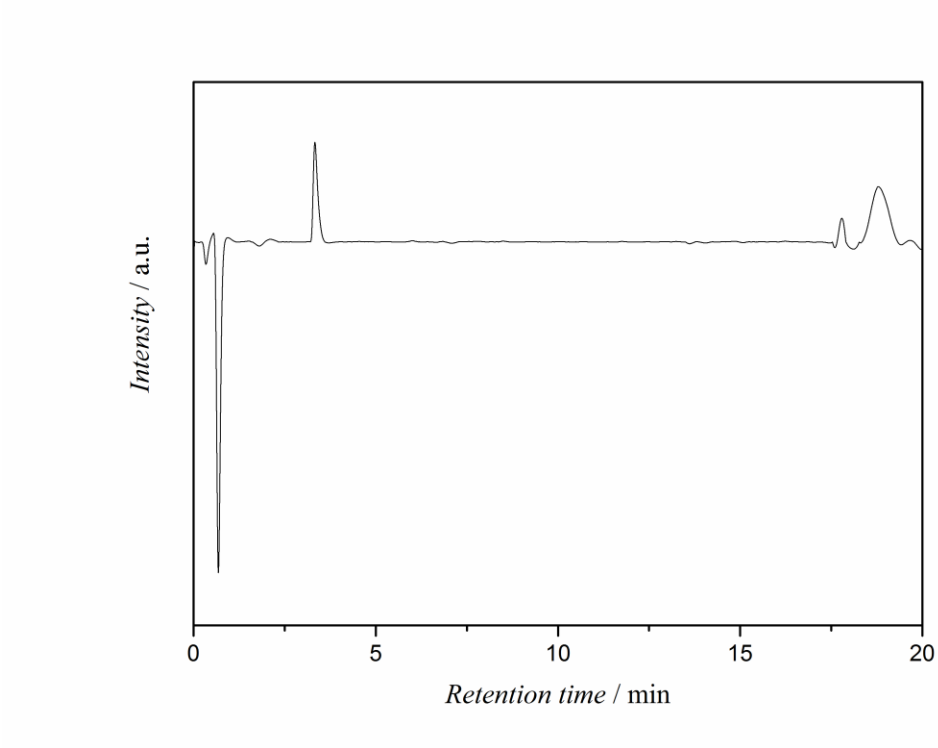

Figure 31: LC-trace oxidation of MKFKFQF after 0 min.

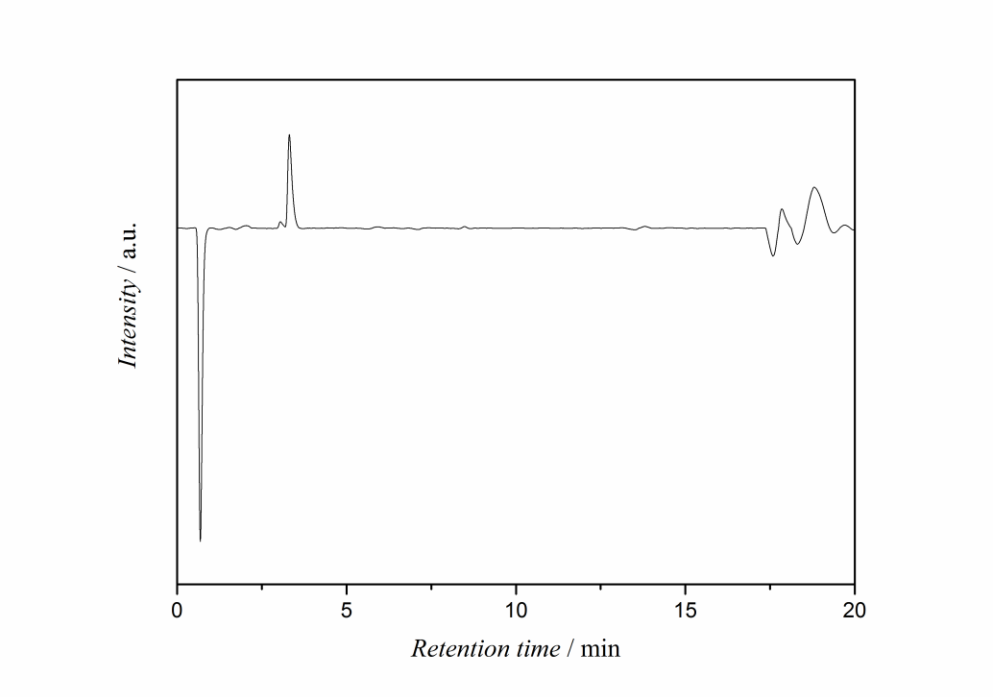

Figure 32: LC-trace oxidation of MKFKFQF after 5 min.

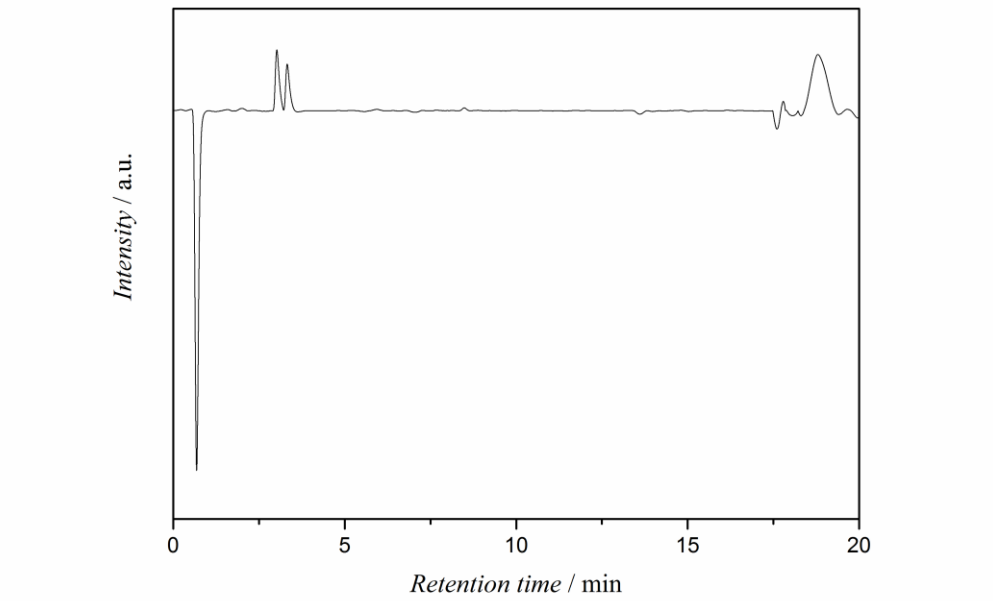

Figure 33: LC-trace oxidation of MKFKFQF after 90 min.

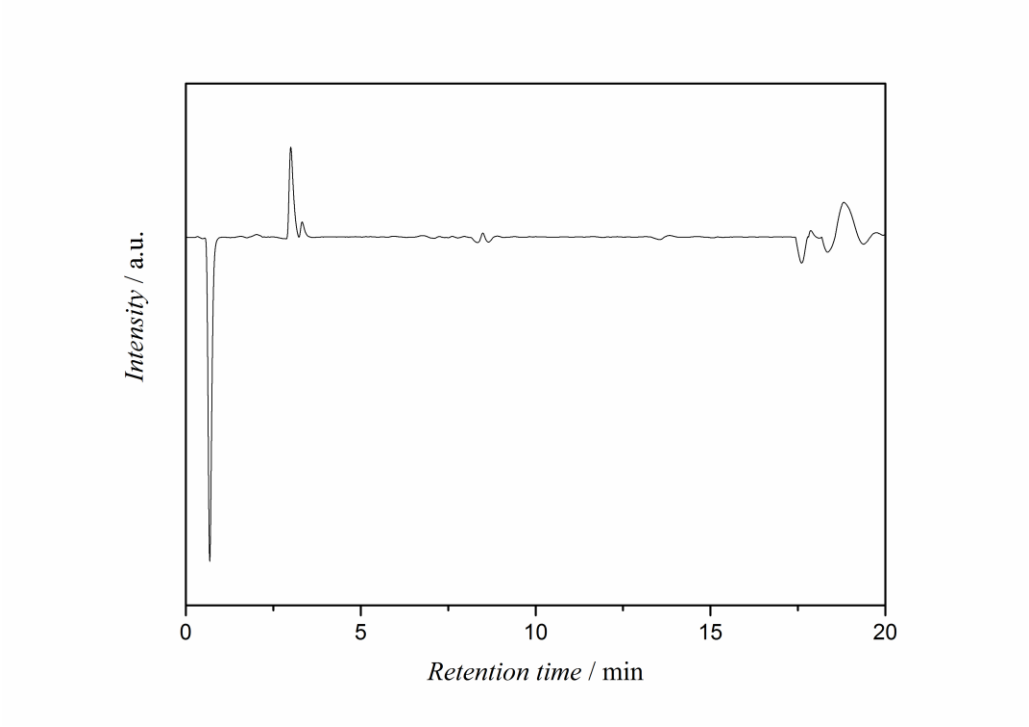

Figure 34: LC-trace oxidation of MKFKFQF after 180 min.

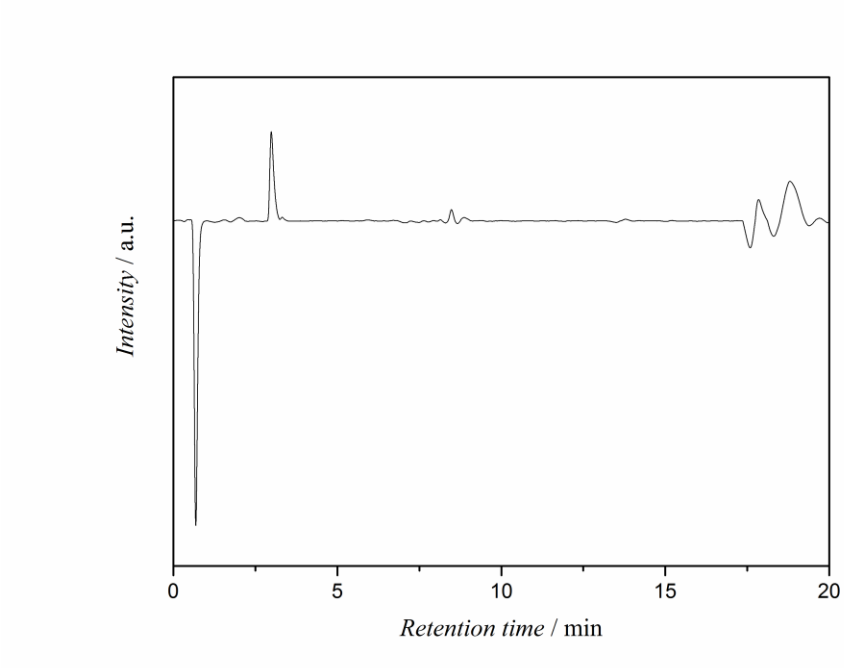

Figure 35: LC-trace oxidation of MKFKFQF after 330 min.

A.2. Table of Figures

A.3. Table of Schemes

A4. Table of Tables

A.4. Literature

1. Heemskerk, B.; Jorritsma, A.; Gomez-Eerland, R.; Toebes, M.; Haanen, J. B.; Schumacher, T. N., Microbead-assisted retroviral transduction for clinical application. *Hum Gene Ther* **2010,** *21* (10), 1335-42.

2. Zufferey, R.; Nagy, D.; Mandel, R. J.; Naldini, L.; Trono, D., Multiply attenuated lentiviral vector achieves efficient gene delivery in vivo. *Nat Biotechnol* **1997,** *15* (9), 871-5.

3. Montini, E.; Cesana, D.; Schmidt, M.; Sanvito, F.; Ponzoni, M.; Bartholomae, C.; Sergi Sergi, L.; Benedicenti, F.; Ambrosi, A.; Di Serio, C.; Doglioni, C.; von Kalle, C.; Naldini, L., Hematopoietic stem cell gene transfer in a tumor-prone mouse model uncovers low genotoxicity of lentiviral vector integration. *Nat Biotechnol* **2006,** *24* (6), 687-96.

4. Schambach, A.; Zychlinski, D.; Ehrnstroem, B.; Baum, C., Biosafety features of lentiviral vectors. *Hum Gene Ther* **2013,** *24* (2), 132-42.

5. Dunbar, C. E.; High, K. A.; Joung, J. K.; Kohn, D. B.; Ozawa, K.; Sadelain, M., Gene therapy comes of age. *Science* **2018,** *359* (6372).

6. Arnold, F.; Schnell, J.; Zirafi, O.; Sturzel, C.; Meier, C.; Weil, T.; Standker, L.; Forssmann, W. G.; Roan, N. R.; Greene, W. C.; Kirchhoff, F.; Munch, J., Naturally occurring fragments from two distinct regions of the prostatic acid phosphatase form amyloidogenic enhancers of HIV infection. *J Virol* **2012,** *86* (2), 1244-9.

7. Yolamanova, M.; Meier, C.; Shaytan, A. K.; Vas, V.; Bertoncini, C. W.; Arnold, F.; Zirafi, O.; Usmani, S. M.; Muller, J. A.; Sauter, D.; Goffinet, C.; Palesch, D.; Walther, P.; Roan, N. R.; Geiger, H.; Lunov, O.; Simmet, T.; Bohne, J.; Schrezenmeier, H.; Schwarz, K.; Standker, L.; Forssmann, W. G.; Salvatella, X.; Khalatur, P. G.; Khokhlov, A. R.; Knowles, T. P.; Weil, T.; Kirchhoff, F.; Munch, J., Peptide nanofibrils boost retroviral gene transfer and provide a rapid means for concentrating viruses. *Nat Nanotechnol* **2013,** *8* (2), 130-6.

8. Meier, C.; Weil, T.; Kirchhoff, F.; Munch, J., Peptide nanofibrils as enhancers of retroviral gene transfer. *Wiley Interdiscip Rev Nanomed Nanobiotechnol* **2014,** *6* (5), 438-51.

9. Lee, N. R.; Bowerman, C. J.; Nilsson, B. L., Effects of varied sequence pattern on the self-assembly of amphipathic peptides. *Biomacromolecules* **2013,** *14* (9), 3267-77.

10. Bowerman, C. J.; Nilsson, B. L., Self-assembly of amphipathic beta-sheet peptides: insights and applications. *Biopolymers* **2012,** *98* (3), 169-84.

11. Habibi, N.; Kamaly, N.; Memic, A.; Shafiee, H., Self-assembled peptide-based nanostructures: Smart nanomaterials toward targeted drug delivery. *Nano Today* **2016,** *11* (1), 41-60.

12. Rubert Perez, C. M.; Stephanopoulos, N.; Sur, S.; Lee, S. S.; Newcomb, C.; Stupp, S. I., The powerful functions of peptide-based bioactive matrices for regenerative medicine. *Ann Biomed Eng* **2015,** *43* (3), 501-14.

13. Gauthier, M. A.; Klok, H. A., Peptide/protein-polymer conjugates: synthetic strategies and design concepts. *Chem Commun (Camb)* **2008,** (23), 2591-611.

14. Castelletto, V.; Newby, G. E.; Hermida Merino, D.; Hamley, I. W.; Liu, D.; Noirez, L., Self-assembly of an amyloid peptide fragment–PEG conjugate: lyotropic phase formation and influence of PEG crystallization. *Polymer Chemistry* **2010,** *1* (4).

15. Couet, J.; Samuel, J. D.; Kopyshev, A.; Santer, S.; Biesalski, M., Peptide-polymer hybrid nanotubes. *Angew Chem Int Ed Engl* **2005,** *44* (21), 3297-301.

16. Sieste, S.; Mack, T.; Synatschke, C. V.; Schilling, C.; Meyer Zu Reckendorf, C.; Pendi, L.; Harvey, S.; Ruggeri, F. S.; Knowles, T. P. J.; Meier, C.; Ng, D. Y. W.; Weil, T.; Knoll, B., Water-Dispersible Polydopamine-Coated Nanofibers for Stimulation of Neuronal Growth and Adhesion. *Adv Healthc Mater* **2018,** *7* (11), e1701485.

17. Matyjaszewski, K.; Spanswick, J., Controlled/living radical polymerization. *Materials Today* **2005,** *8* (3), 26-33.

18. Coessens, V.; Pintauer, T.; Matyjaszewski, K., Functional polymers by atom transfer radical polymerization. *Progress in Polymer Science* **2001,** *26* (3), 337-377.

19. Siegwart, D. J.; Oh, J. K.; Matyjaszewski, K., ATRP in the design of functional materials for biomedical applications. *Prog Polym Sci* **2012,** *37* (1), 18-37.

20. Chen, C.; Thang, S. H., RAFT polymerization of a RGD peptide-based methacrylamide monomer for cell adhesion. *Polymer Chemistry* **2018,** *9* (14), 1780-1786.

21. Perrier, S., 50th Anniversary Perspective: RAFT Polymerization—A User Guide. *Macromolecules* **2017,** *50* (19), 7433-7447.

22. Hentschel, J.; Bleek, K.; Ernst, O.; Lutz, J.-F.; Börner, H. G., Easy Access to Bioactive Peptide–Polymer Conjugates via RAFT. *Macromolecules* **2008,** *41* (4), 1073-1075.

23. Trzebicka, B.; Szweda, R.; Kosowski, D.; Szweda, D.; Otulakowski, Ł.; Haladjova, E.; Dworak, A., Thermoresponsive polymer-peptide/protein conjugates. *Progress in Polymer Science* **2017,** *68*, 35-76.

24. Larnaudie, S. C.; Brendel, J. C.; Jolliffe, K. A.; Perrier, S., pH-Responsive, Amphiphilic Core–Shell Supramolecular Polymer Brushes from Cyclic Peptide–Polymer Conjugates. *ACS Macro Letters* **2017,** *6* (12), 1347-1351.

25. Wolf, K., Prahm, H. Harms, H. , Über den Ordnungszustand der Moleküle in Flüssigkeiten. . *Zeitschrift für Physikalische Chemie 36*, 237-287.

26. Lehn, J.-M., Supramolecular Chemistry -Scope and Perspectives Molecules, Supermolecules, and Molecular Devices (Nobel Lecture). *Angew Chem. Int. Ed.* **1988,** (27), 89-112.

27. Zhao, X.; Pan, F.; Xu, H.; Yaseen, M.; Shan, H.; Hauser, C. A.; Zhang, S.; Lu, J. R., Molecular self-assembly and applications of designer peptide amphiphiles. *Chem Soc Rev* **2010,** *39* (9), 3480-98.

28. Ulijn, R. V.; Smith, A. M., Designing peptide based nanomaterials. *Chem Soc Rev* **2008,** *37* (4), 664-75.

29. Fahy, E.; Subramaniam, S.; Murphy, R. C.; Nishijima, M.; Raetz, C. R.; Shimizu, T.; Spener, F.; van Meer, G.; Wakelam, M. J.; Dennis, E. A., Update of the LIPID MAPS comprehensive classification system for lipids. *J Lipid Res* **2009,** *50 Suppl*, S9-14.

30. Rothemund, P. W., Folding DNA to create nanoscale shapes and patterns. *Nature* **2006,** *440* (7082), 297-302.

31. Alberts, B., *Molecular Biology of the Cell*. CRC Press: 2017.

32. Anfinsen, C. B., Principles that Govern the Folding of Protein Chains. *Science* **1973,** *181* (4096), 223-230.

33. Dill, K. A.; MacCallum, J. L., The protein-folding problem, 50 years on. *Science* **2012,** *338* (6110), 1042-6.

34. Rose, G. D.; Fleming, P. J.; Banavar, J. R.; Maritan, A., A backbone-based theory of protein folding. *Proc Natl Acad Sci U S A* **2006,** *103* (45), 16623-33.

35. Fersht, A., *Structure and Mechanism in Protein Science: A Guide to Enzyme Catalysis and Protein Folding*. World Scientific Publishing Company Pte Limited: 2017.

36. Chan, W.; White, P. D., *Fmoc Solid Phase Peptide Synthesis*. Oxford University Press: 2000.

37. Chen, C.; Liu, K.; Li, J.; Yan, X., Functional architectures based on self-assembly of bio-inspired dipeptides: Structure modulation and its photoelectronic applications. *Adv Colloid Interface Sci* **2015,** *225*, 177-93.

38. Burgess, N. C.; Sharp, T. H.; Thomas, F.; Wood, C. W.; Thomson, A. R.; Zaccai, N. R.; Brady, R. L.; Serpell, L. C.; Woolfson, D. N., Modular Design of Self-Assembling Peptide-Based Nanotubes. *J Am Chem Soc* **2015,** *137* (33), 10554-62.

39. Boyle, A. L.; Woolfson, D. N., De novo designed peptides for biological applications. *Chem Soc Rev* **2011,** *40* (8), 4295-306.

40. Fleming, S.; Ulijn, R. V., Design of nanostructures based on aromatic peptide amphiphiles. *Chem Soc Rev* **2014,** *43* (23), 8150-77.

41. Smith, K. H.; Tejeda-Montes, E.; Poch, M.; Mata, A., Integrating top-down and self-assembly in the fabrication of peptide and protein-based biomedical materials. *Chem Soc Rev* **2011,** *40* (9), 4563-77.

42. De Santis, E.; Ryadnov, M. G., Peptide self-assembly for nanomaterials: the old new kid on the block. *Chem Soc Rev* **2015,** *44* (22), 8288-300.

43. Recio, C.; Maione, F.; Iqbal, A. J.; Mascolo, N.; De Feo, V., The Potential Therapeutic Application of Peptides and Peptidomimetics in Cardiovascular Disease. *Front Pharmacol* **2016,** *7*, 526.

44. Wang, Y.; Yi, S.; Sun, L.; Huang, Y.; Lenaghan, S. C.; Zhang, M., Doxorubicin-loaded cyclic peptide nanotube bundles overcome chemoresistance in breast cancer cells. *J Biomed Nanotechnol.* **2014** 445-54.

45. Hauser, C. A.; Zhang, S., Nanotechnology: Peptides as biological semiconductors. *Nature* **2010,** *468* (7323), 516-7.

46. Kholkin, A.; Amdursky, N.; Bdikin, I.; Gazit, E.; Rosenman, G., Strong piezoelectricity in bioinspired peptide nanotubes. *ACS Nano* **2010,** *4* (2), 610-4.

47. Hansen, S., Die Entdeckung der proteinogenen Aminosäuren von 1805 in Paris bis 1935 in Illinois. 2015.

48. Wagner, I.; Musso, H., New Naturally Occurring Amino Acids. *Angewandte Chemie International Edition in English* **1983,** *22* (11), 816-828.

49. Shafee, T. Wikipedia the free encyclopedia. https://upload.wikimedia.org/wikipedia/commons/5/5f/Protein_structure_(full).png (accessed 24.09.2018).

50. Astbury, W. T.; Dickinson, S.; Bailey, K., The X-ray interpretation of denaturation and the structure of the seed globulins. *Biochem J* **1935,** *29* (10), 2351-2360 1.

51. Astbury, W. T.; Reed, R.; Spark, L. C., An X-ray and electron microscope study of tropomyosin. *Biochem J* **1948,** *43* (2), 282-7.

52. Pauling, L.; Corey, R. B.; Branson, H. R., The structure of proteins; two hydrogen-bonded helical configurations of the polypeptide chain. *Proc Natl Acad Sci U S A* **1951,** *37* (4), 205-11.

53. Chiti, F.; Dobson, C. M., Protein misfolding, functional amyloid, and human disease. *Annu Rev Biochem* **2006,** *75*, 333-66.

54. Zhang, S.; Holmes, T.; Lockshin, C.; Rich, A., Spontaneous assembly of a self-complementary oligopeptide to form a stable macroscopic membrane. *Proc Natl Acad Sci U S A* **1993,** *90* (8), 3334-8.

55. Aggeli, A.; Nyrkova, I. A.; Bell, M.; Harding, R.; Carrick, L.; McLeish, T. C.; Semenov, A. N.; Boden, N., Hierarchical self-assembly of chiral rod-like molecules as a model for peptide beta -sheet tapes, ribbons, fibrils, and fibers. *Proc Natl Acad Sci U S A* **2001,** *98* (21), 11857-62.

56. Sawaya, M. R.; Sambashivan, S.; Nelson, R.; Ivanova, M. I.; Sievers, S. A.; Apostol, M. I.; Thompson, M. J.; Balbirnie, M.; Wiltzius, J. J.; McFarlane, H. T.; Madsen, A. O.; Riekel, C.; Eisenberg, D., Atomic structures of amyloid cross-beta spines reveal varied steric zippers. *Nature* **2007,** *447* (7143), 453-7.

57. Zhao, Y.; Wang, J.; Deng, L.; Zhou, P.; Wang, S.; Wang, Y.; Xu, H.; Lu, J. R., Tuning the self-assembly of short peptides via sequence variations. *Langmuir* **2013,** *29* (44), 13457-64.

58. Deng, L.; Xu, H., Hierarchical processes in beta-sheet peptide self-assembly from the microscopic to the mesoscopic level. *Chinese Phys B* **2016,** *25* (1).

59. Caplan, M. R.; Schwartzfarb, E. M.; Zhang, S. G.; Kamm, R. D.; Lauffenburger, D. A., Control of self-assembling oligopeptide matrix formation through systematic variation of amino acid sequence. *Biomaterials* **2002,** *23* (1), 219-227.

60. Mahadevi, A. S.; Sastry, G. N., Cooperativity in Noncovalent Interactions. *Chem Rev* **2016,** *116* (5), 2775-825.

61. Wang, J.; Liu, K.; Xing, R.; Yan, X., Peptide self-assembly: thermodynamics and kinetics. *Chem Soc Rev* **2016,** *45* (20), 5589-5604.

62. Zhu, P.; Yan, X.; Su, Y.; Yang, Y.; Li, J., Solvent-induced structural transition of self-assembled dipeptide: from organogels to microcrystals. *Chemistry* **2010,** *16* (10), 3176-83.

63. Israelachvili, J. N., *Intermolecular and Surface Forces*. Elsevier Science: 2015.

64. Kabiri, M.; Unsworth, L. D., Application of isothermal titration calorimetry for characterizing thermodynamic parameters of biomolecular interactions: peptide self-assembly and protein adsorption case studies. *Biomacromolecules* **2014,** *15* (10), 3463-73.

65. Tahara, K.; Lei, S.; Adisoejoso, J.; De Feyter, S.; Tobe, Y., Supramolecular surface-confined architectures created by self-assembly of triangular phenylene-ethynylene macrocycles via van der Waals interaction. *Chem Commun (Camb)* **2010,** *46* (45), 8507-25.

66. Zang, L.; Che, Y.; Moore, J. S., One-dimensional self-assembly of planar pi-conjugated molecules: adaptable building blocks for organic nanodevices. *Acc Chem Res* **2008,** *41* (12), 1596-608.

67. Korevaar, P. A.; Schaefer, C.; de Greef, T. F.; Meijer, E. W., Controlling chemical self-assembly by solvent-dependent dynamics. *J Am Chem Soc* **2012,** *134* (32), 13482-91.

68. Boekhoven, J.; Brizard, A. M.; van Rijn, P.; Stuart, M. C.; Eelkema, R.; van Esch, J. H., Programmed morphological transitions of multisegment assemblies by molecular chaperone analogues. *Angew Chem Int Ed Engl* **2011,** *50* (51), 12285-9.

69. Korevaar, P. A.; Newcomb, C. J.; Meijer, E. W.; Stupp, S. I., Pathway selection in peptide amphiphile assembly. *J Am Chem Soc* **2014,** *136* (24), 8540-3.

70. Altman, M.; Lee, P.; Rich, A.; Zhang, S., Conformational behavior of ionic self-complementary peptides. *Protein Sci* **2000,** *9* (6), 1095-105.

71. Zhang, S. G.; Lockshin, C.; Cook, R.; Rich, A., Unusually Stable Beta-Sheet Formation in an Ionic Self-Complementary Oligopeptide. *Biopolymers* **1994,** *34* (5), 663-672.

72. Zhang, S. G.; Altman, M., Peptide self-assembly in functional polymer science and engineering. *React Funct Polym* **1999,** *41* (1-3), 91-102.

73. Caplan, M. R.; Moore, P. N.; Zhang, S.; Kamm, R. D.; Lauffenburger, D. A., Self-Assembly of a β-Sheet Protein Governed by Relief of Electrostatic Repulsion Relative to van der Waals Attraction. *Biomacromolecules* **2000,** *1* (4), 627-631.

74. Hong, Y.; Legge, R. L.; Zhang, S.; Chen, P., Effect of amino acid sequence and pH on nanofiber formation of self-assembling peptides EAK16-II and EAK16-IV. *Biomacromolecules* **2003,** *4* (5), 1433-42.

75. Hoyer, W.; Antony, T.; Cherny, D.; Heim, G.; Jovin, T. M.; Subramaniam, V., Dependence of α-Synuclein Aggregate Morphology on Solution Conditions. *Journal of Molecular Biology* **2002,** *322* (2), 383-393.

76. Hong, Y.; Pritzker, M. D.; Legge, R. L.; Chen, P., Effect of NaCl and peptide concentration on the self-assembly of an ionic-complementary peptide EAK16-II. *Colloids Surf B Biointerfaces* **2005,** *46* (3), 152-61.

77. Lopez De La Paz, M.; Goldie, K.; Zurdo, J.; Lacroix, E.; Dobson, C. M.; Hoenger, A.; Serrano, L., De novo designed peptide-based amyloid fibrils. *Proc Natl Acad Sci U S A* **2002,** *99* (25), 16052-7.

78. Tantakitti, F.; Boekhoven, J.; Wang, X.; Kazantsev, R. V.; Yu, T.; Li, J.; Zhuang, E.; Zandi, R.; Ortony, J. H.; Newcomb, C. J.; Palmer, L. C.; Shekhawat, G. S.; de la Cruz, M. O.; Schatz, G. C.; Stupp, S. I., Energy landscapes and functions of supramolecular systems. *Nat Mater* **2016,** *15* (4), 469-76.

79. Spitzer, D.; Rodrigues, L. L.; Strassburger, D.; Mezger, M.; Besenius, P., Tuneable Transient Thermogels Mediated by a pH- and Redox-Regulated Supramolecular Polymerization. *Angew Chem Int Ed Engl* **2017,** *56* (48), 15461-15465.

80. Moad, G.; Solomon, D. H., *The Chemistry of Radical Polymerization*. Elsevier Science: 2005.

81. Szwarc, M., Living Polymers. *Nature* **1956,** *178* (4543), 1168-1169.

82. Szwarc, M.; Levy, M.; Milkovich, R., Polymerization Initiated by Electron Transfer to Monomer. A New Method of Formation of Block Polymers1. *Journal of the American Chemical Society* **1956,** *78* (11), 2656-2657.

83. Moad, G.; Rizzardo, E., Alkoxyamine-initiated living radical polymerization: Factors affecting alkoxyamine homolysis rates. *Macromolecules* **1995,** *28* (26), 8722-8728.

84. Nicolas, J.; Guillaneuf, Y.; Lefay, C.; Bertin, D.; Gigmes, D.; Charleux, B., Nitroxide-mediated polymerization. *Progress in Polymer Science* **2013,** *38* (1), 63-235.

85. Bachmann, W. E.; Wiselogle, F. Y., The relative stability of pentaarylethanes. III. The reversible dissociation of pentaarylethanes. *J Org Chem* **1936,** *1* (4), 354-382.

86. Fischer, H., The Persistent Radical Effect: A Principle for Selective Radical Reactions and Living Radical Polymerizations. *Chemical Reviews* **2001,** *101* (12), 3581-3610.

87. Kato M.; Kamigaito, M. S., M.; Higashimura,, Polymerization of Methyl Methacrylate with the Carbon Tetrachloride/Dichlorotris(triphenylphosphine)ruthenium(II)/ Methylaluminum

Bis(2,6-di-ferf-butylphenoxide) Initiating System: Possibility of Living Radical Polymerization1. *Macromolecules* **1995,** *28*, 1721–1723.

88. Wang, J.-S.; Matyjaszewski, K., Controlled/"living" radical polymerization. atom transfer radical polymerization in the presence of transition-metal complexes. *Journal of the American Chemical Society* **1995,** *117* (20), 5614-5615.

89. Singleton, D. A.; Nowlan, D. T.; Jahed, N.; Matyjaszewski, K., Isotope Effects and the Mechanism of Atom Transfer Radical Polymerization. *Macromolecules* **2003,** *36* (23), 8609-8616.

90. Becker, M. L.; Liu, J.; Wooley, K. L., Peptide-polymer bioconjugates: hybrid block copolymers generated via living radical polymerizations from resin-supported peptides. *Chemical Communications* **2003,** (2), 180-181.

91. Matyjaszewski, K.; Davis, T. P., *Handbook of Radical Polymerization*. Wiley: 2003.

92. Rettig, H.; Krause, E.; Börner, H. G., Atom Transfer Radical Polymerization with Polypeptide Initiators: A General Approach to Block Copolymers of Sequence-Defined Polypeptides and Synthetic Polymers. *Macromolecular Rapid Communications* **2004,** *25* (13), 1251-1256.

93. Chen, J. G.; Logman, M.; Weber, S. G., Effect of peptide primary sequence on biuret complex formation and properties. *Electroanal* **1999,** *11* (5), 331-336.

94. Chiefari, J.; Chong, Y. K.; Ercole, F.; Krstina, J.; Jeffery, J.; Le, T. P. T.; Mayadunne, R. T. A.; Meijs, G. F.; Moad, C. L.; Moad, G.; Rizzardo, E.; Thang, S. H., Living free-radical polymerization by reversible addition-fragmentation chain transfer: The RAFT process. *Macromolecules* **1998,** *31* (16), 5559-5562.

95. Moad, G.; Rizzardo, E.; Thang, S. H., Living Radical Polymerization by the RAFT Process ? A Third Update. *Australian Journal of Chemistry* **2012,** *65* (8).

96. Moad, G.; Rizzardo, E.; Thang, S. H., Living Radical Polymerization by the RAFT Process—A First Update. *Australian Journal of Chemistry* **2006,** *59* (10).

97. Moad, G.; Rizzardo, E.; Thang, S. H., Living Radical Polymerization by the RAFT Process – A Second Update. *Australian Journal of Chemistry* **2009,** *62* (11).

98. Stenzel, M. H., Hairy Core-Shell Nanoparticles via RAFT: Where are the Opportunities and Where are the Problems and Challenges? *Macromol Rapid Commun* **2009,** *30* (19), 1603-24.

99. An, Z.; Qiu, Q.; Liu, G., Synthesis of architecturally well-defined nanogels via RAFT polymerization for potential bioapplications. *Chem Commun (Camb)* **2011,** *47* (46), 12424-40.

100. Boyer, C.; Stenzel, M. H.; Davis, T. P., Building nanostructures using RAFT polymerization. *Journal of Polymer Science Part A: Polymer Chemistry* **2011,** *49* (3), 551-595.

101. Semsarilar, M.; Perrier, S., 'Green' reversible addition-fragmentation chain-transfer (RAFT) polymerization. *Nat Chem* **2010,** *2* (10), 811-20.

102. Grishin, D. F.; Grishin, I. D., Controlled radical polymerization: Prospects for application for industrial synthesis of polymers (Review). *Russian Journal of Applied Chemistry* **2012,** *84* (12), 2021-2028.

103. Smith, A. E.; Xu, X.; McCormick, C. L., Stimuli-responsive amphiphilic (co)polymers via RAFT polymerization. *Progress in Polymer Science* **2010,** *35* (1-2), 45-93.

104. Beija, M.; Marty, J.-D.; Destarac, M., RAFT/MADIX polymers for the preparation of polymer/inorganic nanohybrids. *Progress in Polymer Science* **2011,** *36* (7), 845-886.

105. Sumerlin, B. S., Proteins as Initiators of Controlled Radical Polymerization: Grafting-from via ATRP and RAFT. *ACS Macro Letters* **2011,** *1* (1), 141-145.

106. Perrier, S.; Takolpuckdee, P.; Westwood, J.; Lewis, D. M., Versatile Chain Transfer Agents for Reversible Addition Fragmentation Chain Transfer (RAFT) Polymerization to Synthesize Functional Polymeric Architectures. *Macromolecules* **2004,** *37* (8), 2709-2717.

107. Merrifield, R. B., Solid Phase Peptide Synthesis. I. The Synthesis of a Tetrapeptide. *Journal of the American Chemical Society* **1963,** *85* (14), 2149-2154.

108. Pandey, M.; Agrawal-Rajput, R.; Kshatriya, V. S.; Shah, D.; P, C. K.; Koshti, B.; Gour, N., Single Amino Acid Based Self-Assemblies of Cysteine and Methionine. **2018**.

109. Sunna, A.; Care, A.; Bergquist, P. L., *Peptides and Peptide-based Biomaterials and their Biomedical Applications*. Springer International Publishing: 2017.

110. Satoyoshi, D.; Hachisu, M.; Amaike, M.; Ohkawa, K.; Yamamoto, H., Methionine-Containing Poly(amino acid) Hybrid Fibers via Self-Assembly at Aqueous Interface. *Macromolecular Materials and Engineering* **2004,** *289* (6), 495-498.

111. Glöckner, P.; Metz, N.; Ritter, H., Cyclodextrins in Polymer Synthesis: Free-Radical Polymerization of Methylated β-Cyclodextrin Complexes of Methyl Methacrylate and Styrene Controlled byN-Acetyl-l-cysteine as a Chain-Transfer Agent in Aqueous Medium. Macromolecules 2000, 33 (11), 4288-4290..

112. ten Cate, M. G. J.; Rettig, H.; Bernhardt, K.; Borner, H. G., Sequence-defined polypeptide-polymer conjugates utilizing reversible addition fragmentation transfer radical polymerization. *Macromolecules* **2005,** *38* (26), 10643-10649.

113. Jones, G. R.; Anastasaki, A.; Whitfield, R.; Engelis, N.; Liarou, E.; Haddleton, D. M., Copper-Mediated Reversible Deactivation Radical Polymerization in Aqueous Media. *Angew Chem Int Ed Engl* **2018,** *57* (33), 10468-10482.

114. Fields, G. B.; Noble, R. L., Solid phase peptide synthesis utilizing 9-fluorenylmethoxycarbonyl amino acids. *Int J Pept Protein Res* **1990,** *35* (3), 161-214.

115. Grant, G., *Synthetic Peptides: A User's Guide*. Oxford University Press: 2002.

116. Guy, C. A.; Fields, G. B., Trifluoroacetic acid cleavage and deprotection of resin-bound peptides following synthesis by Fmoc chemistry. *Methods Enzymol* **1997,** *289*, 67-83.

117. Chen, C.; Kong, F.; Wei, X.; Thang, S. H., Syntheses and effectiveness of functional peptide-based RAFT agents. *Chem Commun (Camb)* **2017,** *53* (78), 10776-10779.

Declaration

Ich, Oliver Ceyhun, Matrikelnummer 2658612 versichere, dass ich meine Diplomarbeit selbstständig verfasst und keine anderen als die angegebenen schriftlichen und elektronischen Quellen, sowie andere Hilfsmittel benutzt habe. Alle Ausführungen, die anderen Schriften wörtlich oder sinngemäß entnommen wurden, habe ich kenntlich gemacht.

Datum _____ Unterschrift _____

Oliver Ceyhun

I, Oliver Ceyhun, matriculation number 2658612, assure that I have written independently my thesis and no other than the written and electronic sources named, as well as other aids were used. All statements, which were taken literally or analogously out of other writings, were identified by me.

Date_____ signature _____

Oliver Ceyhun